Temperature-Responsive Hydrogels with Controlled Water Content and Their Development Toward Drug Delivery and Embolization Applications

by

Derek Overstreet

A Dissertation Presented in Partial Fulfillment
of the Requirements for the Degree
Doctor of Philosophy

Approved July 2012 by the
Graduate Supervisory Committee:

Michael Caplan, Chair
Stephen Massia
Alexander McLaren
Brent Vernon
Ryan McLemore

ARIZONA STATE UNIVERSITY

August 2012

ABSTRACT

Aqueous solutions of temperature-responsive copolymers based on *N*-isopropylacrylamide (NIPAAm) hold promise for medical applications because they can be delivered as liquids and quickly form gels in the body without organic solvents or chemical reaction. However, their gelation is often followed by phase-separation and shrinking. Gel shrinking and water loss is a major limitation to using NIPAAm-based gels for nearly any biomedical application.

In this work, a graft copolymer design was used to synthesize polymers which combine the convenient injectability of poly(NIPAAm) with gel water content controlled by hydrophilic side-chain grafts based on Jeffamine® M-1000 acrylamide (JAAm). The first segment of this work describes the synthesis and characterization of poly(NIPAAm-*co*-JAAm) copolymers which demonstrates controlled swelling that is nearly independent of LCST.

The graft copolymer design was then used to produce a degradable antimicrobial-eluting gel for prevention of prosthetic joint infection. The resorbable graft copolymer gels were shown to have three unique characteristics which demonstrate their suitability for this application. First, antimicrobial release is sustained and complete within 1 week. Second, the gels behave like viscoelastic fluids, enabling complete surface coverage of an implant without disrupting fixation or movement. Finally, the gels degrade rapidly within 1-6 weeks, which may enable their use in interfaces where bone healing takes place.

Graft copolymer hydrogels were also developed which undergo Michael addition *in situ* with poly(ethylene glycol) diacrylate to form elastic gels for

endovascular embolization of saccular aneurysms. Inclusion of JAAm grafts led to weaker physical crosslinking and faster, more complete chemical crosslinking. JAAm grafts prolonged the delivery window of the system from 30 seconds to 220 seconds, provided improved gel swelling, and resulted in stronger, more elastic gels within 30 minutes after delivery.

ACKNOWLEDGMENTS

Lots of people have put me in a position to complete my doctoral work successfully. My advisor, Brent Vernon, comes first—his leadership style has been a perfect fit for me. I am very grateful for the freedom Brent has given me, the open communication that we have maintained, and the valuable advice that he has given me over the last four years. I also want to thank the undergraduate students who have contributed to this work and the work that led to it—Richard Huynh, Elizabeth Lee, Amye Farag, Brandon Doan, and Jorge Valdez—I absolutely would not have been able to complete this work without them.

Many other mentors have helped me grow professionally and personally over my time at ASU, especially Ryan McLemore and Harshil Dhruv. They have shown me more than anyone else what it means to be a Ph.D.

I am also very grateful to the funding sources that have supported me in completing this work. A Science Foundation Arizona Graduate Research Fellowship supported me during my first two years and enabled me the security to try and fail many times, be creative, and finally discover a project that I truly believe in. I also received a GK-12 Graduate Research Fellowship from the National Science Foundation.

Finally I want to thank my wife Cindy for pretending to be interested in my research when I need someone to talk to, for keeping my life balanced, and for being my best friend.

TABLE OF CONTENTS

Page

LIST OF TABLES..... xi

LIST OF FIGURES..... xii

CHAPTER 1. INTRODUCTION 1

1.1. Introduction to *In Situ* Forming Hydrogels 1

1.2. Prevention of Prosthetic Joint Infection..... 2

1.2.1. Total Joint Arthroplasty 2

1.2.2. Antimicrobial-Loaded Cements 4

1.2.3. Antimicrobial Surface Coatings 5

1.3. Cerebral Aneurysm Embolization 7

1.3.1. Cerebral Aneurysms 7

1.3.2. Endovascular Coiling 8

1.3.3. Liquid Embolics 9

1.4. Introduction to Temperature-Responsive Polymers..... 11

1.4.1. *N*-isopropylacrylamide-Based Polymers 11

1.4.2. Copolymer Architecture 12

1.5. Temperature-Responsive Graft Copolymers with Controlled Water Content 15

1.5.1. Graft Copolymer Design 15

1.5.2. Experimental Approach 17

CHAPTER 2. INJECTABLE HYDROGELS FOR DRUG DELIVERY APPLICATIONS..... 19

Page

2.1. Introduction 19

2.2. Temperature-Responsive Hydrogels 21

2.2.1. *N*-isopropylacrylamide-Based Hydrogels 21

2.2.2. Block Copolymer Hydrogels 24

2.2.3. Hybrid Temperature-Responsive Materials 28

2.2.4. Poly(organophosphazene)s 30

2.2.5. Elastin-Like Polypeptides 30

2.3. *In Situ* Crosslinking Hydrogels 31

2.3.1. Natural or Hybrid Materials 32

2.3.2. Synthetic Materials 34

2.4. Hydrogels Forming by Ionic Interactions or Self-Assembly 36

CHAPTER 3. INJECTABLE HYDROGELS FOR SPACE FILLING APPLICATIONS 40

3.1. Introduction 40

3.2. Physically Crosslinked Hydrogels 41

3.3. Chemically Crosslinked Hydrogels 45

3.4. Physically and Chemically Crosslinked Hydrogels 48

CHAPTER 4. TEMPERATURE-RESPONSIVE GRAFT COPOLYMER HYDROGEL DESIGN FOR CONTROLLED SWELLING AND DRUG DELIVERY 50

4.1. Introduction 50

Page

4.2. Materials and Methods 52

4.2.1. Materials 52

4.2.2. Synthesis 53

4.2.3. Composition and Molecular Weight 55

4.2.4. LCST Transition 55

4.2.5. Gelation and Swelling 56

4.2.6. Rheometry 59

4.2.7. Ovalbumin Release Kinetics 60

4.3. Results 61

4.3.1. Composition and Molecular Weight 61

4.3.2. LCST Transition 63

4.3.3. Gelation and Swelling 66

4.3.4. Rheometry 70

4.3.5. Ovalbumin Release Kinetics 71

4.4. Discussion 73

4.4.1. Effect of JAAm on LCST Transition 73

4.4.2. Gel Deswelling 73

4.4.3. Lack of Gelation of Some Poly(NIPAAm-*co*-JAAm) Gels 74

4.4.4. Rheological Properties and Implications for Biomaterials Applications 75

4.4.5. Ovalbumin Release Study Limitations 77

Page

4.4.6. Effect of JAAm on Protein Release 77

4.5. Conclusions 78

CHAPTER 5. TEMPERATURE-RESPONSIVE RESORBABLE HYDROGELS FOR PREVENTION OF PROSTHETIC JOINT INFECTION 80

5.1. Introduction 80

5.2. Materials and Methods 83

5.2.1. Materials 84

5.2.2. Synthesis 84

5.2.3. Composition and Molecular Weight 85

5.2.4. LCST Measurement and Degradation Kinetics . 85

5.2.5. Rheological and Handling Properties 86

5.2.6. Distribution in Cadaveric Human Femur 87

5.2.7. *In Vitro* Antimicrobial Release 89

5.2.8. *In Vitro* Cytocompatibility 91

5.3. Results 93

5.3.1. Composition and Molecular Weight 93

5.3.2. LCST Properties and Degradation 94

5.3.3. Rheological and Handling Properties 98

5.3.4. Distribution in Cadaveric Human Femur 101

5.3.5. *In Vitro* Antimicrobial Release 103

5.3.6. *In Vitro* Cytocompatibility 108

5.4. Discussion 110

Page

5.4.1. Swelling and Degradation Relationship..... 111

5.4.2. Rheological and Handling Properties..... 112

5.4.3. *In Vitro* Antimicrobial Release Kinetics..... 113

5.4.4. Implications for Prevention of Prosthetic Joint Infection..... 116

5.4.5. *In Vitro* Cytocompatibility..... 118

5.5. Conclusions 119

CHAPTER 6. *IN SITU* CROSSLINKING TEMPERATURE-RESPONSIVE HYDROGELS WITH IMPROVED DELIVERY, SWELLING, AND ELASTICITY FOR ENDOVASCULAR EMBOLIZATION 121

6.1. Introduction 121

6.2. Materials and Methods 123

6.2.1. Materials..... 123

6.2.2. Synthesis 124

6.2.3. Hydrogel Preparation 126

6.2.4. Composition and LCST Transition 127

6.2.5. Equilibrium Swelling..... 128

6.2.6. Gelation Kinetics and Rheometry 129

6.2.7. Delivery Window Characterization 130

6.2.8. *In Vitro* Embolization Model 131

6.2.9. *In Vitro* Cytocompatibility 132

Page

6.3. Results 133

6.3.1. Composition and Molecular Weight 133

6.3.2. LCST Transition 134

6.3.3. Swelling 135

6.3.4. Gelation Kinetics and Rheometry 136

6.3.5. Delivery Window 139

6.3.6. *In Vitro* Embolization Model 140

6.3.7. *In Vitro* Cytocompatibility 141

6.4. Discussion 142

6.4.1. Swelling 142

6.4.2. Gelation Kinetics and Delivery 143

6.4.3. *In Vitro* Embolization Model and Cytocompatibility 143

6.4.4. Comparison of pNCJ20 and pNC Gelling Systems for Embolization 145

6.5. Conclusions 146

CHAPTER 7. CONCLUSIONS AND FUTURE WORK 148

7.1. Temperature-Responsive Graft Copolymer Design 149

7.2. Resorbable Temperature-Responsive Graft Copolymer Hydrogels for Drug Delivery 150

7.3. *In Situ* Crosslinking Temperature-Responsive Graft Copolymer Hydrogels for Embolization 151

Page

REFERENCES..... 153

APPENDIX A. STATEMENT OF PERMISSION FROM CO-AUTHORS 181

LIST OF TABLES

Table		Page
4.1.	Composition and Properties of Poly(NIPAAm-*co*-JAAm)	62
5.1.	Composition and Properties of Poly(NIPAAm-*co*-DBLA-*co*-JAAm)	94
5.2.	Cumulative Antimicrobial Release from Hydrogels and Cement After 7 Days.....	105
6.1.	Composition and Properties of Poly(NIPAAm-*co*-cysteamine-co-JAAm)	134
6.2.	Delivery Window of *In Situ* Crosslinking Systems for Embolization	140

LIST OF FIGURES

Figure		Page
4.1.	Synthesis of Poly(NIPAAm-*co*-JAAm)	54
4.2.	Schematic of Swelling Determination	58
4.3.	NMR Spectrum of Poly(NIPAAm-*co*-JAAm)	63
4.4.	DSC Thermograms	64
4.5.	Cloud Point Determination of Poly(NIPAAm-*co*-JAAm)	65
4.6.	Gelation of Poly(NIPAAm-*co*-JAAm) Hydrogels	67
4.7.	Photographs of Gel Shrinking	69
4.8.	Rheological Properties of Poly(NIPAAm-*co*-JAAm)	70
4.9.	Ovalbumin Release Profiles	72
5.1.	Rheological Properties of Radio-Opaque PEG Mock and Poly(NIPAAm-*co*-DBLA-*co*-JAAm) Hydrogel	88
5.2.	Degradation Kinetics	95
5.3.	Photographs of Gel Swelling and Degradation	97
5.4.	Frequency Sweep of Poly(NIPAAm-*co*-DBLA-*co*-JAAm)	98
5.5.	Temperature Sweep of Poly(NIPAAm-*co*-DBLA-*co*-JAAm)	99
5.6.	Handling Data of Resorbable Hydrogels as a Function of Concentration and Drug Loading	101
5.7.	Gel Distribution in Cadaveric Human Femur	102
5.8.	Antimicrobial Release from Resorbable Hydrogels	104
5.9.	Antimicrobial Release from Hydrogels vs. Bone Cement	107
5.10.	*In Vitro* Cytocompatibility Data	109

Figure Page

5.11. Photographs of Cells from *In Vitro* Cytocompatibility Study 110

6.1. Scheme for Synthesis of Poly(NIPAAm-*co*-cysteamine-*co*-JAAm) 125

6.2. Scheme Describing *In Situ* Crosslinking Hydrogel Preparation 127

6.3. NMR Spectrum of Poly(NIPAAm-*co*-cysteamine-*co*-JAAm) 133

6.4. LCST Transition of Poly(NIPAAm-*co*-cysteamine-*co*-JAAm) 135

6.5. Equilibrium Gel Swelling Data 136

6.6. Gelation Kinetics 137

6.7. Frequency Sweep of Gels After Crosslinking 138

6.8. Hydrogel Creep After Crosslinking 139

6.9. *In Vitro* Embolization Model Photographs 141

6.10. *In Vitro* Cytocompatibility Data 142

Chapter 1: INTRODUCTION

1.1. Introduction to *In Situ* Forming Hydrogels

Due to their high water content and mechanical resemblance to natural tissues, hydrogels show promising biocompatibility and potential for medical applications.[1] Injectable hydrogel formulations are particularly attractive due to their minimally invasive delivery procedure, providing reduced healing time, reduced scarring, decreased risk of infection, and ease of delivery compared to surgically implanted materials.[2] Injectable hydrogels are also useful for applications where complete surface coverage or complete filling of a space are required. Examples of how these materials might be used include injectable matrices to restore cardiac function following an infarct,[3] thin protective barriers which conform to irregular physiological geometries,[4,5] or as sustained release drug-eluting matrices.[6,7]

Hydrogels are classically defined as three-dimensional, water-swollen materials formed as a result of physical or chemical crosslinking.[1] There are a variety of mechanisms used to make hydrogel systems injectable. The most common mechanism is the formation of physical or chemical crosslinks between polymer molecules during or subsequent to injection. In the absence of crosslinking, a water-soluble polymer will dilute in the body over time following injection. Physical crosslinking occurs in some injectable hydrogels in response to a change in an environmental condition such as temperature, pH, or ionic strength. Chemical crosslinking between soluble or liquid precursor materials *in*

situ can be achieved through a variety of chemical processes including enzymatic, photoirradiation, and self-reactive reactions.

1.2. Prevention of Prosthetic Joint Infection

1.2.1. Total Joint Arthroplasty

Arthroplasty is the surgical repair of a joint conducted to relieve joint pain. Total hip arthroplasty (THA) and total knee arthroplasty (TKA) are among the most common surgical procedures in orthopaedics.[8] Approximately 1 million of these two procedures combined are performed annually in the United States—a number that is expected to grow to over 4 million by 2030.[9] Both of these procedures involve the total replacement of a joint with prosthetic components.

In THA, a cup is placed into the acetabulum and a femoral prosthesis, sometimes called a stem, is inserted into the femur. The femoral prosthesis is made of metal and consists of a ball end (similar to the femoral head) and a tapered distal portion which is press-fit into the femur. Fixation of the femoral prosthesis can be cemented or cementless—in cemented fixation, poly(methyl methacrylate) bone cement is used to fix the implant in place. Cementless fixation relies initially on press-fitting of the implant into the bone and subsequent osseointegration of the nearby bone onto the implant surface.[10] The vast majority of THAs in the United States are performed using cementless fixation for both the acetabular and femoral components,[10] whereas cemented fixation is more popular in Europe.[11]

In total knee arthroplasty, prosthetic components are placed at the distal end of the femur and proximal end of the tibia.[12] Cemented fixation is commonly performed.[12,13] The femoral component has a rounded shape to simulate the distal end of the femur, allowing for the rolling and gliding motion of a normal knee. The tibial component consists of a flat metal plate with a stem that is inserted into the tibia for fixation. A wear-resistant polyethylene surface is also included to reduce the generation of wear debris.[14–17]

Infection following total joint arthroplasty imposes a considerable financial burden both on patients and our national healthcare system, and it significantly reduces patient quality of life.[18] Though only 1.5-2.5% of primary operations are estimated to result in prosthetic joint infection (PJI),[19] this amounts to thousands of cases annually. Management of infected arthroplasty in the US typically involves resection of the implant, thorough irrigation and debridement of the infected area, implantation of an antibiotic-loaded spacer, and—in a separate procedure—re-implantation of a new implant.[20–22] This approach is called a two-stage revision. The overall cost associated with a single infection is substantial, with estimates ranging from $70,000-$114,000 per case in today's dollars.[23–25]

Orthopaedic implant infections are caused by organisms adhering to implant surfaces and then forming a biofilm, producing an established infection.[26,27] Microbes (bacteria, fungi, yeast) in biofilm are resistant to the antimicrobial concentrations that can be achieved safely by systemic delivery. They also elicit little to no immune response. The antimicrobial concentrations required to kill bacteria in biofilm can be 100-1000 times greater than those which

kill planktonic (free floating in fluid) bacteria.[28–30] Such concentrations can only be safely achieved by local delivery.

There is an opportunity to reduce overall costs and improve patient care by taking measures during surgery which reliably prevent infection from arising. The current standard of care for prevention of orthopaedic implant infections is systemic delivery of antimicrobials for 24 hours starting an hour before surgery, strict sterile technique to minimize intra-operative contamination, meticulous surgical technique to minimize soft tissue injury, and optimization of the patient's immune function before surgery. Unfortunately, this does not eliminate all contamination at surgery or completely prevent bacteria from adhering to implant surfaces. In the best possible situation, the infection rate may be less than 1 in 1000, but suboptimal circumstances usually exist, resulting in higher infection rates.[31–33]

1.2.2. Antimicrobial-Loaded Cements

Antimicrobial-loaded bone cement (ALBC) is currently the only option available to deliver antimicrobials directly to the surface of an implant. Some improvement in infection rates has been shown with ALBC in large retrospective analyses.[34,35] However, ALBC is not compatible with cementless fixation which is common in THA. In TKA, although cemented fixation is common, the ALBC remains almost completely entrapped under the implant, affording very limited delivery of antimicrobial to the surgical wound and articulating implant surfaces. Furthermore, when ALBC is used for implant fixation, the dose must be limited to

prevent the cement from becoming too weak.[36,37] The dose of antimicrobials in ALBC for prophylactic use is typically 0.5–2 grams of antimicrobial powder per batch of cement. These preparations render the antimicrobial highly entrapped such that a small fraction (<20%) of the drug is released within several weeks.[38,39] There also is concern that long term, subtherapeutic antimicrobial delivery from ALBC may give rise to resistant organisms.[40]

Other hard materials like calcium phosphate cement (CPC) are unsuitable because they provide rapid drug release,[41] inadequate mechanical properties for fixation (4-37 MPa for CPC[42] vs. 80-90 MPa for low dose ALBC), and do not match bone healing rates in their resorption.[43] The design of these materials presents an inherent tradeoff between mechanical strength and drug delivery—to be structurally supportive, they must have low porosity, which is in direct opposition to efficient delivery of water-soluble antimicrobials.

1.2.3. Antimicrobial Surface Coatings

Though none are yet approved for use, there are active efforts toward developing antimicrobial surface coatings for prosthetic joint components. Several major challenges exist for the use of antimicrobial-loaded polymeric surface coatings on prosthetic joints. In particular, femoral prostheses indicated for cementless fixation are placed under high stress when hammered into the femur to obtain a press-fit, and the volume available for a coating between an implant and the nearby bone is very small. In a knee, there is a significant amount of load and shear on the prosthetic components such that hard surface coatings

would be prone to generate wear debris. Modifying the surface of an implant can change the ability of the bone to achieve good osseointegration with the implant.[44]

A drug-eluting coating must allow for healing, carry and deliver a therapeutic dose of antimicrobial in a controlled fashion, and maintain good surface contact with the prosthesis after implantation. Surface treatments which anchor antimicrobials to a surface typically originate from a silane or other surface-bound reactive molecule,[45,46] meaning that small scratches on the implant can create crevasses prone to bacterial adherence and growth.

Materials in currently FDA-approved products are poorly suited to use in a total joint arthroplasty. Biodegradable hydrophobic polyesters such as PLGA have moderate mechanical strength which may disrupt fixation and slow degradation times exceeding the healing time of bone.[47–49] Alternatively, hydrophilic crosslinked gels such as those based on poly(ethylene glycol) (PEG) tend to release a high fraction of drug quickly.[50] These and other devices, such as those based on gelatin,[51] tend to form a weak yet solid implant—upon experiencing the forces associated with implantation of a hip stem, these materials would break into many pieces rather than continuously coat an implant.

Thus the major obstacle to a viable approach using local antimicrobial delivery to protect to the entire surface of a total joint against infection is the lack of a suitable drug delivery system. There is no available material which can conform to the surface of an implant, protect effectively against biofilm, avoid the generation of wear debris, and allow for osseointegration.

1.3. Cerebral Aneurysm Embolization

1.3.1. Cerebral Aneurysms

An aneurysm is a bulge in a weakened blood vessel wall. While aneurysms can develop in vessels throughout the body, cerebral aneurysms are especially dangerous due to the risk of subarachnoid hemorrhage upon aneurysm rupture. Large autopsy series have shown that cerebral aneurysms are present in 1-6% of the population, but most remain asymptomatic and small.[52] Cerebral aneurysms form in the arteries at the base of the brain called the Circle of Willis. However, only about 1 in 10,000 people experience aneurysmal subarachnoid hemorrhage. Patients who have already had one hemorrhage have an increased likelihood of development of new aneurysms.[53] As a result, this patient group is targeted for preventative treatment to prevent any aneurysms they may develop from bursting.[54]

Prior to the early 1990s, aneurysms were most commonly treated using microsurgical clipping.[55,56] This technique first requires a craniotomy to access the aneurysm, after which a neurosurgeon uses a device to "pinch off" the aneurysm neck. This technique is effective but has fallen out of favor due to its invasiveness. When better endovascular tools were developed, such as flow-directed catheters and balloon remodeling techniques, embolization arose as another option for aneurysm treatment.[57,58] Embolization refers to the placement of a material into an aneurysm in order to reduce blood flow into an aneurysm and prevent the aneurysm from rupturing.

1.3.2. Endovascular Coiling

Platinum coils are the standard of care in endovascular embolization of aneurysms today.[55] Coils are the standard of care for endovascular aneurysm treatment, but lead to poor recanalization rates (>25%) in large or wide-neck aneurysms.[59–61] Failure is most often attributed to the low volume fraction that the coils occupy within the aneurysm, relying on clot formation to occlude the entire volume rather than the coils themselves.[62–64] Placing a coil into an aneurysm increases the amount of force required to place the next coil, thus increasing the risk of accidentally puncturing the aneurysm while placing coils.[65] Even in the best case scenario, coil embolization has only been shown to fill about 50% of the total aneurysm volume.[63,66–69] However, the aneurysm filling percent attained by coil placement is directly related to the re-bleeding rate, indicating that the body's response will not completely suffice to block aneurysms if they are not initially filled to a certain degree.[62,70] While coil embolization is a widely used endovascular technique for treating intracranial aneurysms, some new hydrogel-coated coil designs are being developed to address some of the drawbacks of bare platinum coils to achieve better volumetric filling,[66,71–73] accelerate thrombus formation[74–76] or structurally support the coils.[77,78] However, there is a lack of well-designed trials demonstrating evidence in favor of these newer coil systems.[79]

1.3.3. Liquid Embolics

Materials that form *in situ* from liquid precursors have the potential to fill aneurysms more completely than endovascular coils, making them an attractive option.[80–86] Poly(ethylene-*co*-vinyl alcohol) polymer dissolved in DMSO and marketed under the trade name Onyx® (eV3 Neurovascular; Irvine, CA), is the only liquid embolic device currently approved by the FDA (as a Humanitarian Use Device in 2007) "for the treatment of intracranial, saccular, sidewall aneurysms that present with a wide neck (≥ 4mm) or with a dome-to-neck ratio < 2 that are not amenable to treatment with surgical clipping." The polymer utilizes a solvent exchange process in which the DMSO is gradually replaced by blood in the aneurysm, rendering the polymer insoluble.[87–91] While studies have supported Onyx's potential as an embolic agent for aneurysm treatment,[81] solvent exchange systems have inherent limitations. First, the polymer must be delivered in DMSO, an organic solvent. As the polymer is delivered, it is released into the body. DMSO has been linked to angiotoxicity and vasospasm when injected too quickly.[89,92,93] As a result, Onyx® must be delivered very slowly, requiring repeated steps allowing for the DMSO to gradually leave the aneurysm site and be replaced by water. Delivery can take over an hour to complete,[81] which is undesirable and leads some surgeons to not use the product. Prolonged use or oscillating on-off use of balloon occlusion during the procedure also increases the risk of vascular damage.[81]

Other water-borne systems based on *in situ* physical[85] or chemical[83,86] crosslinking have also been reported in the literature but none have yet been

successfully translated to clinical use. For example, the ability of alginate to form a gel in the presence of calcium-rich solutions was evaluated for embolization using a dual-lumen microcatheter.[94] These hydrogels form very quickly once the precursor solutions are mixed *in situ*, resulting in the polymer forming a string-like shape upon delivery. Despite this and alginate gels being relatively soft, successful embolization was observed in eight swine,[95] however these materials have not been reported on recently. Lightly crosslinked temperature-responsive polymer gels have also been used, with partial recanalization observed in swine at 2 weeks unless used in combination with a second device such a flow-diverting stent.[85] These gels were elastic, but very weak (G' < 1000 Pa) and required a cooling jacket to inject, hindering the delivery of the gel and adding cost to the procedure. Recently, a chemical gelling system based on poly(propylene glycol) diacrylate and a thiol-based crosslinker were demonstrated as a water-borne polymer gel for embolization.[83] Despite promising *in vitro* data demonstrating these gels' very high strength and easy delivery, complete aneurysm filling or overfilling led to fatal outcomes in swine.[84] While the high strength of a liquid embolic is good for retention of the gel within the aneurysm, it also may enable the gel's swelling to distend or rupture the aneurysm. This device's prospects may be limited given that a relatively minor misuse could bring severe risk to the patient.

1.4. Introduction to Temperature-Responsive Polymers

Some temperature-responsive polymers hold promise for biomedical applications because they are soluble in water at ambient (or slightly cooler) temperatures and then precipitate to form a gel when heated to body temperature. These temperature-responsive polymers can be delivered into the body as a liquid and allow for fast gelation *in situ* without requiring organic solvents or chemical reaction. Fast gelation might be important for example in order to keep the polymer from diluting in the surrounding media or to limit the burst release of drugs loaded into the gelling solution. Such polymers are said to have a lower critical solution temperature, or LCST, the temperature above which a polymer becomes insoluble.

1.4.1. *N*-isopropylacrylamide-based Polymers

Among temperature-responsive polymers, polymers of *N*-substituted acrylamides are desirable because they exhibit an LCST transition over a narrow temperature range in aqueous solution[96] and their properties can be easily modified by copolymerization with vinyl/acrylic comonomers. Poly(*N*-isopropylacrylamide) (poly(NIPAAm)) is by far the most commonly investigated, as it has a convenient LCST of about 30°C which can be further controlled by the content and composition of additional comonomers.[97,98] Relative to multiblock copolymers having an LCST,[99] an advantage of using poly(NIPAAm) is that the LCST is relatively insensitive to a number of design parameters, such as molecular weight,[100,101] concentration,[101] crosslinking,[102] pH,[103] and ionic strength,[104] and so

a wide range of gel properties is attainable by adjusting these parameters. However, the LCST is very sensitive to the hydrophilicity of other comonomers. Hydrophilic comonomers such as acrylic acid (AAc) can increase the LCST by as much as 12°C per wt%.[105] The high sensitivity of LCST to hydrophilic groups limits the amount that can be copolymerized with NIPAAm while retaining an LCST lower than body temperature.

1.4.2. Copolymer Architecture

Polymers are molecules consisting of one or more repeat units connected in a particular arrangement. It is well known that using different individual repeat units lead to vastly different material properties. For example, polystyrene, polyethylene, PEG, poly(NIPAAm), polypropylene, nylon, etc. have different properties which lead to their suitability for various uses. It is slightly more subtle but still true that the arrangement of the repeat units, also called the polymer architecture, can also be controlled to provide new, different, and potentially useful properties. Polymers can be made to be linear, branched, crosslinked, block, star-shaped, comb, graft, or dendrimers.[106] As an example, poly(NIPAAm) crosslinked gels containing graft chains of poly(NIPAAm) were shown to undergo much faster deswelling than gels which did not contain side chains.[107] A more obvious example is that if a given linear polymer is water-soluble, a crosslinked architecture will yield a swollen, solid gel.

Copolymers can be made by combining multiple types of repeat units. Copolymers can exhibit:

1. New properties not shared with homopolymers of either of its repeat units;

2. Intermediate (blended) properties compared to those derived from each repeat unit;

3. Combined properties while more completely retaining properties derived from each repeat unit separately.

The way that properties of repeat units combine in a copolymer depends on the copolymer's architecture. Block copolymers can result in completely new properties. For example, multiblock copolymers of poly(ethylene glycol) with either poly(propylene glycol) or poly(lactic acid) can have LCST behavior, though none of the respective homopolymers do. These copolymers can act as surfactants or form micelles because their hydrophilic and hydrophobic repeat units are separated into distinct blocks.

Random copolymers tend to have a blend of the properties expected from their repeat units. Consider the copolymerization of NIPAAm with acrylic acid (AAc). Poly(AAc) is a hydrophilic, water-soluble polymer at neutral pH. Poly(NIPAAm) is hydrophilic below its LCST and hydrophobic above its LCST. When NIPAAm and AAc are randomly copolymerized, LCST increases linearly with AAc content.[98,105] In this system, LCST is very sensitive to AAc content—just 2 mol% of AAc is enough to increase the LCST by approximately 10°C. If enough AAc is added, the LCST can cease to exist altogether (or increase to above the boiling point of water), as the hydrophilicity of AAc dominates the temperature-responsiveness of poly(NIPAAm). Obtaining a blend of properties in

the case of poly(NIPAAm) is undesirable for medical applications—nearly all comonomers broaden and change the average temperature of the LCST transition. Random copolymerization can also lead to unique behavior (such as the faster degradation and lower crystallinity of lactic and glycolic acid random copolymers relative to a homopolymer of either)[108] but it is not well-suited to lead to retention of the properties of multiple comonomers.

Graft and block copolymers tend to retain the properties of each type of repeat unit more separately. Chen and Hoffman demonstrated that a graft copolymer consisting of poly(NIPAAm) grafts on a main chain of poly(AAc) has an LCST identical to that of poly(NIPAAm) and identical pH response to that of poly(AAc).[109] This finding demonstrated that the LCST of a copolymer with NIPAAm in particular is not a function of the weight fraction of a comonomer. Instead, an improved explanation is that the LCST is related to the uninterrupted chain length of NIPAAm repeat units,[110] such that in a block or graft copolymer, the LCST is almost identical to that of poly(NIPAAm) homopolymer. As a general rule, a block of repeat unit A contributes the properties of poly(A) when incorporated within a copolymer architecture and likewise for B. A graft or block copolymer of A and B would thus retain some properties of poly(A) and some of poly(B). However, despite work having been done using graft copolymers of poly(NIPAAm) and hydrophilic polymers,[109,111–113] none have captured the appropriate ratios, molecular weights, and concentrations necessary to form a hydrogel.

1.5. Temperature-Responsive Graft Copolymers with Controlled Water Content

A major limitation of NIPAAm-based hydrogels for nearly any biomedical application is that the gels tend to exhibit substantial shrinking and solvent loss (syneresis) when heated above the LCST.[97,107,114–117] Previous strategies for controlling gel swelling have led to undesirable properties, including large LCST increase with a small swelling effect,[105,110,118] limited deliverability,[119,120] or leaching of high molecular weight byproducts.[121]

1.5.1. Graft Copolymer Design

Rapid water loss and shrinking of poly(NIPAAm) gels is a major limitation to their viability as materials for medical applications in drug delivery and embolization. Thus, the overall goal of this work was to develop a novel copolymer platform in which the water content of poly(NIPAAm)-based gels could be controlled independently of other properties such as LCST, deliverability, or degradability. Previously reported materials have required tradeoffs where the component used to control swelling has also reduced or eliminated the benefits of using poly(NIPAAm)

Put another way, the goal was to develop materials which combine the injectable nature of poly(NIPAAm) with the hydrophilicity of PEG. Such a system would overcome the inherent limitation of poly(NIPAAm) related to its shrinking upon gelation. The hypothesis as the basis for this design was that polymer LCST is related to mol% content of comonomers with NIPAAm, but gel swelling is related to wt%. Therefore, a design was used which uses a comonomer

with NIPAAm with a disproportionately higher wt% relative to mol%--i.e., a high molecular weight comonomer. For this reason, a graft copolymer design was pursued.

The graft copolymers consisted of a main chain rich in NIPAAm repeat units, with hydrophilic side-chain grafts based on Jeffamine® M-1000 (Huntsman Corp., The Woodlands, TX, USA) to control the swelling and hydrophilicity of the polymer. Jeffamine® M-1000 is a random copolymer of ethylene oxide (EO) and propylene oxide (PO) in a 19:3 EO:PO ratio and approximately 1000 Da molecular weight. Jeffamine® M-1000 was chosen as the hydrophilic graft (as opposed to a PEG diacrylate or other hydrophilic polymer) for the following reasons:

1. It forms a stable linkage to the main polymer chain. Because Jeffamine® M-1000 has an amine end, it allows for an amide linkage between the main chain and the graft. Thus the swelling control over the material does not change as a function of time and does not introduce a confounding effect of degradation due to the graft component. The grafts themselves are also hydrolytically stable.
2. It is not a crosslinker. Crosslinking of NIPAAm chains yields materials which are gels both below and above the transition temperature. Because the resulting polymer is not chemically crosslinked, it has improved flexibility in its delivery properties by virtue of the material being liquid below the LCST. This also allows for conversion from gel to sol in a resorbable polymer formulation.[122–124]

3. It is easy to synthesize the graft copolymer. Because Jeffamine® M-1000 can be incorporated using a simple two-step chemistry—first, by acryloylation with acryloyl chloride, and second, by radical copolymerization with NIPAAm. Such a synthesis scheme allows for good yields and is reproducible.

4. It is inexpensive. Heterobifunctional PEG of similar molecular weight can cost $300 per gram or more for research grade material, whereas Jeffamine® M-1000 is mass produced and costs under $20 per kg. A lower cost of materials enables a wider range of potential applications and also improves the potential of these copolymers to be commercialized so long as the material properties are appropriate.

1.5.2. Experimental Approach

The first segment of this work (as reported in Chapter 4) was to synthesize and characterize graft copolymers of NIPAAm and Jeffamine® M-1000 acrylamide (JAAm). Characterizing the effects of JAAm and molecular weight on LCST, gel swelling, gel strength, and drug elution were emphasized. This data was intended to provide proof-of-principle that a graft copolymer design can lead to NIPAAm-based polymers where gel swelling can be tuned nearly independently of LCST. In the following segments of this work, the novel graft copolymer design was utilized to develop polymers for drug delivery (Chapter 5) and endovascular embolization (Chapter 6).

To develop an injectable and resorbable material for controlled drug delivery, a third co-monomer was included which causes an increase in LCST over time as a result of hydrolysis, leading to dissolution of the polymer. The degradation time and elution of antimicrobials were evaluated as a function of polymer JAAm content and compared to that of clinically used antibiotic-loaded bone cement. The goal of this work was to develop a candidate material with appropriate properties as a local drug-eluting material for prevention of prosthetic joint infection following total joint arthroplasty.

For use in embolization, side groups available for *in situ* crosslinking were added, and gels were prepared by mixing with a second precursor solution containing a reactive crosslinker. Physical crosslinking is intended in these gels to stop them from diluting in the surrounding media whereas subsequent chemical crosslinking causes the gel to become stronger and more elastic. Gels containing various JAAm content were characterized with emphasis on their rheological properties relevant to their ability to be delivered in an endovascular procedure and their stability after crosslinking.

Chapter 2: INJECTABLE HYDROGELS FOR DRUG DELIVERY APPLICATIONS

2.1. Introduction

Injectable hydrogels are often engineered to function as carriers that provide controlled drug release.[7,125–128] Injectable hydrogels can also be easily delivered into sites that are difficult or infeasible to access surgically. These formulations are typically designed to provide prolonged activity from a single administration, reducing risks associated with patient compliance. Because the size and shape of an injectable hydrogel is determined by its local environment,[129] good interfacial contact is usually achieved between the hydrogel and the nearby tissue,[130] allowing for drug to elute directly into the local tissue and, in some cases, facilitating healing. Further, injectable and degradable materials allow for easy delivery of additional doses to the same site.

Some drawbacks exist for using injectable hydrogels for drug delivery. Most hydrogels are too weak to be load-bearing, and some (physical gels, in particular) are prone to plastic deformation in response to stress due to their viscoelastic character. Insoluble drugs can become heterogeneously distributed within the gels, leading to sample-to-sample variability of drug release rates. The greatest drawback is typically that drug release from hydrogels suffers from either a rapid initial burst release of drug followed by sustained release, or rapid release of drug altogether.[125] Burst release is a primary concern for injectable

formulations because slow gelation *in situ* can lead to loss of drug before the gel fully forms. Changes in gel volume after gelation can also cause rapid release.

Though the ideal properties of the hydrogel depend heavily on the application for which it is intended, there is a basic set of properties that are advantageous for drug delivery.[6,131] Desirable hydrogel properties for drug delivery include:

i) Low/medium viscosity of the solution prior to injection.

ii) Fast gelation which minimizes the initial burst release of drug.

iii) High water content and good biocompatibility.

iv) Compatibility with a wide variety of drugs (low molecular weight, proteins, nucleic acids).

v) Efficient drug loading.

vi) Maintenance of volume and interfacial contact with tissue after gelation.

vii) Control of drug release rate over a range of time frames.

viii) Long (>3 month) shelf life.

ix) Easy to purify and sterilize.

x) Degradability into low molecular weight, soluble byproducts either by hydrolysis or enzymatic degradation.

xi) Suitable drug release profile (i.e. cumulative release vs. time) for the application.

2.2. Temperature-Responsive Hydrogels

2.2.1. *N*-isopropylacrylamide-Based Hydrogels

Typically, poly(NIPAAm) gels tend to undergo a high degree of syneresis (i.e. shrinking and separation from solvent) upon gelation, which can result in high burst release, particularly of hydrophilic drugs. Another disadvantage of poly(NIPAAm) homopolymer for drug delivery is its lack of degradability, and therefore additional comonomers must be included to make the gel degradable.

For a copolymer containing NIPAAm to form an injectable hydrogel, it must initially have an LCST below body temperature. Before injection below the LCST, this polymer is soluble in an aqueous solution. Then, upon injection (body temperature > LCST), this polymer precipitates and forms a hydrogel if the polymer concentration is sufficient. The release rate from physical (i.e. not crosslinked) gels is inversely proportional to the gel's viscosity in the absence of intermolecular interactions between the polymer and the drug.[125,132] For a formulation to be degradable based on hydrolysis[122,133–136] or enzymatic degradation[137] of side chains, the LCST must increase to above body temperature upon hydrolysis or enzymatic degradation and the polymer must not be sufficiently chemically crosslinked to remain as a solid below the LCST so that the polymer re-dissolves. In these types of materials, the LCST starts below the body temperature to make the material injectable, but becomes resorbed after the LCST increases to above body temperature. The use of dynamic LCST polymers based on NIPAAm was first demonstrated by Neradovic et al.[133] using

hydrolyzable poly(NIPAAm-*co*-hydroxyethylmethacrylate (HEMA)-monolactide), though these materials did not have a final LCST above body temperature. Similar materials were subsequently developed by Lee and Vernon[136] using poly(NIPAAm-*co*-AAc-*co*-HEMA-lactide) and Ma et al.[135] using poly(NIPAAm-*co*-lactide methacrylate-*co*-HEMA) which exhibited LCST increase to above body temperature upon hydrolysis. In the former case, the degradation was rapid (2-8 days) due to increased hydration of the polymer chains owing to the hydrophilicity of acrylic acid (AAc), whereas Ma et al. reported much longer degradation times of about 200 days due to grafting of the lactide side group onto methacrylic acid, leading to a much more hydrophobic material. However, these materials also underwent rapid deswelling over the course of 2-6 hr and had an equilibrium water content under 50%,[135] likely rendering them unsuitable for delivery of hydrophilic drugs that will partition into the water phase as it leaves the hydrogel system during syneresis.

Alternatively, copolymers of NIPAAm containing hydrolyzable dimethyl-γ-butyrolactone acrylate (DBLA) were shown by Cui et al. to exhibit degradability without the loss of low molecular weight byproducts.[122] Copolymers containing NIPAAm, DBLA, and AAc were subsequently shown to have favorable biocompatibility *in vivo.*[123] Li et al. used similar copolymers of NIPAAm, DBLA, AAc, and HEMA-poly(trimethylene carbonate) (HEMA-PTMC) to deliver the protein superoxide dismutase.[124] The release profile was highly dependent on the protein loading. Gels physically mixed with collagen at high protein loading (4 mg/mL) exhibited nearly constant protein release over a

period of 3 weeks; however, all gels with low protein loading (2 mg/mL) showed fast release over the first day and almost no release thereafter.

Another method allowing for gel degradation is crosslinking NIPAAm-based polymer chains with degradable crosslinkers such as poly(lactic acid),[138] dextran,[138,139] or peptide sequences[140,121]—however, in this approach, unless the LCST of the individual polymer chains increases to above body temperature, the poly(NIPAAm) portions will remain permanently insoluble at the injection site. In order to be injectable, crosslinked materials must have a very low crosslink density, as they will otherwise form solid, swollen hydrogels below the transition temperature.

As a poly(NIPAAm)-based gel is heated above its LCST, a homogeneous polymer-rich phase (i.e. the gel) separates from a fraction of the original solvent and then tends toward an equilibrium.[141] Usually, solutions are formulated at <30 wt% and deswell such that the final polymer concentration in the gel is about 50%,[115,118,105,142] so a significant fraction of water is lost during gelation. Rapid deswelling and syneresis (i.e. loss of the initially entrapped aqueous liquid) has been shown to be associated with fast drug release upon heating above the LCST of NIPAAm-based physical gels.[116,143,144]

A promising and yet rarely used method for controlling drug release from these materials may be the copolymerization a drug derivative as a hydrolyzable side group. Such a strategy was reported by Shah et al. using *N*-hydroxysuccinimide as a model drug in the polymer-drug conjugate poly(NIPAAm-*co*-*N*-acryloxysuccinimide).[145] These materials have the advantage

of releasing drug in concert with the rate of degradation of the bond linking the drug to the polymer backbone, and degradation leaves an acid group on the polymer backbone, raising the LCST and allowing for dissolution of the polymer. However, this strategy is only compatible with certain drugs (those containing hydroxyl groups).

Dual-responsive polymers sensitive to both temperature and pH have been developed by copolymerizing NIPAAm with either AAc[109] or pH-sensitive substituted acrylates such as 2-(dimethylamino)ethyl methacrylate (DMAEMA).[146] In terms of drug delivery, it is convenient to have a pH-induced transition at 37°C that occurs over the neutral range of pH around 5.0-7.4.[103] Using propylacrylic acid as a second monomer having pKa near 6.0, Garbern et al. reported prolonged release of active VEGF up to 4 weeks at pH 5.0 and for between 1-4 days at pH 7.4, despite the polymer being soluble.[147] Such prolonged release at low pH may have been due to the high content of propylacrylic acid (17 mol%) affecting the overall properties of the polymer in its protonated (insoluble) state. The somewhat prolonged release at neutral pH despite the polymer being soluble was attributed to electrostatic affinity between the VEGF (isoelectric point pI = 8.5) and the negatively-charged polymer.

2.2.2. Block Copolymer Hydrogels

Solutions of block copolymers with alternating hydrophilicity (usually ABA triblock or alternating multi-block copolymers) have LCST in aqueous solution which is dependent on block length, composition, and polymer

concentration. Typically relatively high polymer concentrations (>10 wt%) are required for these materials to exhibit LCST behavior, though exceptions do exist.[148] These materials often have a central hydrophobic block such as poly(propylene oxide) (PPO) or poly(lactide-*co*-glycolide) (PLGA) and hydrophilic blocks which are almost always comprised of PEG (also called PEO for poly(ethylene oxide)). The LCST of these materials is thought to be due to increased hydrophobicity of the hydrophobic segment upon heating, leading to micellar aggregation.[149,150]

Much of the early work on this family of polymers was based on PEO-PPO-PEO block copolymers such as the Pluronics made by BASF,[149–154] but these are non-degradable, mechanically weak, and tend to be highly permeable to drugs.[57] The first degradable block copolymer hydrogels with LCST behavior for drug delivery were reported by Jeong et al., who used poly(L-lactic acid) (PLLA) as the hydrophobic central block.[155] Unlike poly(NIPAAm)-based systems, these polymers are backbone degradable and become soluble after a single ester is hydrolyzed. These gels were shown to release FITC-dextran (20 kDa) over at least 12 days with very low initial burst release. Increasing the polymer concentration from 25 to 35 wt% led to a more constant-release profile *in vitro*.[155] Similar materials of PEG-PLGA-PEG (500-2810-500) were shown to have convenient LCST below body temperature above about 16 wt%.[156] These materials released the hydrophilic low molecular weight drug ketoprofen mostly over the first 3-5 days *in vitro*, with very low release thereafter. The release rate was not tunable over a wide time frame, with similar release observed from 20%,

25% and 33% gels. Using the same copolymers, the hydrophobic drug spironolactone was released in an S-shaped release profile, with the first part being due to diffusion over about 4 days, followed by almost no release for the next 10 days, and then accelerating release thereafter for the next 35 days due to degradation of the gels. Much work over the last decade has utilized this block copolymer design with various degradable hydrophobic groups and various architectures, such as PEG-PTMC diblocks,[157] poly(caprolactone) (PCL) groups,[158,159] modified Pluronics,[160–162] enzyme-degradable poly(amino acid)s,[163] and even hydrophobic segments of poly(NIPAAm),[164,165] which give rise to a sharp gelation temperature based on the LCST of the NIPAAm chains.

For drug release, block copolymer hydrogels are rather flexible in terms of the types of drugs that can be loaded. A formulation of PLGA-PEG-PLGA developed under the name ReGel® showed nearly linear *in vitro* release of paclitaxel over 50 days with about 20% initial burst release over the first day at 23 wt% concentration.[166] Similar gels showed first-order release of various proteins over 1-2 weeks. The difference in release among these can be explained by the fact that hydrophobic drugs are relatively immobile due to poor solubility and hence exhibit partition-controlled release, whereas hydrophilic drugs (either small molecules or proteins) tend to release more quickly and in a first-order profile based on diffusion. Partition-controlled release refers to the phenomena that hydrophobic drugs preferentially dissolve (partition) in the hydrophobic polymer phase and only slowly diffuse into the water phase and thus become released due to their low water solubility. The release of the protein GLP-1 was slowed from

about 2 days to 15 days and made nearly linear by complexing the drug with zinc, thereby reducing its solubility while preserving its activity.[167] Injection of the ReGel® into diabetic rats led to reduced blood glucose levels for 15 days post-injection. A similar system using cationic poly(β-amino ester) (PAE) as the outside blocks of a PAE-PCL-PEG-PCL-PAE pentablock copolymer resulted in electrostatic retention of insulin and a linear release profile for up to 20 days *in vitro*, with sustained insulin concentrations provided *in vivo* for up to 18 days.[168] Still, this class of materials tends to release hydrophilic drugs very quickly. For example, Gong et al. reported PEG-PCL-PEG gels which released the hydrophilic model drug VB_{12} completely over about 24 hr, with high burst and incomplete release of both bovine serum albumin (BSA) and the hydrophobic model drug honokiol after 14 days (about 20% cumulative release), though it is worth noting that the release was not measured throughout the 50 day degradation of the gels.[169] Tang and Singh synthesized 11 variants of mPEG-PLGA-mPEG and reported release of lysozyme over 20 days at the longest from very high concentration (40 wt%) gels.[170]

Block copolymer hydrogels can be made to respond to both temperature and pH. Determan et al. modified Pluronic F127 with end blocks of poly(2-diethylaminoethyl-methyl methacrylate), having pKa near 7.5.[171] They showed linear release of lysozyme over about 4 days at pH 7.0 and slightly slower release, projected to last about 6 days, at pH 8.0. Pluronic® P104-based gels with acid-sensitive acetal linkages were reported by Garripelli et al.[172] They reported release of FITC-dextran (40 kDa) over 2 days at pH 5.0, 9 days at pH 6.5, and about 30

days with an S-shaped release profile at pH 7.4. Such pH-dependent release might be useful in terms of releasing drugs more quickly in response to local acidic conditions.

2.2.3. Hybrid Temperature-Responsive Materials

Natural and natural/synthetic hybrid temperature-responsive materials which thicken or gel upon warming to body temperature have been reported, usually with the goal of prolonging release using high molecular weight natural polymers or for combining the advantages of high biocompatibility and degradability of natural materials with the control over composition and properties of synthetic materials.

Aqueous solutions of chitosan in the presence of glycerophosphate salts can undergo gelation upon heating at neutral pH.[173] Gelation time is affected by salt concentration, temperature, degree of deacetylation, and slightly by drug loading.[174] These materials were shown to release paclitaxel *in vitro* at a rate which was dependent on the drug loading, with 40% cumulative release in 30 days when loaded at 64 mg/mL.[175] When evaluated *in vivo* in a subcutaneous tumor model, gels showed some antitumor efficacy both in the presence and absence of drug, indicating an antitumor effect of chitosan alone.[175] Gels with drug showed tumor volumes at 17 days that was similar to that of daily intravenous injections for the first 4 days. However, it is unclear whether the higher efficiency (similar outcome using a single administration) of the gels is related to the material or simply the intratumoral administration of the drug in the

gel group. A notable disadvantage of these natural materials is that the release rate of the drug is not easily controlled by adjusting the properties of the device. While the authors note that the drug itself could be modified to alter the release (in this case, to increase the release rate for a high drug loading), this approach is undesirable in terms of cost and regulatory issues. Crosslink density of chitosan-glycerophosphate interpenetrating polymer networks (IPNs) with hydrophilic poly(vinyl alcohol) was used to control the release of lysozyme,[176] though it is worth noting that covalently crosslinked gels are likely to not be injectable or to break into many pieces upon injection through a needle, and the poly(vinyl alcohol) used was of relatively high molecular weight (66 kDa), which could lead to renal toxicity.

A common design for hybrid temperature-responsive hydrogels is to graft temperature-responsive synthetic polymers, such as poly(NIPAAm), onto a natural, hydrophilic polymer such as hyaluronic acid,[177] gelatin,[178] or chitosan.[179–181] The poly(NIPAAm) chains in these materials tend to be of low molecular weight, and so the resulting gels tend to be very weak and viscous. Further, the drug release is typically fast. A variety of low molecular weight drugs were shown to release from NIPAAm-grafted gelatin within 6 hours,[178] and proteins released from NIPAAm-grafted hyaluronic acid within 12 hours.[177] Similarly fast release over 2 days or less was observed for NIPAAm-grafted chitosan for various model drugs[179–181]—to prolong the release of hydrophobic drugs to 14 days, the authors embedded PLGA microparticles within the gel.[181] In addition to the short duration of drug release so far demonstrated from this class of materials, another

disadvantage is that the thermosensitive polymer chains in these designs will remain insoluble after degradation of the natural component.

2.2.4. Poly(organophosphazene)s

Another group of linear polymers having LCST-like behavior in aqueous solution are the poly(organophosphazene)s, which can be made degradable through the incorporation of amines, amino acids, or alkoxy groups. These gels thicken over a wide range of temperatures and remain transparent rather than phase-separating like most other LCST materials, and so the thermal transition is typically characterized by viscometry. Drug release can be controlled either by incorporation into the polymer[182,183] or simply by diffusion or degradation, over a period of up to about 35 days.[184] Kang et al. used hydrophobic side groups of L-isoleucine ethyl ester and hydrophilic side groups of α-amino-ω-methoxy-PEG (MW 550) and reported duration of release for two model protein drugs to be between 3 and 15 days.[185] Similar gels released the hydrophobic low molecular weight drug doxorubicin steadily over about 30 days.[186]

2.2.5. Elastin-Like Polypeptides

Elastin-like polypeptides (ELPs) contain pentapeptide repeat units Val-Pro-Gly-X-Gly, where X is any natural amino acid except proline.[187] These materials have an LCST which tends to occur over a narrow temperature range. Since they are genetically encoded, they can be made to be monodisperse, and are enzymatically degradable *in vivo.* While these materials have also been

investigated as thermally triggered polymer-drug conjugates,[188–191] hydrogels have also been made from these materials for injectable drug delivering matrices, primarily complexed with silk to comprise so-called silk-elastin like polypeptides or SELPs. These materials show injectability due to reduced crystallinity of the silk component by mixing with ELPs.[192] However, the release from these matrices is rapid, occurring almost completely in a matter of hours, even for large protein drugs.[193]

2.3. *In Situ* Crosslinking Hydrogels

Hydrogels can be formed from liquid or soluble precursors by *in situ* chemical reaction by a number of mechanisms including thermal polymerization, photopolymerization, or *in situ* polymer-polymer crosslinking reactions. For any application, it is desirable for such reactions to take place under biologically-compatible conditions and usually with minimal side reactions to nearby tissue. *In situ* crosslinking is ideal for incorporating a wide variety of biocompatible hydrophilic biomaterials (such as natural soluble polymers or PEG) into an injectable hydrogel. The kinetics of gelation is an important consideration for drug delivery, particularly for systems which do not gel beginning on the outside, forming an initial 'skin' and then proceed to gel toward the center of the material. The material must have low enough viscosity to be injectable and yet gel quickly enough after injection to avoid burst release. Efficient crosslinking is also important for minimizing the toxicity associated with reactive chemical species or leachable small molecules (e.g. monomers, crosslinkers). Discussion of these

systems will be divided into natural or hybrid materials which are comprised of at least one natural component, and materials made from fully synthetic precursors.

2.3.1. Natural or Hybrid Materials

Natural biomaterials are often high molecular weight, linear polymers which can subsequently be crosslinked together through a controlled fraction of functional groups on their sides, most commonly hydroxyls or amines. Alginate oxidized to contain terminal aldehyde groups can crosslink through proteins such as gelatin, which is accelerated in the presence of borax.[194] The gelation time of these materials was 20-50 seconds, and even when the materials were allowed to gel for 10 minutes before release was measured *in vitro*, a 30% or greater burst release of primaquine was observed within 6 hr for all gels tested. The remainder of the drug was released slowly over at least 5 days. Similar chemistry has been used with an aldehyde-functionalized alginate derivative crosslinking through adipic acid dihydrazide, crosslinking upon the formation of two hydrazone linkages.[195] A disadvantage of aldehyde chemistry is its lack of specificity—aldehydes are prone to react with amines which are present in proteins, as is the case for the fixatives glutaraldehyde and formaldehyde. Conversely, a chemistry which has not been evaluated for drug delivery but is capable of forming crosslinked networks with high specificity is high-affinity non-covalent binding, such as that between avidin and biotin.[196]

A common crosslinking chemistry in both synthetic and natural materials is the Michael addition reaction between thiols and acrylates. Cai et al. developed

thiol-modified hyaluronic acid and chondroitin sulfate materials for *in situ* crosslinking with PEG diacrylate (PEGDA) and release of basic fibroblast growth factor (bFGF).[197] Gelation time was dependent on pH, with gels forming more rapidly at higher pH. Gels formed within 1 minute at pH 8.5. Release of FITC-HSA was prolonged over about 5 days *in vitro*. Using covalently bound heparin to complex with the bFGF, its release was prolonged over about 28 days, and this formulation showed improved neovascularization relative to gels without heparin or bFGF alone. Hiemstra et al. used thiol-modified dextran with either 4-arm PEG-tetraacrylate or dextran functionalized with vinyl sulfone to form gels in under 1 minute.[198] At 20 wt%, these gels became rather strong, with storage modulus near 100 kPa. The gel properties of these materials are particularly sensitive to the ratio of reactive groups, with the strongest gels obtained using a thiol:acrylate ratio near 1:1.

Enzyme-mediated *in situ* crosslinking can be done using tyramine-functionalized materials. Jin et al. functionalized hydroxyl groups on dextran with pendant phenol moieties, which are coupled to each other in the presence of hydrogen peroxide and horseradish peroxidase.[199] Similar systems based on hyaluronic acid showed fast burst release in the first 5 hours up to a fraction of the total protein which was related to the crosslink density of the gels.[200] This period was followed by degradation-based release of the entrapped model proteins lysozyme and α-amylase only in the presence of hyaluronidase.

Crosslinking can also be initiated using light as an external energy source. For example, chitosan functionalized with azide and lactose groups was

crosslinked by UV light with a gelation time under 30 seconds and used for release of FGF-2 in a wound dressing.[201–203] The reaction proceeds by release of nitrogen gas from azide groups, converting them to reactive nitrene groups which then crosslink either with amines or other nitrenes to yield a stable azo linkage. These materials provided some release for 1 day after gelation and then nearly zero release thereafter, though protein release was measured to be incomplete.[202] It is unclear what fraction of the FGF-2 remained active following the UV exposure, but improved wound closure with time was observed, indicating that some active protein was released.[203] These materials released the alkaline model drug toluidine blue completely within one day *in vitro*, while almost no acidic model drug (trypan blue) was released for 5 days. This difference was attributed to the alkaline character of the chitosan itself, demonstrating the potential for control over release rate depending on the affinity between the drug and the device.

2.3.2. Synthetic Materials

In situ polymerization of monomers with macromolecular crosslinkers can be used for controlled drug delivery applications provided that gelation is fast and the monomers have low toxicity. For example, West and Hubbell developed gels based on PEGDA and *N*-vinyl pyrrolidone (NVP) which crosslink by radical polymerization into solid gels within 20 seconds of exposure to UV light.[204] The crosslinker in these designs can be engineered to control the degradability of the gels due to either hydrolysis[204] or the action of specific enzymes.[205] These gels

were shown to release a variety of proteins (6-66 kDa) *in vitro* at a steady rate over a period of up to 5 days depending on molecular weight. The UV photopolymerization was also shown to not substantially affect the activity of entrapped tissue plasminogen activator (tPA). *In situ* photopolymerized gels using poly(ε-caprolactone fumarate) diacrylate as the macromer required over 3 minutes to form gels when exposed to blue light.[206] Thin cylindrical shaped gels (8 mm diameter, 2 mm thickness) optimized for maximum crosslinking showed diffusion-based release of the low molecular weight, hydrophobic drug tamoxifen citrate over a period of about 5 days *in vitro*. While the crosslinked gels are relatively non-toxic to cells, the macromers themselves can be relatively cytotoxic. Studies on acrylate-functionalized macromers[207] and initiators[208] show concentration-dependent toxicity of these components of *in situ* polymerizing hydrogels.

Some systems rely on crosslinking reactions between individual low molecular weight precursors to form gels rather than a polymerization reaction. This approach may be advantageous in that it does not require an external energy source or give rise to radicals. The most common among these *in situ* crosslinking systems are systems of thiols and acrylates, of which the average functionality of the precursors must be greater than 2 for network formation (i.e. gelation) to occur.[209,210] Elbert et al. mixed PEG-dithiol and multi-arm PEG acrylates at 40 wt% to yield gels which released albumin over 8-12 days, with slower release and longer degradation time observed in gels with greater average functionality.[211] Vernon et al. used PEGDA and the tetra-thiol precursor

pentaerythritol tetrakis(3-mercaptopropionate) (QT) at a very high concentration (75 wt%) for partition-controlled release of progesterone.[212] Gels with high drug loading showed prolonged and steady release over at least 50 days.

Drug release data from studies using *in situ* crosslinking gels must be evaluated carefully because the data is likely to underestimate the amount of burst release that would occur from the gels if used *in vivo*. Because the standard method in the literature involves curing the liquid precursors completely before exposing the gels to the release medium, most measurements of drug release behavior provided by these materials represent a "best case" in terms of minimizing burst release. While studies on temperature-responsive hydrogels may show similar bias by pre-gelling a drug-loaded injectable solution before exposing the gel to the release medium, burst release from temperature-responsive hydrogels tends to occur more slowly upon syneresis after gelation, and is therefore still likely to be reflected more accurately *in vitro*.

2.4. Hydrogels Forming By Ionic Interactions or Self-Assembly

Systems that undergo gelation in the presence of ions in the solvent have also been evaluated.[213] A change in the concentration of specific ions in solution can trigger solution to gel (sol-gel) transition in some materials due to ion exchange that causes a change in the interactions between polymer molecules and the solvent. For example, alginate, a naturally derived polymer, undergoes gelation in the presence of Ca^{2+} and other divalent ions.[1] This material was shown to release active VEGF for over 2 weeks when first allowed to gel for 30

minutes[214,215] and show improved motor function in a rat model of Huntington's disease relative to a control without VEGF.[216] While alginates can entrap a wide variety of drugs, they have a long *in vivo* degradation time.[217] Alginate gels also have a time-sensitive gelling process which poses a challenge for drug delivery—too fast, and the material is not injectable; too slow, and the drug is released rapidly before gelation can occur. Alginate gels undergo faster gelation without a preliminary mixing step when used in ophthalmic applications because the higher calcium concentration in the eye allows for alginate gelation without an initial mixing step. In these applications, release of low molecular weight drugs was prolonged over less than 12 hours.[218,219]

Electrostatic interactions between oppositely charged materials yield hydrogels following a pre-mixing step. Van Tomme et al. reported formation of mostly elastic gels upon mixing of oppositely charged microspheres comprised of dextran crosslinked either with negatively charged methacrylic acid or positively charged DMAEMA.[220] These gels showed degradation-based release of rhodamine-B-dextran (70 kDa), which can be controlled by adjusting the crosslink density, microsphere weight fraction and charge balance.[221] Negatively charged chondroitin 6-sulfate and positively charged type A gelatin were used to form a gel by complex coacervation which was used to control the gelation and drug release from a methylcellulose hydrogel.[222] However, this system involves a salt (ammonium sulfate) which is unlikely to remain in the gel for several days after injection *in vivo*, limiting its use to short-term formulations.

Hydrogels can form due to non-covalent interactions between similar molecules[223–226] or complexation of two mixed precursors.[227,228] Such gels are often referred to as self-assembling or nano-assembling gels. Self-assembling hydrogels are shear thinning which allows for injectability after subjecting the material to stress and then gels upon subsequent recovery of its mechanical properties *in situ*. Injectable self-assembling peptide nanofibers comprised of short peptides were shown to release PDGF-BB in vivo in a myocardial infarct model for up to 14 days.[223] These peptides contain an alternating polar / non-polar pattern of amino acids which allows them to form nanofibers or other nanostructures which form gels upon entanglement of those structures.[229] This design is advantageous because of the low molecular weight of the gelator, the low concentration required for gelation, and the enzyme-degradable nature of the materials. Using a similar approach, amphiphilic prodrugs based on acetominophen conjugated to fatty acids were shown to deliver drugs without initial burst release.[225] Alternatively, a non-drug gelator such as ascorbyl palmitate can be used to entrap drugs.[226] Drug release was enzyme-mediated, with almost zero release of physically entrapped drugs in the absence of enzyme.[225,226] Such low release in the "off" state over as long as 7 days is remarkable for a hydrogel material. This design is particularly promising because it uses materials which are natural and generally regarded as safe, offers flexibility for the incorporation of multiple types of drugs (hydrophilic drugs in the gelator itself and hydrophobic drugs entrapped physically), and allows for very high drug loading since a significant fraction of the device itself is composed of drug.

However, because the degradation and release are dependent on enzyme action, the rate of release is likely to be governed mostly by the amount of enzyme activity in the injection site. As injection of any foreign material is likely to induce some acute inflammatory response, proteases involved in this process might trigger faster release of drug. The release of the hydrophilic compound in such a case could be controlled through changing the gelator concentration. Another concern with these materials is their long gelation time, which may produce burst release *in vivo* even if not observed after the 15-45 minute gelation time. Over this amount of time, it is reasonable to expect that some release might occur as the gel recovers its properties.

Synthetic polymers can also be utilized in injectable self-assembling hydrogels. One synthetic approach utilizing segments of PEG-poly(hydroxybutyrate)-PEG block copolymer hydrogels with α-cyclodextrin has been used to cause gelation, compared to the block copolymer alone which is soluble.[230,231] Cyclodextrins form a necklace-like molecular structure with linear polymers such as PEG,[232,233] which contribute to the crystallinity of the polymer. The gels are shear-thinning and thixotropic, reducing in viscosity by about 5-fold after 10 minutes of agitation and then recovering over a period of 12 hours. The gels released entrapped FITC-dextran (20 kDa) over 25 days at a nearly constant rate after gelation. However, the same concern as above applies—the gels were allowed to thicken for 12 hours prior to the start of the release study. Also the viscous and weak (~100 Pa*s viscosity at low shear rate)[231] rheological properties of these gels may lead to irreversible deformation under nearly any load.

Chapter 3: INJECTABLE HYDROGELS FOR SPACE FILLING APPLICATIONS

3.1. Introduction

Because injectable hydrogels assume the shape of the environment into which they are placed, they are suitable choices for some materials which neither release drugs nor serve as tissue engineering matrices, but instead provide a structural, barrier, or space-filling function.[3,5,234–238] For plastic surgery or tissue filling applications, minimally invasive administration and minimized scar formation make injectable materials ideal. Using embolic agents for diverting or eliminating flow in blood vessels can be useful for treatment of arteriovenous malformations or aneurysms. Similar materials might also be useful for contraception. Injectable hydrogels have also been investigated as tissue barriers for adhesion prevention or as bulking agents to reinforce weakened tissue.

There are several design considerations for hydrogels to be used in space-filling applications. Typically, the primary consideration is that hydrogels tend to be relatively weak, and so both the modulus and the viscoelastic character (i.e. phase angle) of the gel must be suitable for the application. For a material to be resilient and resistant to creep in response to constant or periodic stresses, it must lose very little of the energy put into it—i.e. the material must be highly elastic (phase angle near zero). Deswelling is likely to be problematic in applications such as endovascular embolization where full occlusion of a space is a necessary function of the material. Swelling in the same applications should also be limited

to avoid exerting undue forces on weakened vessel walls. Other considerations include bioadhesion, solute transport through the device, biocompatibility, sterilization, deliverability (such as through a catheter), delivery time, gelation time, and degradability (and if so, degradation time).

In this section, injectable space-filling hydrogels reported in the recent literature will be presented according to the type of crosslinking responsible for *in situ* gelation (physical, chemical, or multiple). While many materials such as pre-fabricated gels and silicone are used as injectable fillers in cosmetic surgery[239–242] and as tissue bulking agents,[243–245] this section will focus on materials which undergo an increase in mechanical properties after administration.

3.2. Physically Crosslinked Hydrogels

Physical gels form associative networks without covalent crosslinks connecting the constituent molecules. Whereas chemical gels tend to be highly elastic, some physical gels tend to be viscoelastic[144,246] which is disadvantageous for most space-filling applications. For example, physical gels of poly(*N*-isopropylacrylamide) are formed due to hydrophobic interactions between side groups.[247–249] During deformation of the material, hydrophobic interactions between side groups can be "broken" and then reformed between different combinations of polymer side groups. The interchangeable nature of the hydrophobic interactions can result in a viscous or viscoelastic gel.[135,144,250] The phase angle can be controlled by a number of factors including

concentration,[130,246] polymer architecture,[250] light pre-crosslinking,[118,119] *in situ* crosslinking,[136,251] or molecular weight.[130]

One application of injectable hydrogels is intra-myocardial injection following myocardial infarction slow the progression of heart disease by reducing stresses on the infarcted tissue.[3,252] Degradable physical gels of poly(NIPAAm-*co*-AAc-*co*-HEMA-poly(trimethylene carbonate)) were shown to lead to improved contractility, ventricular wall thickness, and capillary density at 8 weeks after injection.[253] Though no rheological data was reported, the gels were initially able to be stretched to ~200% strain. However it is unclear whether the gels were effective after 8 weeks and especially after degradation of the gel. If not, gel would need to be re-injected to be effective for more than a few months, which would be impractical. Self-assembling peptide hydrogels have been investigated for myocardial injection as well, but gels alone did not lead to improved outcome as measured by cardiac function or ventricular wall thickness.[223,254,255] These hydrogels did show encouraging results in a rat model when releasing growth factors in a tissue engineering approach,[254,255] but the data from hydrogels without growth factors suggests that the gels' mechanical properties are insufficient to provide an improved outcome.

Copolymer architecture was used by Lin and Cheng to make injectable gels of elastic modulus between 1000-2500 Pa using block and star copolymers with a central PEG group and terminal poly(NIPAAm) groups.[250] The materials exhibited reversible gelation due to the poly(NIPAAm) groups above the LCST of 26-29°C. These gels show limited syneresis, a fast injection time, and some

elasticity (tan δ between 0.24-0.62). Stereocomplexing degradable star copolymers containing 8-arm PEG and terminal segments of either poly(D-lactic acid) (PDLA) or poly(L-lactic acid) (PLLA) were shown to exhibit lower gelation concentrations and higher strengths when equimolar amounts of each enantiomer were present compared to PEG-PLLA alone and compared to triblock copolymers.[256] These gels were relatively strong, with the gels having up to 14 kPa storage modulus and low phase angle.

Lightly crosslinked temperature-responsive gels based on poly(NIPAAm) have been developed for space-filling applications. Below the LCST, light crosslinking allows for the material to behave as a liquid, and yet above the LCST allows for improved elasticity characteristic of a chemical gel. In general, temperature-responsive materials with light pre-crosslinking tend to be weaker than temperature-responsive materials which undergo crosslinking *in situ* because the crosslink density is limited to a low fraction of comonomers. However these polymers do not have reactive groups present which may improve their biocompatibility. A lightly crosslinked copolymer of poly(NIPAAm-*co*-butyl methacrylate) lightly crosslinked with PEG-diacrylamide groups[119,257] was investigated for embolization of cerebral aneurysms alone or in combination with protection devices such as stents and coils.[85] Because of the low LCST of 13-18°C, a cooling jacket had to be continuously flushed with 4°C saline to prevent gelation inside the microcatheter containing the polymer prior to delivery. Complete occlusion was observed after 14 days when the polymer was co-administered with a stent or both stent and coil, but partial recanalization was

observed in aneurysms with neither, likely due to the low modulus of the polymer (storage modulus ~ 1000 Pa). It is also difficult to assess the effectiveness of the polymer alone because the study was only carried out for 14 days and the untreated control aneurysms did not rupture.[85]

Vernengo et al. used a similar polymer design of poly(NIPAAm) lightly crosslinked with PEG-dimethacrylate of various molecular weights for nucleus pulposus replacement.[235] These materials are injectable and are reported to maintain their mass for up to 90 days *in vitro*, with compressive moduli over 50 kPa seen in several of the formulations, particularly those with lower molecular weight PEG (below 4.6 kDa). However, using this range of PEG resulted in equilibrium water content that was near or below 50 wt% when the polymers were formulated at 15 wt%. Therefore, the gels shrank to approximately 30% of their initial volume within 90 days. This degree of shrinking could be problematic for a load-bearing material, due to concentration of stress on the shrunken implant, absence or deformation of the material potentially allowing for bone-bone contact, or even risk of the implant being displaced.

Another material design used for intra-myocardial injection involves the use of a dextran and PCL-based degradable macromolecular crosslinker subsequently copolymerized with NIPAAm to yield a pre-crosslinked injectable hydrogel.[258] The materials had storage modulus up to 1500 Pa depending on the crosslinker content. This material was injected into infarcted heart tissue in rabbits 4 days post-infarct.[259] After 4 weeks, they showed increased ejection fraction and lower left ventricular end diastolic diameter (LVEDD). While no material was

observed at 4 weeks in the histology due to degradation of the crosslinker, it is unclear if this material has longer term effects either on cardiac function or biocompatibility due to its partial non-degradability.

Ionic crosslinking of alginate gels that occurs based on local tissue calcium concentration has also been used as an injectable bulking agent in myocardium.[260] Alginate solution was injected 7 days post-infarct in rats. After 8 weeks, animals receiving alginate injections showed increased wall thickness and lower LVEDD. It was shown by staining that most of the material was not present in the infarct by 6 weeks. However, as with other myocardial bulking agents, it is unclear how the heart performs well past degradation. There is also evidence suggesting that increases in wall thickness are insufficient to prevent unwanted left ventricular remodeling post-infarct,[261] and that long-term improvement in function may depend as much or more on healing in the infarct site rather than the stresses being absorbed by the injected gel.[261–263]

3.3. Chemically Crosslinked Hydrogels

Covalently crosslinked materials based on liquid or injectable precursors are useful for space-filling applications because they form highly elastic network polymers with phase angles near zero. These materials are not as prone to creep as physical gels, and therefore tend to be suitable for applications that require load bearing or long-term exposure to stress. The precursor materials can potentially be delivered through a catheter without solidification, and gelation time can be easily controlled.

In situ photopolymerization of a PEG-based crosslinker and *N*-vinyl pyrrolidone has been used to form a thin barrier on the interior of blood vessels to reduce thrombosis following vascular injury.[5] The photoinitiator was first adsorbed onto the vessel surface followed by polymerization, creating a hydrogel with a nearly uniform thickness conforming to the surface of the vessel wall. The liquid precursor materials can also penetrate into the tissue, leading to adhesion between the gel and the tissue. Gel formation took place within seconds, and gel thickness was well controlled by adjusting the polymerization time. The gels significantly reduced thrombosis and reduced neointimal thickening by 80% after 2 weeks in a rabbit balloon injury model.

In situ crosslinking between two soluble or liquid precursors has been used in a variety of bioinert or structural materials. One of the strongest is a reverse-emulsion (water-in-oil) system developed by Vernon et al. consisting of 3 mass equivalents of a mixture of two organic precursors (one functionalized with thiols and the other with acrylates) mixed with 1 equivalent of aqueous buffer, resulting in 75 wt% gels.[264] Reverse-emulsion gels made of tetrafunctional pentaerythritol tetrakis(3-mercaptopropionate) (QT) and pentaerythritol triacrylate (TA) had ultimate strength in compression exceeding 6 MPa and ultimate deformation of 37%. Stabilization with a surfactant was required for gelation to provide high surface area between the oil phase containing the precursors and the alkaline aqueous phase which activates the reaction. A similar system based on QT and poly(propylene glycol) diacrylate (PPODA) has recently been developed for intracranial aneurysm embolization.[83,84] The gelation kinetics of this system

are desirable for embolization because there is a time after mixing during which the material is still injectable as a liquid with a phase angle near 90° (purely fluid versus elastic) and low viscosity. Then gelation occurs quickly, resulting in a material with low phase angle near 0° (purely elastic). A number of factors affect the gelation time and final properties of these materials, including mixing time and the composition of the aqueous phase.[83] *In vivo* studies of the PPODA-QT system in swine showed neointimal growth at 1 month when the material was used to incompletely fill (80-90 vol%) aneurysms to avoid re-entry of material into the parent vessel.[84] Based on the high strength of these gels, they were able to be deployed successfully without a second device such a stent to retain the gel inside the aneurysm. Also the deliverability time of these strong gels is much lower and the delivery process easier than for the solvent-exchange Onyx system (poly(ethylene-*co*-vinyl alcohol) delivered in DMSO)[81,265] currently approved in the US.

Natural-synthetic hybrid *in situ* crosslinking materials have been developed for bioinert applications as well. Cloyd et al. screened a variety of gel types for mechanical matching of human nucleus pulposus and concluded that *in situ* crosslinking hydrogels based on hyaluronic acid and PEG-grafted chitosan was an appropriate match.[234] These materials had moduli in compression between 5-20 kPa. Hybrid hydrogels based on HA and methylcellulose crosslinking by aldehyde reaction with hydrazides showed moderate cytotoxicity *in vitro*, but were effective in preventing peritoneal adhesions *in vivo* in a rabbit cecal injury-side wall defect model.[266] Gels with methylcellulose were shown to be stronger

than *in situ* crosslinking HA gels, but all of the gels tested were weak, with shear moduli below 500 Da. These gels exhibited slower degradation than HA-based gels, dependent on the type of cellulose derivative used. This material design is suitable for prevention of peritoneal adhesions because complete surface coverage and biocompatibility are primary concerns, while the strength requirement is relatively low.

So-called "fibrin glue" forms upon the conversion of fibrinogen to fibrin by thrombin, and so gels can be made on demand by mixing thrombin and fibrinogen solutions together—for example, using a double-barreled syringe. These gels have good biocompatibility, are degradable, and can form gels rapidly. Fibrin glues have long been used as surgical sealants,[267–269] and more recently have been evaluated for intramyocardial injection after infarction. Mukherjee et al. evaluated the injection of a fibrin-alginate composite gel into infarcted myocardium in pigs and found that infarct expansion was prevented for 2 weeks after injection.[270] Promising results have also been obtained using fibrin glue in the same application both alone and seeded with skeletal myoblasts in smaller animal models.[271,272]

3.4. Physically and Chemically Crosslinked Hydrogels

Gels which crosslink both physically and chemically have potential to combine the advantages of fast gelation typical of temperature-responsive physical gels with the strength and elasticity of a covalently crosslinked material. Combining poly(NIPAAm-*co*-HEMA-acrylate) with either thiol-functionalized

poly(NIPAAm)[273,274] or thiol-functionalized crosslinkers[142] yields stronger gels with improved elastic properties at low frequency compared to physical gels. Alternatively, thiol-functionalized poly(NIPAAm) forms strong and elastic physical-chemical gels upon mixing with PEGDA below the LCST, which, when heated, reach storage moduli near 1 MPa, an exceptionally high value for a hydrogel.[275] Alternatively, NIPAAm-based macromers can be polymerized *in situ* to obtain physical-chemical gels.[276] Yet some frequency response is still observed in physical-chemical gels when allowed to crosslink above the LCST, and the gel moduli plateaus at lower values when the gels are heated to 37°C more quickly,[274] which indicates that crosslinking may be incomplete when the polymers must crosslink at temperatures above the LCST. These materials also are non-degradable.

Degradable physical-chemical gelling systems based on Michael addition reactions between poly(organophosphazene)s with other poly(organophosphazene)s or PEG-based crosslinkers have recently been reported.[251,277,278] Some of these gels with 8-arm PEG-based crosslinkers[251] showed the highest storage moduli (over 40 kPa) and slow degradation, with over half the gel mass remaining after 90 days after subcutaneous injection in mice. FT-IR data also suggests that the gels are capable of crosslinking at 37°C over about 40 minutes. While the poly(organophosphazene) acrylated precursor was found to be somewhat cytotoxic even at a very low concentration of 0.05 wt%, the same concentrations of the crosslinked hydrogel led to cell viability similar to cells without polymer.

Chapter 4 – TEMPERATURE-RESPONSIVE GRAFT COPOLYMER HYDROGEL DESIGN FOR CONTROLLED SWELLING AND DRUG DELIVERY

4.1. Introduction

Poly(NIPAAm) gels exhibit substantial syneresis (shrinking and expulsion of solvent) when heated above the LCST,[115–117,279] and so resistance to shrinking is an important consideration for the design of nearly any NIPAAm-based biomaterial. For most applications of *in situ* forming hydrogels, the ideal case is that the material transitions quickly from liquid to solid with no change in volume. For example, wound healing and embolization applications require retention of the hydrogel's original size to maintain contact with the surrounding tissue. For controlled drug delivery, a fast sol-to-gel transition without syneresis could reduce the high initial burst release of hydrophilic drugs typical of many *in situ* forming materials.[7,143]

There is evidence which suggests that the LCST depends on the number of consecutive NIPAAm repeat units in a polymer chain,[110,111] while swelling depends on the mass of water that a hydrophilic comonomer retains within the gel.[109,110,130] In other words, the LCST can be considered as a function of comonomer molar fraction, while swelling is a function of weight fraction. Copolymerization of NIPAAm with low molecular weight hydrophilic comonomers has failed to achieve full volume retention and an LCST below body temperature.[105,118,280] Alternatively, graft copolymer architecture allows for a

comonomer to comprise a low molar fraction of the comonomers but a higher weight fraction of the polymer. For example, a poly(NIPAAm) or poly(NIPAAm-*co*-BMA) backbone crosslinked with 6 kDa NH_2-PEG-NH_2 (~1 mol% or 38 wt% PEG) provides swollen and hydrophilic temperature-responsive gels with a minimal increase in LCST due to the PEG.[257,119] Random copolymers of NIPAAm with methoxy-PEG-methacrylate (mPEGMA) have been reported as candidate materials for cell encapsulation or *in situ* forming implants.[130] These extremely high molecular weight (3-4 MDa) polymers formed elastic gels at low polymer concentrations which retained their volume for over 10 days. However, because PEG is linked to the polymer backbone via an ester group in this and other similar materials, the side chains will eventually hydrolyze over a physiologically relevant time, leaving ionized methacrylic acid units which cause increased LCST and either partial or complete dissolution of the polymer under physiological conditions.[145,210,281]

Here, the synthesis and characterization of new water-stable graft copolymers with controlled equilibrium swelling based on NIPAAm and Jeffamine® M-1000 acrylamide (JAAm) is reported. Jeffamine® M-1000 is a random copolymer of ethylene oxide (EO) and propylene oxide (PO) in a 19:3 EO:PO ratio and approximately 1000 Da molecular weight [282], with one methoxy end and one primary amine end, affording a stable amide linkage to the polymer backbone. The methoxy end group may decrease the material LCST and improve gel stability via interactions between the chain end and the hydrophobic poly(NIPAAm) core relative to the hydroxyl end group of PEG.[130,283] The

hypothesis for this work was that JAAm would be useful as a component in a graft copolymer architecture for control of the swelling and release properties of NIPAAm-based gels with a minimal effect on LCST. The use of crosslinkers was avoided in the present work to isolate the LCST and swelling effects of JAAm rather than confounding those with the effects of the crosslinker itself. A secondary reason for this decision is that physical gels have improved flexibility by virtue of their convenient handling properties as liquids below the LCST and also their potential for conversion from gel to sol in a resorbable polymer.[122–124]

Copolymers of NIPAAm with or without various amounts of JAAm were synthesized in two ranges of molecular weights in order to ascertain the effect of JAAm on gelation and swelling at various polymer concentrations. These materials were synthesized and characterized via ^{1}H nuclear magnetic resonance spectroscopy (NMR), differential scanning calorimetry (DSC), cloud point determination, and high-performance liquid chromatography (HPLC). Two high molecular weight polymers with markedly different equilibrium swelling behavior were further characterized for rheological properties and protein release kinetics, using ovalbumin as a model drug.

4.2. Materials and Methods

4.2.1. Materials

All materials were reagent grade and obtained from Sigma-Aldrich unless otherwise noted. NIPAAm monomer was recrystallized from hexane.

Azobisisobutyronitrile (AIBN) was recrystallized from methanol. Benzene and 1,4-dioxane were anhydrous and used as received. Triethylamine (TEA) was distilled and stored under nitrogen. HPLC grade tetrahydrofuran (THF) was used for low molecular weight polymerizations and as the mobile phase for molecular weight and polydispersity determination. Jeffamine® M-1000 polyetheramine was donated by Huntsman Corporation (The Woodlands, TX, USA).

4.2.2. Synthesis

Jeffamine® M-1000 acrylamide (JAAm) was synthesized from Jeffamine® M-1000 polyetheramine as shown in Figure 4.1A. Jeffamine® M-1000 (20 g, 20 mmol) was dissolved at 10 w/v% in dichloromethane (DCM) along with TEA (3.3 mL, 24 mmol) and maintained at 0°C under nitrogen atmosphere. Acryloyl chloride (1.95 mL, 24 mmol) was then added dropwise into the solution under stirring and the reaction was allowed to proceed for at least 6 hours at 0-4°C at under nitrogen atmosphere. Following the reaction, DCM was evaporated and the residue was dissolved in 0.1 N sodium bicarbonate (200 mL). The product was extracted into DCM and the organic layer evaporated once more. JAAm was solidified by cooling on ice, vacuum dried, and stored at 4°C until use.

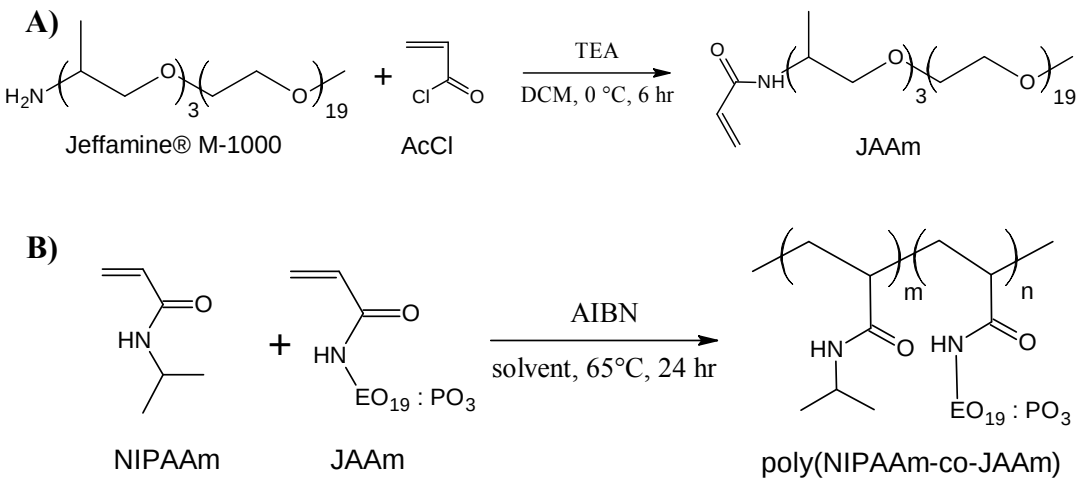

Figure 4.1. Synthesis of A) Jeffamine® M-1000 acrylamide (JAAm) macromer and B) poly(NIPAAm-*co*-JAAm)

Poly(NIPAAm-*co*-JAAm) copolymers were synthesized by radical polymerization in each of two solvent mixtures, either 90:10 benzene: dioxane (high molecular weight, HMW) or 80:20 dioxane: THF (low molecular weight, LMW), as shown in Figure 4.1B. Feed ratios in the polymerizations were either 100:0, 85:15, or 70:30 NIPAAm: JAAm by mass. Direct polymerization of monomers was chosen rather than side-chain substitution (for example, using *N*-acryloxysuccinimide) because direct polymerization allows for one-step synthesis and easy purification without hydrolysis of the reactive intermediate [145]. Monomer solutions were bubbled with nitrogen for at least 20 minutes prior to addition of the initiator to reduce dissolved oxygen. Polymerizations were conducted at 65°C for 24 hr under a slight positive pressure of nitrogen, with AIBN (0.007 mol AIBN/mol of total monomer) as the initiator. For HMW polymerizations only, approximately half of the solvent was either decanted or

evaporated and then replaced by an equivalent volume of acetone to reduce the viscosity of the polymer solution. Copolymers were collected by precipitation in 10-fold (HMW) or 15-fold (LMW) excess of 0-4°C diethyl ether, filtered, and vacuum-dried overnight. The product was then dissolved in deionized water, dialyzed against deionized water at either 10,000 MWCO (HMW) or 3,500 MWCO (LMW) for at least 3 days at 4°C, and lyophilized.

4.2.3. Composition and Molecular Weight

^{1}H NMR (Varian Inova, 400 MHz) was used to confirm successful synthesis and determine the composition of JAAm and the synthesized polymers. D_2O was used as the NMR solvent.

The molecular weight and polydispersity of the synthesized polymers was determined by gel permeation chromatography (Shimadzu Corp.) in conjunction with static light scattering (MiniDawn, Wyatt Technology Corp.) with THF as the mobile phase. Samples were prepared by dissolving the polymers in THF with a concentration of 10 mg/mL.

4.2.4. LCST Transition

The LCST transitions of the synthesized copolymers were evaluated by DSC (MC-DSC, Calorimetry Sciences Corp.). Samples were dissolved at 5 wt% in 150 mM PBS (pH 7.4). Scans were taken from 10°C to 80°C at a heating rate of 1°C/min. Samples were measured in triplicate.

Synthesized copolymers were dissolved at 0.1 wt% in 150 mM PBS (pH 7.4) and the LCST transition characterized by cloud point determination. This concentration was chosen because none of the polymer solutions saturated the detector when heated above the LCST. Cuvettes containing the polymer solutions were allowed to equilibrate in a water bath for at least 90 s prior to each measurement. Absorbance at 450 nm was measured every 1°C by a UV/Vis spectrometer from 25-45°C with buffer alone as the reference. Some polymers precipitated and formed aggregates upon heating. In this case, the greatest value of absorbance before observed aggregation was recorded as the maximum value and all previous values were normalized relative to the maximum value. Absorbance values for polymers that did not aggregate were normalized to the absorbance at 55°C.

4.2.5. Gelation and Swelling

The swelling behavior and gel stability of the synthesized copolymers were characterized at various concentrations and molecular weights. Solutions of each low molecular weight (LMW) polymer were prepared at 5, 10, 20, and 30 wt% and of each high molecular weight (HMW) polymer at 5, 10, and 20 wt%. Solutions of HMW polymers at 30 wt% were very viscous and difficult to dispense, particularly for the homopolymer. Three approximately 1 g aliquots of each polymer solution were placed into each of three 2 mL glass vials and heated to 37°C in a water bath. After 30 minutes, vials were photographed and then 1 mL of 37°C pre-warmed PBS was added to each sample. Solutions were maintained

in a 37°C room for the remainder of the study. Vials were photographed at various time points to assess gel swelling.

A diagram depicting the method used to calculate swelling is shown in Figure 4.2. Images of the vials were cropped to contain only the entire water volume in the vial. Images for each vial at each time point were converted to grayscale and then thresholded into either white (gel) or black (not gel) pixels both manually and using MATLAB (Version R2009b, The MathWorks, Inc.). Manual thresholding was done only to remove image artifacts such as light reflections. The initial gel height in pixels corrected for any differences in image size was calculated for each sample in MATLAB using the equation

$$h_t = w_t\left(\frac{h_i}{w_i}\right)$$

where w_t is the width in pixels of the image at time t, and h_i and w_i are the height and width, respectively, in pixels of the image of the same sample (gel plus any expelled water) at 30 minutes after gelation (before any additional buffer was placed on top of the gels). Gel volume was determined by assuming that horizontal cross sections of each gel were cylindrical. The number of white (gel) pixels in each row of an image was calculated, then each row's pixel count divided by 2 and squared. The sum of these values over all rows is a measure of volume, V. The initial gel volume for the same sample, V_0, was determined using the formula

$$V_0 = h_t\left(\frac{w_t}{2}\right)$$

Swelling was then reported as a fraction of the initial gel volume, i.e. V/V_0. Significant differences in swelling between gels at the same concentration and time point were determined by Student's *t*-test ($\alpha = 0.05$).

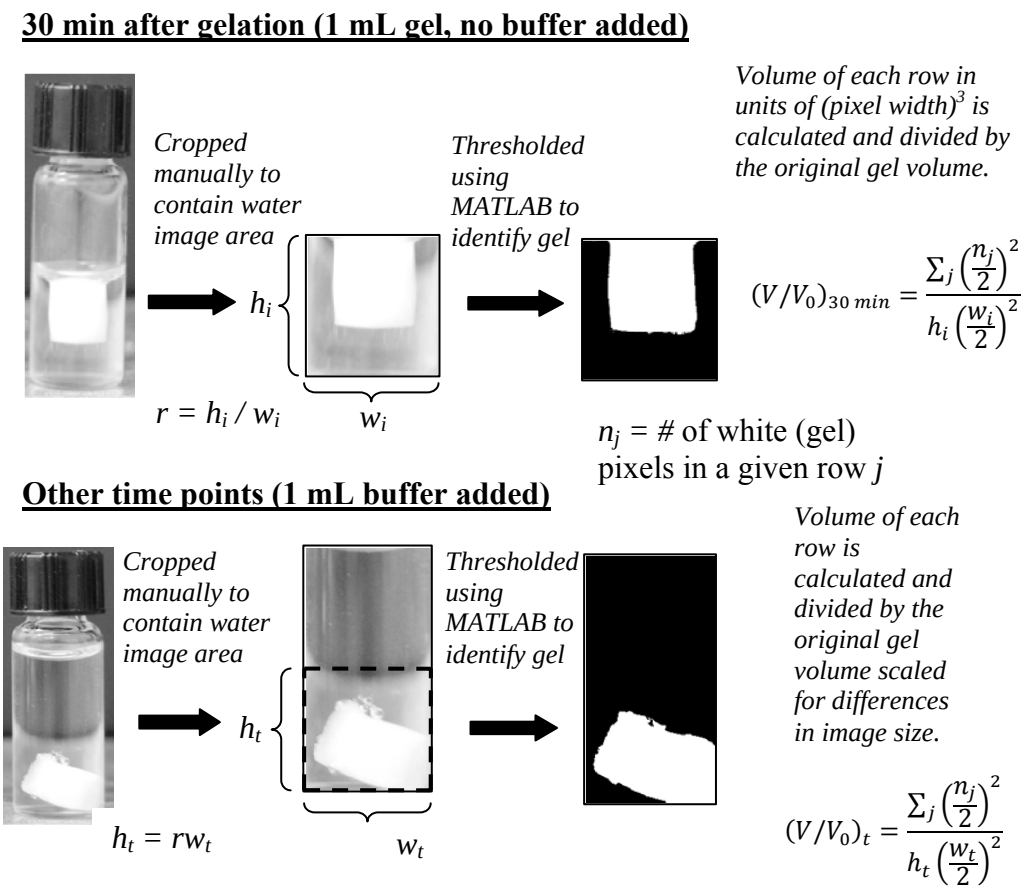

Figure 4.2. Method of swelling measurement. Images were cropped manually and thresholded into white (gel) or dark (no gel) pixels. Assuming cylindrical cross-sections, the gel volume was calculated and then divided by the initial volume of the same sample (i.e. the volume of the gel plus any excess water at $t = 30$ min).

4.2.6. Rheometry

Rheological properties of 20 wt% HMW poly(NIPAAm) and HMW poly(NIPAAm-*co*-JAAm) (70:30 feed ratio) hydrogels at equilibrium were measured. For copolymer gels, about 400 μL of polymer solution was placed on the stage of a rheometer (MCR-101, Anton Paar USA Inc.), and the flat 25 mm diameter plate set to a gap height of 0.5 mm. The rheometer stage was initially 20°C and then heated to 37°C for 60 seconds before measurements were taken. Because homopolymer gels shrank rapidly after gelation, the methods were altered to measure the properties of the gels at equilibrium. 1 mL of the homopolymer solution was first dispensed into the well of a 6-well tissue culture plate, heated to 37°C until completely opaque, and then incubated in excess PBS at 37°C for 24 hr to reach equilibrium. The gel was then quickly transferred to the pre-warmed rheometer stage and measurement started immediately. Gels were evaluated with normal force maintained during measurement at 100 +/- 50 mN and a humidity chamber placed over the sample to reduce evaporation. The linear viscoelastic region for each gel was determined by varying the oscillatory strain applied to the gels between 0.01% and 25% at 1 Hz frequency (not shown). The materials were then subjected to oscillatory strain within the linear viscoelastic region and the frequency varied from 0.1 to 100 Hz.. Storage modulus (G') and loss modulus (G") were determined at each frequency.

4.2.7. Ovalbumin Release Kinetics

Protein release kinetics from 20 wt% HMW poly(NIPAAm) and HMW poly(NIPAAm-*co*-JAAm) (70:30 feed ratio) hydrogels were measured at 37°C using ovalbumin (44.3 kDa) as a model drug. Ovalbumin (10 mg/mL) was dissolved in the polymer solutions at 4°C and then 1 g samples (n = 3) were weighed out of each common solution into 4 mL vials. Gels were formed by incubation in a 37°C water bath for 15 minutes. The 4 mL vials with gels were then inserted into pre-warmed 20 mL vials which were then filled to the top with 20 mL pre-warmed PBS and maintained in a 37°C room. This system was used because the copolymer gels were adhesive and difficult to handle above the LCST. Buffer was completely replaced for homopolymer samples after 1 day incubation in order to maintain infinite sink conditions. Aliquots were taken at various time points and frozen at -20°C. Protein concentration in the aliquots was measured at the end of the study using the BCA Protein Assay (Pierce Biotechnology) according to the manufacturer's instructions using a UV/Vis spectrophotometer (Fluostar Omega, BMG Labtech). An uncontrolled factor in this experiment was the surface area of the gels through which ovalbumin was able to diffuse out of the gel. To fairly compare the gels despite this lack of control, release rate normalized by gel surface area was reported in addition to cumulative release. The surface area of the homopolymer gels was assumed to be equal to the initial surface area of the gels (i.e. shrinking was not accounted for). Statistical analysis was performed on release rate data using repeated measures ANOVA with the factors being gel type and time ($\alpha = 0.05$).

4.3. Results

4.3.1. Composition and Molecular Weight

Successful synthesis of JAAm was confirmed by the appearance of two new peaks in ^{1}H NMR (not shown) at 6.1 ppm (2H) and 5.6 ppm (1H) from the protons adjacent to the double bond of the acrylamide group. The polymer feed ratios, composition, molecular weight, and LCST as measured by DSC are shown in Table 4.1. Polymer batches are abbreviated in terms of their molecular weight (H for high, L for low) and JAAm fraction in the feed (0, 15, or 30 wt%). When applicable, polymer concentration is written before the molecular weight (i.e. 20 H 30). LMW polymers each had a polydispersity near 2.0 and M_w between 28.8 and 37.2 kDa. HMW poly(NIPAAm) had a weight-average molecular weight (M_w) of 861 kDa, while the molecular weights of both HMW copolymers containing JAAm were considerably lower with M_w near 230 kDa, possibly due to lower reactivity for chain propagation steps involving JAAm or chain transfer caused by impurities. Polydispersities of HMW copolymers were slightly lower than those of LMW polymers, ranging from 1.67 to 1.90.

Table 4.1 Composition, molecular weight distribution, and LCST of poly(NIPAAm-*co*-JAAm) copolymers

	JAAm content (wt%)				
Polymer	**Feed Ratio**	**Composition**	**M_w (kDa)**	**Pd (M_w/M_n)**	**LCST (°C)**
H 0	0	0	861.0	1.90	27.83 ± 0.06
H 15	15	11.9	226.6	1.84	31.07 ± 0.06
H 30	30	22.4	229.1	1.67	33.87 ± 0.15
L 0	0	0	30.0	2.03	29.6 ± 0.06
L 15	15	12.1	28.8	2.02	32.4 ± 0.06
L 30	30	24.2	37.2	2.02	35.4 ± 0.06

Successful synthesis of poly(NIPAAm-*co*-JAAm) copolymers was confirmed by ^{1}H NMR, as shown in Figure 4.3. JAAm content in the copolymers was calculated from the integration ratios of the peak at 3.5 ppm ascribed to the oxyethylene protons of the EO units (CH_2CH_2O) of JAAm relative to the peak at 3.7 ppm (1H) of the lone isopropyl proton of NIPAAm ($CH(CH_3)_2$). JAAm weight fraction was calculated by assuming a 19:3:1 ratio of EO: PO: acrylamide units per macromer. JAAm content in the copolymers is reported as wt% in this work because weight fraction is thought to determine equilibrium swelling rather than the molar fraction.[235] All copolymers exhibited lower incorporation of JAAm relative to the feed ratio, likely due to low reactivity of JAAm caused by steric hindrance. Batch-to-batch variability was low; in each copolymer, JAAm content was 74-81% of that in the feed ratio.

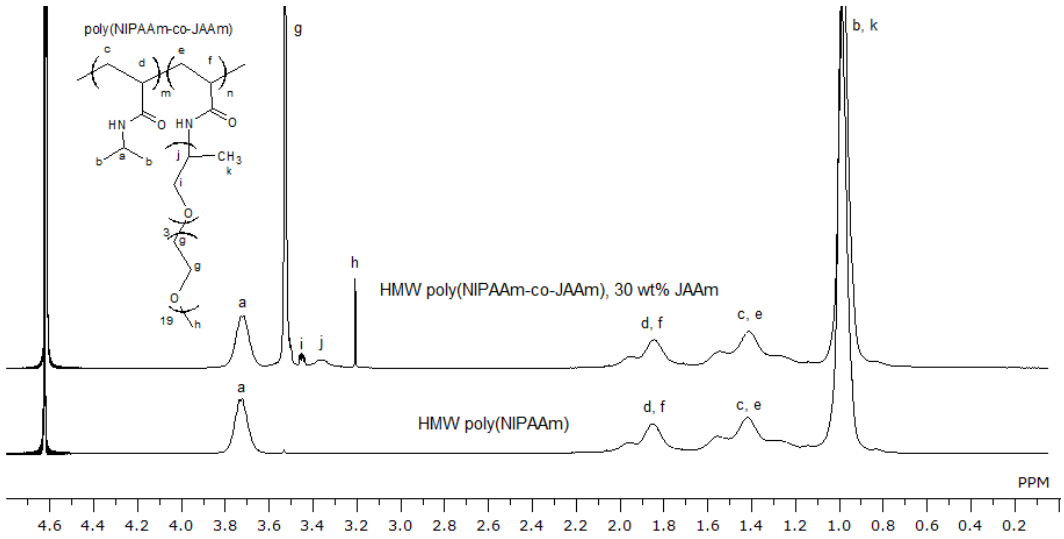

Figure 4.3. ^{1}H NMR spectra of high molecular weight poly(NIPAAm) and poly(NIPAAm-*co*-JAAm) in D_2O.

4.3.2. LCST Transition

The LCST transition of each polymer at 5 wt% in PBS was characterized by DSC as shown in Figure 4.4. For both HMW and LMW copolymers, increasing JAAm content in the polymer caused an increase in the material LCST, which is consistent with previously reported data for copolymers of NIPAAm with PEG (meth)acrylates.[130,257,235] The onset of the transition for each molecular weight range is about 5°C higher for H 30 and L 30 compared to the respective homopolymers. Increasing JAAm content also leads to broadening of the LCST endotherm.

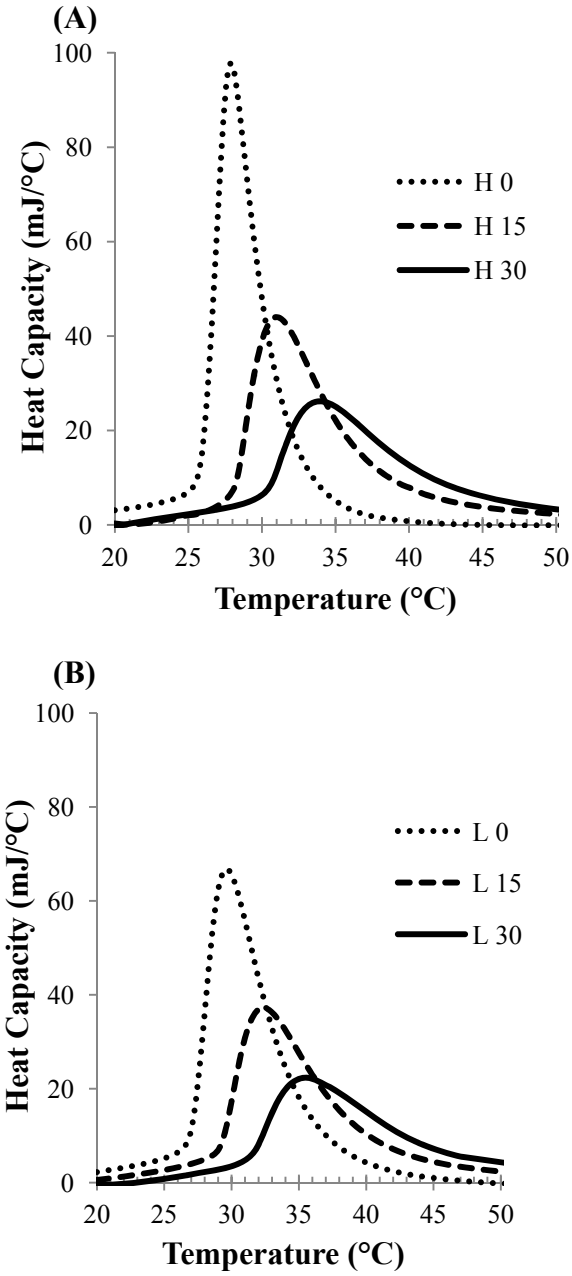

Figure 4.4. Representative differential scanning calorimetry thermograms for 5 wt% solutions of (A) HMW and (B) LMW copolymers of poly(NIPAAm-*co*-JAAm) in 150 mM PBS.

Cloud point determination was done to evaluate the broadness and average temperature of the sol-gel transition of the synthesized copolymers and is shown

in Figure 4.5. Incorporation of JAAm caused an increase in the cloud point and a broadening of the material LCST. Both homopolymers, H 0 and L 0, exhibited a sharp transition near 27°C and 29°C, respectively. H 15 and L 15 surpassed half-maximum absorbance at 30°C and 32°C, and H 30 and L 30 did the same at 33°C and 35°C. Linear regression gives the following correlation coefficients for LCST vs. JAAm wt%: LMW by DSC: 0.240°C/wt%; HMW by DSC: 0.270°C/wt%; LMW by cloud point: 0.248°C/wt%; HMW by cloud point: 0.268°C/wt% (all R^2 > 0.998). Though LCST can vary depending on the measurement technique, these results indicate that LCST is approximately 40 times less sensitive to JAAm than AAc[105] on a wt% basis.

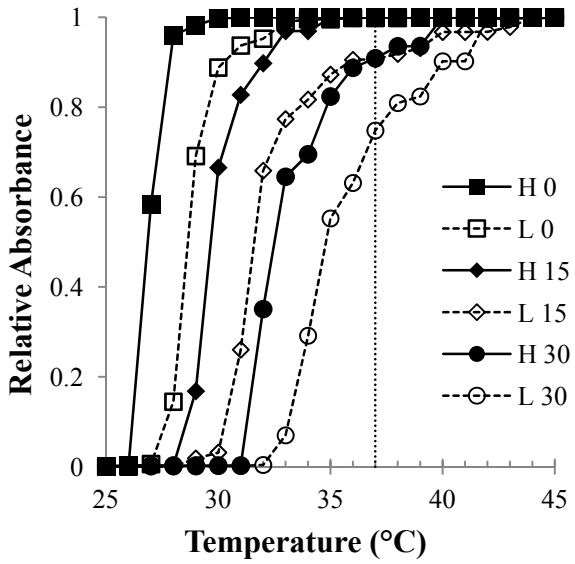

Figure 4.5. Relative absorbance (λ = 450 nm) of 0.1 wt% solutions of synthesized copolymers in 150 mM PBS, pH 7.4. The dotted vertical line denotes body temperature.

4.3.3. Gelation and Swelling

Gelation and swelling of synthesized copolymer solutions at various concentrations was observed at 37°C. Figure 4.6A shows the gelation and swelling behavior of those HMW polymer solutions which formed opaque gels after 5 days. Polymer solutions not shown in the legend of Figure 4.6 (5 H 30, 10 H 30) separated into a translucent phase and settled on the bottom of the vials within 2 hr upon heating to 37°C. The difference in gel formation between H 15 and H 30 demonstrates that the critical polymer concentration required to form a gel increases with JAAm content at a given molecular weight. Greater polymer concentration is necessary to form copolymer gels because the EO-rich Jeffamine grafts play a role in hindering the chain entanglement required to form a physical gel.[284] This is in agreement with other studies on physical gels of NIPAAm-based copolymers in the presence of hydrophilic molecules which show weak and viscous properties rather than elastic behavior when covalently bound to hydrophilic macromolecules.[134,177]

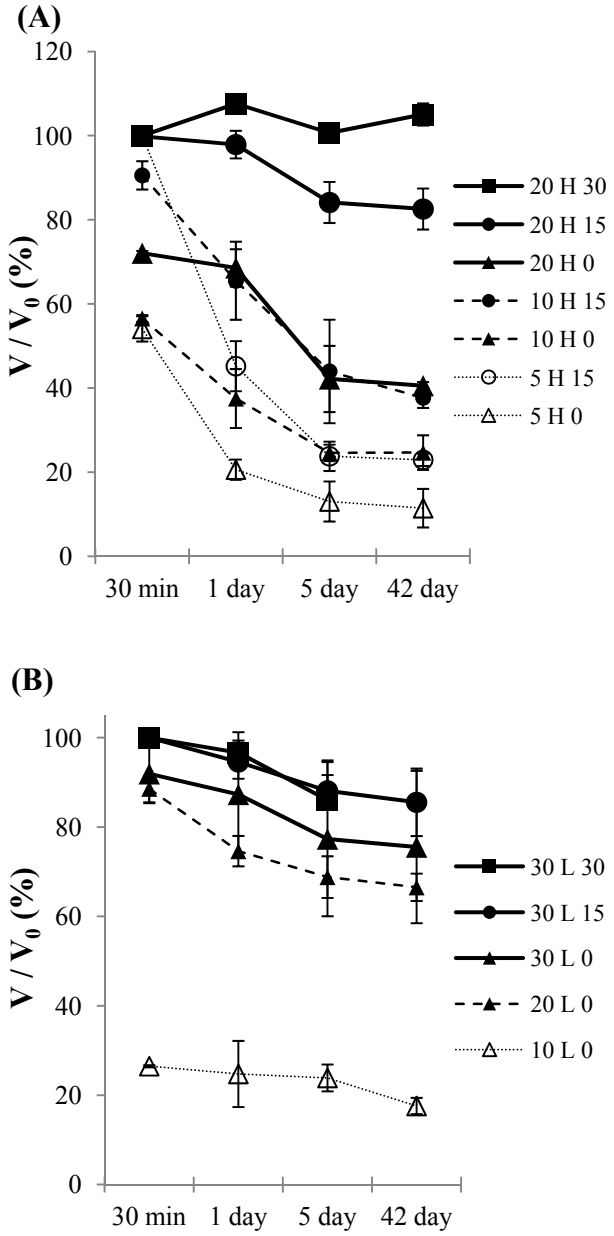

Figure 4.6. Percentage of initial gel volume at various times after gelation for (A) HMW and (B) LMW copolymers of poly(NIPAAm-*co*-JAAm). Shape indicates polymer composition by feed ratio (square: 30% JAAm; circle: 15% JAAm; triangle: 0% JAAm). Symbols indicate polymer concentration (from highest to lowest concentration: large solid symbol > small solid symbol > small open symbol). Data are reported as mean ± s.d. (n = 3).

Statistically significant differences in swelling ratio due to JAAm inclusion after 42 days were observed at 5 wt% between 5 H 0 and 5 H 15 (p = 0.014), at 10 wt% between 10 H 0 and 10 H 15 (p = 0.009), and at 20 wt% between each pair of sample groups (20 H 0 vs. 20 H 15, 20 H 15 vs. 20 H 30, and 20 H 0 vs. 20 H 30) (all $p < 0.005$). While 20 H 30 was the only solution with 30% JAAm in the feed that yielded gels at 37°C, those gels exhibited excellent resistance to shrinking and stability under physiological conditions, maintaining 105 ± 3% of their initial volume after 42 days. Accordingly, 20 H 15 gels underwent minimal syneresis (83 ± 5%), and 20 H 0 homopolymer gels collapsed to a much greater extent, decreasing to 41 ± 1% of their initial volume. Representative gels of 20 H 0 and 20 H 30 are shown at various times after gelation in Figure 4.7.

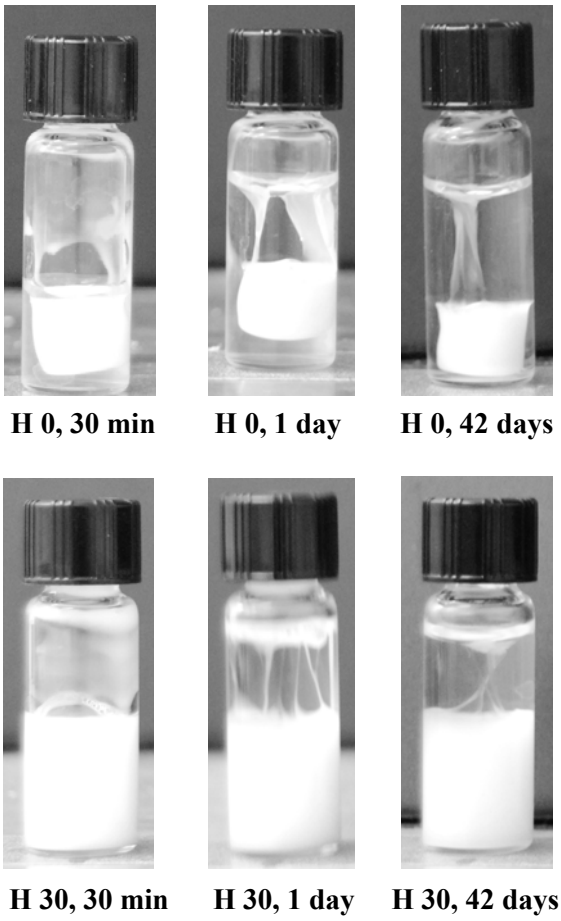

Figure 4.7. Gel swelling of 20 wt% H 0 (top row) and H 30 (bottom row) at various times after gelation at 37°C.

Copolymers with low molecular weight in general had much poorer gelation characteristics, as shown in Figure 4.6B. Polymer solutions not shown in the legend of Figure 4.6B separated into a small translucent or opaque phase and settled on the bottom of the vials within 2 hr upon heating to 37°C. Homopolymer solutions at 10 wt% and greater formed gels at 37°C, while polymers containing JAAm only formed gels at 30 wt%. At 42 days, 30 L 30 became translucent and

flowed when inverted, so it was not considered a gel at that time, perhaps due to sensitivity to small temperature fluctuations (as low as 35°C) during incubation.

4.3.4. Rheometry

Frequency-dependent storage and loss moduli of 20 H 0 and 20 H 30 under oscillatory strain at 37°C are shown in Figure 4.8. Each gel exhibits increased resistance to deformation at higher frequencies which is characteristic of physical gels.[275] In the frequency range 0.1-10 Hz, both gels have a phase angle near 45° (i.e. G'=G"), characteristic of a viscoelastic material. Homopolymer gels have both storage and loss moduli in the 5-50 kPa range, while the moduli for copolymer gels are lower, in the 10-100 Pa range.

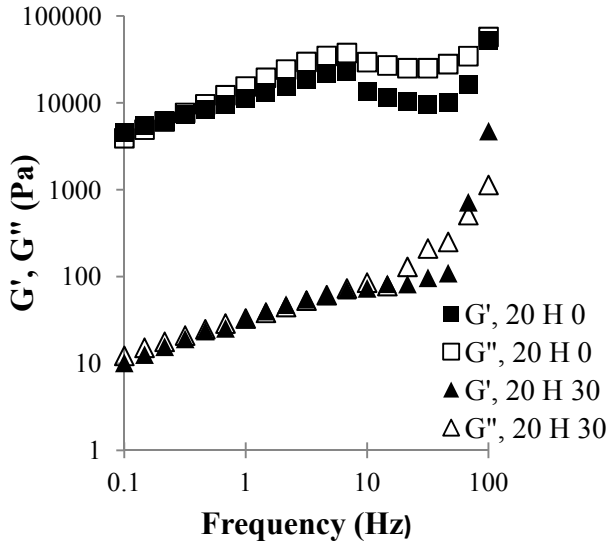

Figure 4.8. Storage (G') and loss (G") moduli of 20 H 0 and 20 H 30 at equilibrium subjected to oscillatory frequency sweeps with active normal force control at 37°C.

4.3.5. Ovalbumin Release Kinetics

Release kinetics of ovalbumin from 20 H 0 and 20 H 30 gels at 37°C is shown in Figure 4.9. Gel type and time were both significant factors ($p < 0.001$) with respect to release rate per surface area. Homopolymer gels provided fast release. During the first 15 minutes after gelation, gels decreased in volume by only about 20%, yet over 50% of the loaded ovalbumin was released in the same time. Over 90% of the loaded ovalbumin was released within 3 hours. The release rate from homopolymer gels decreased to near zero after 2 days. Release from the 20 H 30 gels was much slower. Only 8% release was observed within one day after gelation, and an additional 7% was released over the following 5 days.

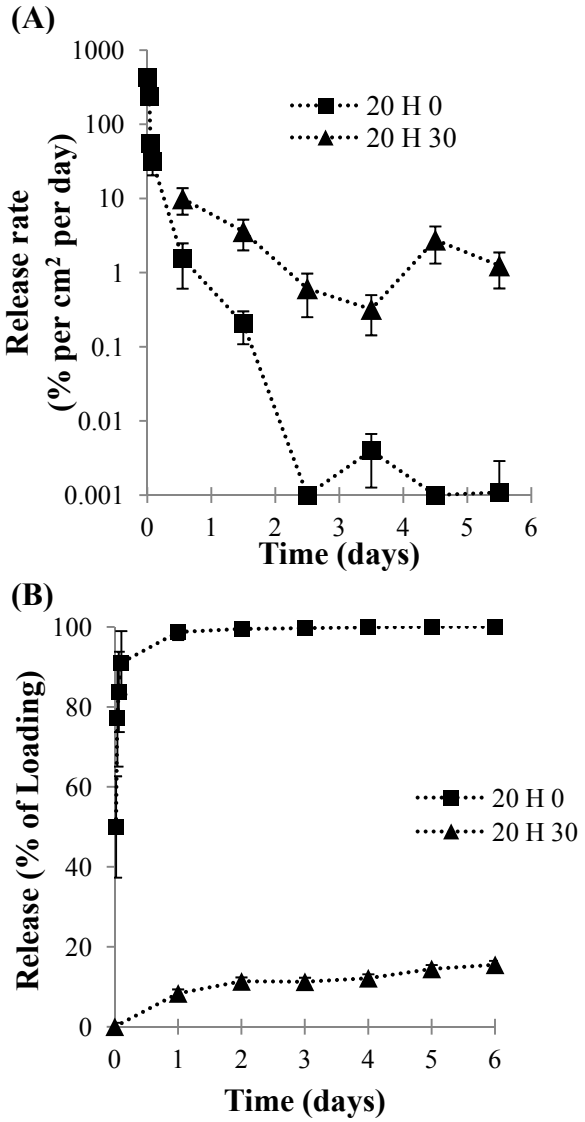

Figure 4.9. (A) Ovalbumin release rate in percent of loading per cm^2 per day and (B) Cumulative fraction released from 20 H 0 and 20 H 30 hydrogels at 37°C in 150 mM PBS, pH 7.4. Error bars represent one standard deviation (n = 3). Some error bars are smaller than the data points.

4.4. Discussion

4.4.1. Effect of JAAm on LCST Transition

JAAm incorporation and low molecular weight both contributed to increased broadness of the LCST transition, especially above 0.5 relative absorbance. For example, the absorbance of a solution of H 0 completes over 90% of its transition within a range of 2°C, while L 30 must be heated over a range of 10°C to do the same. L 15, H 30, and L 30 copolymers were all not completely transitioned at body temperature. The increase in broadness of the polymer LCST shown in both DSC and cloud point characterization can be attributed to the heterogeneity within a single batch of material produced by free radical copolymerization. It has previously been shown that both lower molecular weight[100,285] and higher content[98,105] of hydrophilic comonomers lead to higher polymer LCST, and that heterogeneity in both molecular weight and comonomer content are responsible for the broadness of the LCST transition within a single batch of material prepared by radical polymerization.[284] In this case, molecules with less JAAm and higher molecular weight will transition at lower temperatures, while those with more JAAm and lower molecular weight will transition at higher temperatures.

4.4.2. Gel Deswelling

Gel deswelling is a thermodynamically driven process. When a solution of a NIPAAm-based polymer is heated above its LCST, a homogeneous gel forms

that phase-separates into a polymer-rich gel phase and a phase consisting of almost pure solvent.[141] This polymer-rich phase then tends toward an equilibrium volume.[286,287] In cases where HMW polymer solutions formed stable gels, those with greater JAAm incorporation underwent less and slower syneresis on average. Homopolymer gels with low equilibrium swelling ratios began to separate from a substantial fraction of PBS within 30 minutes of heating above the LCST, while gels with JAAm and similarly low equilibrium swelling retained more water for hours after gelation. Afterward, the gels tended toward equilibrium over another 2-5 days in a slower rearrangement process, during which local contacts between polymer molecules become increasingly favorable.[141]

4.4.3. Lack of Gelation of Some Poly(NIPAAm-*co*-JAAm) Gels

The lack of gelation observed in copolymers containing JAAm may be attributed to the observations that 1) the transition temperatures of L 15 and L 30 are both higher and more broadly distributed than HMW polymers with similar composition, and so fewer chains are insoluble at 37°C; and 2) LMW polymers require greater concentrations to form gels compared to HMW polymers. Additionally, JAAm may contribute to reduced polymer-polymer interactions or chain entanglement, as seen in previous studies with high collagen content limiting the gelation of NIPAAm-based polymers above the LCST.[134] Equilibrium (42 day) swelling of LMW homopolymer gels increased with polymer concentration, with 30 L 0 having V/V_0 of 76 ± 17%. While 30 L 30 and 30 L 15 gels retained a greater volume on average than 30 L 0 for the first 3 days, V/V_0

between any pair of these gels was not significantly different at any time point. There is an inverse relationship between the fraction of JAAm required to adequately control shrinking and the polymer concentration required to form a stable gel. An explanation for the lack of swelling difference observed in this molecular weight range (M_w 28-38 kDa) is that the minimum concentration required to form copolymer gels was so high that even homopolymer did not shrink much. However, JAAm may still provide controlled shrinking and drug delivery properties to more hydrophobic polymers in this molecular weight range. In particular, our group and others have previously developed resorbable materials with initial LCST below 25°C in the 10-80 kDa molecular weight range which undergo substantial shrinking even at high concentrations.[123,124]

4.4.4. Rheological Properties and Implications for Biomaterials Applications

The lower strength of gels with JAAm can be attributed to their lower molecular weight, higher water content, and incomplete LCST transition at 37°C. The latter could be addressed by fractionation in aqueous medium, incorporating a hydrophobic comonomer, or modifying the composition of the JAAm comonomer to reduce its effect on increasing the LCST--for example, using an alkyl substitution.[103]

In terms of their potential for use as biomaterials, copolymers with JAAm (though weak) maintain consistent properties after gelation and lower modulus whereas homopolymer gels have highly dynamic properties but higher modulus. As both materials are hydrogels, neither is suitable for hard tissue or load-bearing

applications—the shear modulus of bone tissue exceeds 1 GPa.[288] The weak and viscoelastic character of the copolymer gels renders them unsuitable for any application in which the material needs to retain its shape in the presence of nearly any amount of loading. Without further modification, these physical gels are likely only useful for drug delivery to non-load bearing sites or perhaps for cell encapsulation or drug delivery in soft tissues.[130,289] However, these materials could be made stiffer (and more elastic) to allow for other applications by crosslinking—in particular, an *in situ* crosslinking and swelling-controlled material based on these materials might be useful for space-filling applications such as embolization[83,142,275] or contraception[237,290] while remaining injectable. Because the material is so weak and viscous above the LCST in the absence of crosslinking, it could potentially be injected via a catheter and then crosslink *in situ* to become stronger and more elastic. Crosslinking *in situ* of 2 mol% of monomers in a NIPAAm-based polymer gel has been shown to increase the storage modulus by over three orders of magnitude at 1 Hz frequency.[275] On the other hand, homopolymer gels are strong enough to withstand greater stresses and retain their shape, yet their deswelling precludes them from being useful in space-filling applications despite their potentially sufficient modulus. Additionally, purely physical gels tend to have phase angles well above zero and are therefore subject to creep in response to a low-pressure constant stress such as blood flow.[275]

4.4.5. Ovalbumin Release Study Limitations

Both gel type and time were significant factors affecting release. However, due to lack of control over exposed gel surface area in the release experiment, the release data from gels with and without JAAm are not directly comparable due to differences in gel surface area during the release study. When normalized to account for the difference in gel surface area, the release rate from 20 H 30 gels remained in the range 0.32-3.5% of loading per cm^2 per day throughout the experiment, whereas the release rate from homopolymer gels was initially very high and fell to near zero after 2 days as the drug payload was exhausted. The influence of geometric differences is still not completely removed from the release rate data because the surface area to volume ratio (and hence the mean diffusion distance required for release) is different between polymers, which is a shortcoming of the study. Yet the vast difference in release rates cannot be sufficiently explained by this difference in geometry alone, as the release is prolonged by more than an order of magnitude in copolymer gels. Thus the more steady release rate per surface area observed from 20 H 30 gels indicates that the diffusivity of ovalbumin is greatly reduced in copolymer gels relative to homopolymer gels.

4.4.6. Effect of JAAm on Protein Release

The lack of high initial burst release from 20 H 30 gels can be attributed to resistance to syneresis. Upon heating above the LCST, the polymer solution phase-separates into two phases—a homogeneous polymer-rich gel phase—

consisting of nearly all of the polymer plus some fraction of water—and a nearly pure solvent phase.[114,141] For 20 H 30 gels, the equilibrium water content of the gel being near the initial content led to a phase transition with minimal phase separation—therefore it can be assumed the protein is retained almost entirely within the polymer-rich gel phase. As the rate of release from non-crosslinked physical gels is known to be inversely related to their viscosity,[125,132] it follows that the high viscosity of the 20 H 30 gel phase combined with little to no phase separation is the primary cause of the slow and sustained release of ovalbumin observed. Similarly low burst release and sustained release of dextran has been reported in temperature-responsive block copolymer physical gels which are also rich in PEO.[155] Conversely, the phase transition of homopolymer gels leads to a high degree of phase separation following gelation, resulting in a hydrophobic polymer-rich gel phase and excess water. A possible explanation for the rapid albumin release is that, after phase separation, the albumin preferentially dissolved (partitioned) into the excess water phase based on its hydrophilicity and therefore rapidly diffused from the homopolymer gels. The vast difference in protein release kinetics from the two polymers used in this study demonstrates the potential utility of NIPAAm-based graft copolymer hydrogels for controlled drug delivery applications.

4.5. Conclusions

Water-stable temperature responsive copolymers poly(NIPAAm-*co*-JAAm) were successfully synthesized. Incorporation of JAAm was slightly lower

than feed ratio. JAAm caused a small increase in polymer LCST of 0.24-0.27°C/wt% and increased broadness of the sol-gel transition. The gelation of poly(NIPAAm-*co*-JAAm) solutions in physiological saline depends on JAAm incorporation, polymer molecular weight, and polymer concentration. Significant differences in swelling behavior were observed between poly(NIPAAm) and poly(NIPAAm-*co*-JAAm) at high molecular weights (M_w > 225 kDa). Some copolymer gels underwent a sol-gel transition with almost no change in volume. Gelation of poly(NIPAAm-*co*-JAAm) solutions was generally poor at low molecular weight (M_w ~ 30 kDa) due to the high critical gelation concentration and incomplete precipitation of the polymer under physiological conditions. Physical gels of poly(NIPAAm-*co*-JAAm) are viscoelastic and have shear moduli approximately 500-fold lower than comparable homopolymer gels. Ovalbumin release from high molecular weight gels was slowed from a duration of minutes to a duration of over 6 days via incorporation of JAAm. The hydrolytic stability, hydrophilicity, and minimal LCST effect of JAAm make it suitable for inclusion in a variety of temperature-responsive biomaterials where control over swelling or drug release is required.

Chapter 5: TEMPERATURE-RESPONSIVE RESORBABLE HYDROGELS FOR PREVENTION OF PROSTHETIC JOINT INFECTION

5.1. Introduction

Currently, injectable microsphere suspensions based on poly(lactic-*co*-glycolic acid) (PLGA) provide one of the main clinically available degradable drug delivery vehicles.[291,292] *In situ* forming hydrogels share this system's advantages of injectability and potential for controlled release, but can undergo degradation much more uniformly with reduced generation of charges.[122,124,293] Hydrogels also provide viscoelastic properties that cannot be replicated with particulate systems, which may enable their use in additional applications in areas under cyclic mechanical loads, since wear debris from harder materials in joint spaces can lead to local toxicity.[294,295] Because hydrogels contain a higher fraction of water compared to hard non-hydrogel materials (e.g., PLGA, hydroxyapatite), they offer potential for faster hydrolytic degradation. The slow degradation of hard materials may also be a drawback when administration of a second dose is desired, or in orthopaedic applications, as bone healing occurs within 6-8 weeks.[44,296] Using soft *in situ* forming hydrogels with tunable degradation may therefore enable drug delivery in many applications which are not amenable to sustained release carriers in currently approved products.

Temperature-responsive hydrogels based on *N*-isopropylacrylamide (NIPAAm) are particularly well-suited to drug delivery applications due to rapid physical crosslinking which takes place in physiological conditions without

chemical reaction. Poly(NIPAAm) has a sharp lower critical solution temperature (LCST) in aqueous media near 30°C.[97,285,297] As a sufficiently concentrated solution of poly(NIPAAm) is heated above the LCST, a hydrogel is formed. Various properties such as LCST, pH-sensitivity, or gel swelling can be controlled by incorporating small molar fractions (<10%) of comonomers with NIPAAm.[98,111,103] For example, hydrophobic comonomers decrease the LCST while hydrophilic comonomers increase the LCST.[98] Accordingly, copolymers of NIPAAm can be made to be degradable by incorporating comonomers with side chains which become more hydrophilic upon degradation either by water[122,124,135,136,293] or specific enzymes,[137] causing an increase in LCST. When the LCST increases to above body temperature, the polymer re-dissolves.

Effective controlled drug delivery from NIPAAm-based hydrogels is limited primarily by high burst release following gelation. As a poly(NIPAAm)-based gel forms as a result of physical crosslinking, a homogeneous polymer-rich phase (i.e., the gel) separates from a fraction of the original solvent and then tends toward an equilibrium composition.[141,297] Macroscopically, this is observed as shrinking and expulsion of solvent. While the polymer solutions tend to be formulated at 30 wt% or less for ease of handling, the final polymer concentration in the gel is about 50 wt%.[115,118,105,142] Upon phase separation, hydrophilic drugs are prone to distribute predominantly into the solvent phase rather than the gel phase. As a result of shrinkage and drug distribution into the expelled solvent, most of the payload of both low molecular weight hydrophilic drugs[116] or proteins[143,298] is typically released quickly and completely upon the phase

transition of crosslinked NIPAAm-based gels. Poly(NIPAAm) gels without chemical crosslinking show even more burst release, with >90% protein release occurring in under 1 hr.[144]

Several methods have been reported for slowing or controlling drug release from temperature-responsive materials. Crosslinked NIPAAm copolymer gels have been demonstrated for on-off release, with the on (drug-releasing) state being either below[117,143,299] or above[116] the gel transition temperature. Prolonged protein release on the order of weeks has been reported from some crosslinked gels as well[300]—however, crosslinked gels must be loaded with drug by soaking in a drug solution, and none of these studies report resorbable materials. Recently, alternative strategies relying on electrostatic interaction between the polymer and drug,[147] covalent conjugation of the drug by a labile linkage,[293] and co-delivery of embedded drug-loaded microspheres[293] have been demonstrated for prolonged protein release from temperature-responsive resorbable hydrogels.

This chapter describes the development of a resorbable NIPAAm-based polymer system which is capable of providing controlled release on its own, without requiring covalent crosslinking, intermolecular interactions, covalent conjugation of drug, or separately prepared embedded particles. Such a system would be simple to reliably manufacture and use and would have potential for a variety of local or sustained drug delivery applications. In Chapter 4, it was demonstrated that incorporating hydrophilic grafts of Jeffamine® M-1000 on a poly(NIPAAm) backbone yields physical gels which exhibit controlled swelling and slow protein release.[144] Here, the hypothesis was that using Jeffamine® M-

1000 grafts in a resorbable copolymer gel would reduce burst release upon gelation and, instead, cause any entrapped drugs to be subsequently released by diffusion or hydrogel degradation. These copolymers were synthesized and characterized to evaluate the effect of graft content on hydrogel properties and the feasibility of using these gels for delivery of low molecular weight drugs was evaluated.

One application for this these materials is especially well suited is for controlled release in a joint space. In particular, antibiotic delivery following total joint replacement could be used to prevent infections from arising by delivering antimicrobials directly at the surface of a joint prosthesis. There is no current opportunity for local antimicrobial delivery over the entire surface of a cementless prosthetic hip or over the majority of the surface of a prosthetic knee. Thus the feasibility of using soft, cohesive materials developed in this work was evaluated, and antimicrobial release kinetics were compared to that of antimicrobial-loaded bone cement.

5.2. Materials and Methods

5.2.1. Materials

All materials were reagent grade and obtained from Sigma-Aldrich unless otherwise noted. NIPAAm was recrystallized from hexane. Azobisisobutyronitrile (AIBN) was recrystallized from methanol. HPLC grade tetrahydrofuran (THF) was used for polymerizations and as the mobile phase for molecular weight

determination. Jeffamine® M-1000 was donated by Huntsman Corporation (The Woodlands, TX, USA).

5.2.2. Synthesis

JAAm was described as reported in Section 4.2.2 with the exception that the organic phase from the extraction was purified by column chromatography. After evaporation of DCM, JAAm was obtained as a viscous clear to light yellow liquid. JAAm was solidified by cooling on ice, vacuum dried overnight, then collected and stored at -20°C until use.

Copolymers of NIPAAm, (*R*)-α-Acryloyloxy-β,β-dimethyl-γ-butyrolactone (DBLA), and JAAm were synthesized by radical polymerization with 80% dioxane / 20% THF as the solvent. This solvent blend was chosen to obtain a weight-average molecular weight near 40 kDa. The molar amount of DBLA relative to NIPAAm was held fixed at 92.8:7.2, as this was shown in previous work to provide a material with an LCST after degradation that exceeds 37°C.[122] JAAm was fed into the reaction as 0, 15, or 30% of the mass relative to NIPAAm. Monomer solution (10 w/v%) was bubbled with nitrogen for at least 20 minutes prior to addition of initiator. After this time, AIBN was added (0.007 mol AIBN/mol of total monomer) and the reaction allowed to proceed for 18 hr at 65°C under nitrogen. Copolymers were collected by precipitation into 10- to 15-fold excess of chilled diethyl ether. Following precipitation, the product, poly(NIPAAm-*co*-DBLA-*co*-JAAm) (abbreviated pNDJ) was collected by filtration and dried overnight under vacuum. The product was then dissolved in

deionized water and dialyzed against 3500 MWCO at 4°C for 20 hours with the excess water replaced 3 times. Materials were then lyophilized and stored under nitrogen at -20°C until use.

5.2.3. Composition and Molecular Weight

^{1}H NMR (Varian Inova, 300 MHz) was used to confirm successful synthesis and determine the chemical composition of the synthesized polymers. $CDCl_3$ was used as the NMR solvent.

The molecular weight and polydispersity of the synthesized polymers was determined by gel permeation chromatography (Shimadzu Corporation) in conjunction with static light scattering (MiniDawn, Wyatt Technology Corporation) with THF as the mobile phase.

5.2.4. LCST Measurement and Degradation Kinetics

Synthesized copolymers were dissolved at 0.25 wt% in 150 mM PBS (pH 7.4) and analyzed for LCST properties by cloud point determination. None of the polymer solutions saturated the detector when heated above the LCST. Cuvettes containing the polymer solutions were allowed to reach the desired temperature in a water bath for at least 90 s prior to each measurement. Absorbance at 450 nm was measured every 1°C by a UV/Vis spectrometer throughout the range of the LCST transition with buffer alone as the reference. Some polymer solutions reached a temperature at which the absorbance began to decrease due to precipitation and settling out of polymer particles from the solution. In this case,

the last value of absorbance before observed aggregation was recorded as the maximum value and all previous values were normalized relative to this maximum value. Absorbance values for polymers that did not show a decrease in absorbance with heating were normalized to the absorbance at 55°C.

Solutions of pNDJ15 and pNDJ30 were dissolved at 5 wt% in 150 mM PBS (pH 7.4) and several samples of each were incubated separately at 37°C. After various time points, single samples of polymer solution were removed and frozen at -20°C to stop degradation. The study was stopped for each material after the polymer solution was completely transparent at 37°C. After the end of the study, all of the frozen samples were thawed, diluted to 0.25 wt%, and measured for LCST by cloud point determination as described above. LCST is reported as the temperature at which the absorbance was at least half of the maximum observed. The degradation kinetics of pND have been reported previously.[122]

5.2.5. Rheological and Handling Properties

For each run, about 400 μL of polymer solution was placed between the flat 25 mm plates of a rheometer (Anton Paar MCR-101), with a gap height of 0.5 mm. For frequency sweeps, polymer solutions were placed on the rheometer at 20°C and then heated to 37°C for 60 seconds before measurements were taken. Because pND gels underwent significant shrinking throughout the first 15 minutes after gelation, pND gels of similar size to the other gel samples were quickly placed on the rheometer stage after being incubated in excess PBS at 37°C for 24 hr to allow the gels to reach equilibrium. Gels were evaluated at 37°C with

normal force maintained throughout the measurement at 100 ± 50 mN and a humidity chamber placed over the samples to reduce evaporation. The gels were then subjected to 1% oscillatory strain and the frequency varied from 0.1 to 10 Hz. For temperature sweeps, 400 μL of polymer solution was placed on the rheometer stage maintained at 10°C. The gels were evaluated under 1% oscillatory strain at 1 Hz frequency as the rheometer stage was heated to a final temperature of 50°C at a rate of 2°C/min with a humidity chamber used as above. Frequency sweeps of pNDJ30 were also done at 20, 25, 30, and 35 wt% with and without 50 mg/mL of added vancomycin both at 20°C and 37°C. The complex viscosity, which was nearly constant as a function of frequency was taken at 1 Hz and the phase angle reported for each sample at each temperature.

5.2.6. Distribution in Cadaveric Human Femur

In situ distribution of a radio-opaque mock polymer solution in cadaveric femur was evaluated by fluoroscopy. Because the poly(NIPAAm-*co*-DBLA-*co*-JAAm) solutions behave as viscoelastic fluids above the LCST, a viscoelastic fluid mock was made using Conray™ 60 (60 w/v% iothalamate meglumine, Covidien Pharmaceuticals, Hazelwood, MO) as the solvent and 600 kDa PEO as the solute. It was determined by rheometry that 13 wt% and 4 wt% solutions of 600 kDa PEO in Conray™ exhibited similar viscoelastic properties (complex viscosity and phase angle vs. frequency) to a 30 wt% solution of pNDJ30a containing 50 mg/mL vancomycin HCl at 37°C and 20°C, respectively (see

Figure 5.1). This substitution was made because pNDJ is not soluble at 30 wt% in Conray™. It also facilitated conducting the experiment at room temperature.

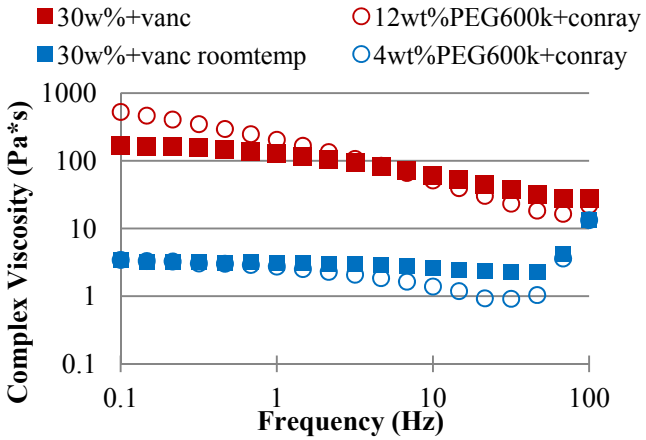

Figure 5.1. Matching of rheological properties between pNDJ30a above (red squares) and below (blue squares) the LCST using radio-opaque solutions of PEG (600 kDa) in Conray™ 60.

Cadaveric human femur was prepared by making a guided cut through the base of the femoral neck, getting rid of the femoral head and allowing access to shaft's marrow cavity. Femurs were then cut to be 2 inches longer than the implant. The marrow was then evacuated and the distal end of the femur was fitted with a PMMA plug in the base approximately 1 inch thick. The femur construct was then reamed and broached appropriately to accommodate implant size. The broach was removed and radio-opaque polymer solution was added to the intramedullary canal, followed by re-insertion of the broach to the proper depth. Images were acquired at a variety of angles at each of three stages: 1) bone without broach inserted; 2) bone with broach inserted; and 3) bone with broach

inserted containing polymer. No polymer solution was lost during the second implantation of the broach except out of the proximal cavity in the medullary canal.

5.2.7. *In Vitro* Antimicrobial Release

Release of cefazolin (454.5 g/mol) and vancomycin (1449.3 g/mol) from copolymer gels was evaluated at 37°C. The model antimicrobials were chosen because they are frequently used in surgeon-mixed high dose cement to manage infection and have different solubility at neutral pH. The solubility of a drug can substantially affect its release kinetics.[156]. Cefazolin is a readily accessible cephalosporin which inhibits the synthesis of bacterial cell wall peptides and is efficacious against gram-positive bacteria.[301] Vancomycin is a glycopeptide antimicrobial that inhibits bacterial cell wall synthesis, and is a typical second-line treatment against methicillin resistant staphylococcus aureus (MRSA).[302,303] Cefazolin exhibits considerable water solubility, similar to the aminoglycosides (gentamicin and tobramycin) commonly used in orthopaedic infection management and prophylaxis.[34,304,305] Vancomycin is less soluble at neutral pH, and is used in clinical preparations as the hydrochloride salt.

Polymer solutions were prepared at 30 wt% and allowed to dissolve overnight at 4°C. Gel samples were prepared by measuring one gram of polymer solution into a 20 mL glass vial (inner diameter ~ 25 mm, resulting in gel thickness of approx. 2 mm), and then the desired amount of drug (either 5 or 50 mg) was added to the solution and vortex mixed to dissolve or suspend the drug.

The mass of drug (+/- 0.1 mg) loaded into each sample was recorded due to some error in adding 5.0 mg of drug to each low-dose sample. Only the low dose cefazolin-loaded polymer solutions were transparent after mixing; the high dose samples contained evenly distributed but insoluble drug. Gels were formed by incubation in a 37°C water bath for 15 minutes. After 15 minutes, vials were filled to the top with 20 mL pre-warmed PBS and maintained at 37°C. pND hydrogels evaluated for release used only polymer batch pNDb, while the batches of pNDJ15 and pNDJ30 were used interchangeably for various studies.

For cement samples, a quarter batch (10 g powder) of Simplex bone cement (Stryker, Kalamazoo, MI) was prepared and finely ground antimicrobial powder. High dose samples had 2.5 g of antimicrobial powder added, equivalent to a clinical load of 10 g per batch. This loading is similar to those used by infection surgeons to control active infection, but is weaker than allowed for fixation (ISO 5833, 70 MPa required after 24 hours). Low dose samples had 0.25 g of antimicrobial powder added, equivalent to a clinical load of 1 g per batch. This is similar to cement formulations approved for fixation. Antimicrobial powder was uniformly mixed with polymer powder using a spatula, after which 5 mL of methyl methacrylate monomer was added, and the material was stirred approximately 3 minutes as it entered the dough phase. Cement was mixed at room temperature without vacuum, similar to methods used by surgeons who choose to mix their own antimicrobials into cement. Approximately 1 g portions of drug-loaded cement were weighed and then pressed into cylinders while in the dough phase using the flat bottom of a 20 mL scintillation vial pressed onto a

plastic weigh boat. Both the gel and cement samples had a thickness of approximately 2 mm and diameter of approximately 25 mm. Release from cement discs was evaluated in beakers containing 20 mL of PBS. Samples were maintained at 37°C throughout the course of the experiment.

At selected time points, aliquots were removed and stored at -20°C, and the release buffer was completely replaced with pre-warmed PBS to maintain infinite sink conditions. Drug concentration in the aliquots was measured at the end of the study by UV spectrophotometry (BMG Labtech, Fluostar Omega) at 280 nm for vancomycin and 272 nm for cefazolin. Calibration curves for each drug were used on each plate. It was verified that degraded polymers exhibited minimal absorbance at 1.5 wt% (corresponding to complete gel dissolution in the release medium in a single time point) at the wavelengths used for drug detection.

5.2.8. *In Vitro* Cytocompatibility

The cytocompatibility of degraded poly(NIPAAm-*co*-DBLA-*co*-JAAm) (batch pNDJ30a) was characterized at various polymer concentrations between 1-25 mg/mL. These concentrations were chosen as they are likely to represent the range of concentration of soluble polymer byproducts to which cells in local tissues would be exposed for a sustained period of time (i.e., days). Studies on similar and lower concentrations have been reported in the literature to assess the cytocompatibility of the soluble precursors or degradation byproducts of resorbable hydrogel materials.[251,306] Polymer was dissolved at 10 wt% in PBS titrated to pH 12 with 1 N NaOH and degraded by stirring for 3 days at room

temperature with the pH titrated to pH 12 twice daily. Following degradation, the polymer solution was dialyzed for 5 days against deionized water (3500 MWCO) with frequent water changes, and then lyophilized. Lyophilized polymer and glass scintillation vials were then treated with ethanol and exposed to UV light in a laminar flow hood for at least 1 hr. Then the polymer was dissolved at various concentrations in sterile DMEM supplemented with penicillin (100 units/mL), streptomycin (100 μg/mL), and l-alanyl-l-glutamine (2 mM). Solutions were then filter sterilized using a 0.45 μm filter and placed into scintillation vials. MC3T3 mouse osteoblasts (MC3T3-E1) and NIH3T3 mouse fibroblasts (clone A31) were seeded at 10,000 cells/well in separate 24 well plates and allowed to adhere for 24 hr (37°C, 5% CO_2) in 550 μL control media (DMEM supplemented with 1% glutamine, 1% pen-strep, and 10% bovine calf serum) per well. The media was then replaced with either degraded polymer solution (n=4 for each concentration) or control media without polymer. Calf serum (50 μL) was added to the polymer-media solutions in each well individually. NIH3T3 cultures were analyzed after 3 days. MC3T3 cultures (including controls) took longer to approach confluency, so the media was exchanged after 3 days and the cultures were analyzed after a total of 6 days incubation in polymer solutions. Cells were then rinsed with PBS and evaluated for live cell number using the CellTiter 96® AQueous Cell Proliferation Assay (Promega, Inc.) according to the manufacturer's instructions. The assay uses the tetrazolium salt 3-(4,5-dimethylthiazol-2-yl)-5-(3-carboxymethoxyphenyl)-2-(4-sulfophenyl)-2H-tetrazolium) (MTS) which is reduced by metabolically active cells. Before evaluation of cell number, cells

were imaged by light microscopy to observe any differences in cell morphology. Significant differences in cell number between cells in media without polymer and cells in each concentration of polymer were determined using Student's t-test ($\alpha = 0.05$).

5.3 Results

5.3.1. Composition and Molecular Weight

The polymer feed ratios, composition, molecular weight, initial LCST as measured by cloud point, and degradation time are shown in Table 5.1. Polymer batches are abbreviated in terms of the JAAm weight fraction in the feed (0, 15, or 30 wt%). Additional batches of polymer made using the same feed ratios are denoted by a letter. The molecular weight distributions of all the polymer batches were relatively consistent, with number-average molecular weight between 13-28 kDa and weight-average molecular weight between 28-54 kDa. Because the polymer backbone remains intact after degradation of these materials, their molecular weight should be near or below 40 kDa in order to facilitate rapid clearance through the kidneys.[307]

Table 5.1. Selected properties of degradable temperature-responsive polymers poly(NIPAAm-*co*-DBLA-*co*-JAAm).

Polymer	Feed ratio (mol%)		Composition* (mol%)		Molecular weight (g/mol)		Initial LCST (°C)	Degradation time (37°C, pH 7.4)
	DBLA	JAAm	DBLA	JAAm	M_n	M_w		
pNDa	7.2	-	5.6	0.0	13,100	32,100	18	-
pNDb	7.2	-	6.4	0.0	14,890	28,940	19	~180 days**
pNDJ15a	7.1	1.7	6.8	1.2	28,000	54,440	21	40 days
pNDJ15b	7.1	1.7	6.6	1.2	19,060	36,980	21	-
pNDJ30a	6.9	4.1	6.4	2.8	19,100	35,330	27	9 days
pNDJ30b	6.9	4.1	6.4	2.8	19,820	49,680	27	-

**Measured by ^1H NMR, **estimated from accelerated degradation reported previously*[122]

Successful synthesis was confirmed by ^1H NMR. JAAm content in the copolymers was calculated from the integration ratios of the peak at 3.5 ppm ascribed to the oxyethylene protons of the EO units (CH_2CH_2O) of JAAm relative to the peak at 3.7 ppm (1H) of the lone isopropyl proton of NIPAAm ($CH(CH_3)_2$). DBLA content was determined using the peaks near 5.3-5.5 ppm (1H) of the lone proton on the acryloyloxy-substituted carbon of the butyrolactone ring group. All copolymers exhibited lower incorporation of JAAm relative to the feed ratio, and DBLA content was also slightly lower than feed. Batch-to-batch variability in content was low.

5.3.2. LCST Properties and Degradation

The initial LCST of all synthesized materials was between 18-27°C, with JAAm incorporation being positively correlated with LCST. Solutions of these polymers will thus be flowable at ambient or slightly cooler temperatures and will

gel at body temperature. Degradation kinetics of pNDJ30a and pNDJ15a at 5 wt% are shown in Figure 5.2. Similar data on pND copolymers without JAAm have been previously reported by our lab using an accelerated degradation study[122] due to the longer degradation time of these polymers. Arrhenius kinetics suggest a degradation time for pND of approximately 180 days at 37°C. In this work, degradation time of the copolymers varied greatly with JAAm content, with JAAm leading to faster degradation. pND gels exhibit an initially slow increase in LCST, followed by a linear increase in LCST as the hydrophilicity of gels increases.[122,123] A similar but faster process was observed for pNDJ15, with minimal LCST change over the first two weeks of degradation, followed by a linear ($R^2 = 0.995$) increase in LCST with time between day 18 and day 54, and a final degradation time of about 40 days. pNDJ30a exhibited a linear ($R^2 = 0.992$) increase in LCST throughout the first 14 days of degradation.

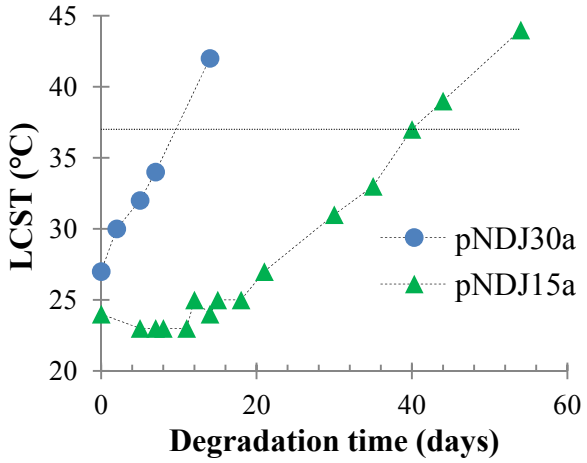

Figure 5.2. Degradation kinetics of poly(NIPAAm-*co*-DBLA-*co*-JAAm) hydrogels at 5 wt% (PBS, pH 7.4). Increased JAAm content resulted in higher initial LCST and faster degradation.

The degradation time of this system at 5 wt% can thus be tuned between about 9-180 days depending on JAAm content. This agrees well with previous work showing that JAAm functions to retain water (reducing shrinkage) within the polymer-rich "gel" phase at temperatures above the LCST.[144] As more water is retained within the polymer-rich phase, the rate of hydrolysis increases. While these polymers did not form gels at 5 wt%, 30 wt% gels in release studies exhibited degradation kinetics similar to the results reported in Figure 5.2. Whereas 30 wt% p(ND) gels showed no marked change in appearance in over 15 weeks at 37°C, pNDJ15b gels degraded over about 4-5 weeks at 37°C, and pNDJ30a gels with 2.8 mol% JAAm (about 21 wt%) became translucent within as little as 3 days.

Inclusion of JAAm grafts in the polymer design leads to more uniform degradation throughout the resulting hydrogel (Figure 5.3). Gels of 30 wt% pNDJ30 maintained their initial volume (or slightly increase in volume) and underwent gradual degradation. Gels of 30 wt% pND that have low equilibrium water content underwent rapid shrinking and slower degradation (Figure 5.3, top row). Interestingly, pNDJ gels degrade over a similar period of time but in a much different process than poly(NIPAAm-*co*-DBLA-*co*-acrylic acid) (pNDA) gels. Whereas pNDJ gels exhibit degradation which appears to be approximately uniform, the degradation of pNDA gels (which shrink) has been shown to occur primarily at the surface, leading to re-swelling of the periphery of the gel and formation of an inward-moving front between the swollen, translucent outer phase

and the shrunken inner gel core.[123,308] After the swelling front reaches all parts of the pNDA gel, the swollen phase then disintegrates to yield a solution.[123]

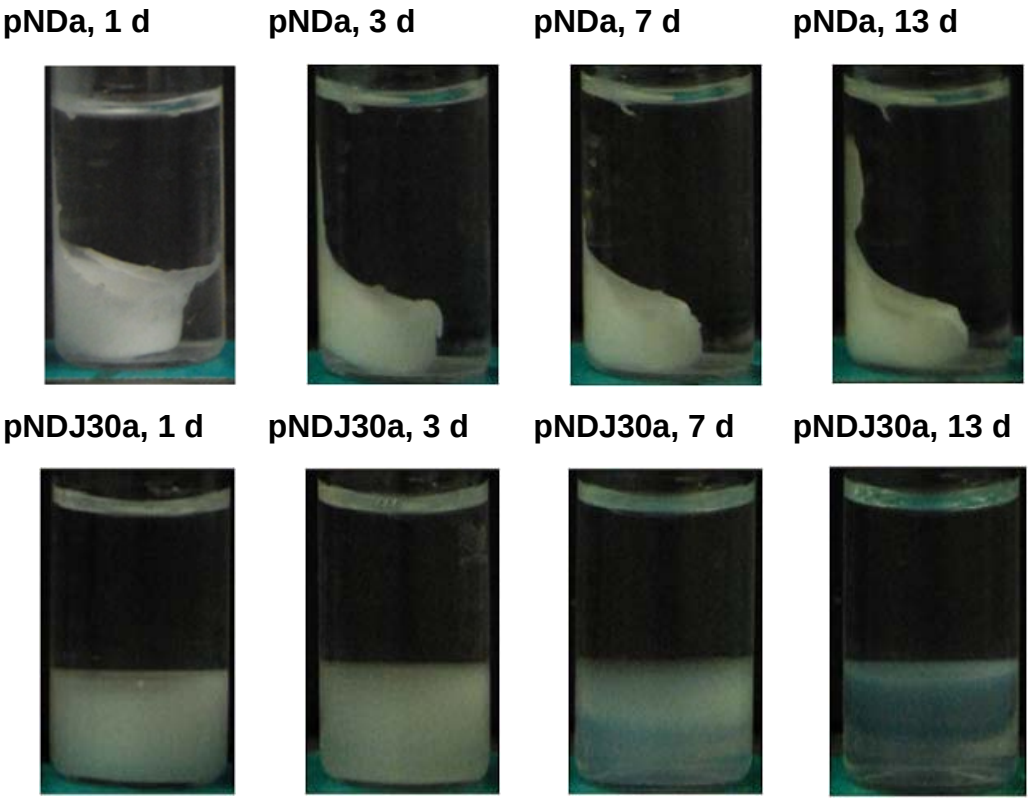

Figure 5.3. Swelling and degradation behavior of 30 wt% pND (top row) and pNDJ30 (bottom row) hydrogels incubated in PBS (pH 7.4) at 37°C. Gels were 1 mL with 1.5 mL excess PBS added after gelation. pND gels shrink and expel solvent and do not degrade within 13 days, whereas pNDJ30 gels maintain their initial volume, but dissolved in the excess PBS when buffer was replaced at 13 days. PBS was replaced at 1,3,7, and 13 days.

5.3.3. Rheological and Handling Properties

Rheological properties of 30 wt% hydrogels at 37°C as a function of frequency are shown in **Figure** 5.4. All of the gels were viscoelastic above the LCST, with phase angles greater than 45° (i.e., the gels are more viscous than elastic). Gels containing JAAm had storage and loss moduli in the 100-500 Pa range at 1 Hz, while pND gels were considerably stronger, particularly at lower frequencies. All of the gels showed increasing modulus with frequency which is characteristic of physical gels.[135,144,250]

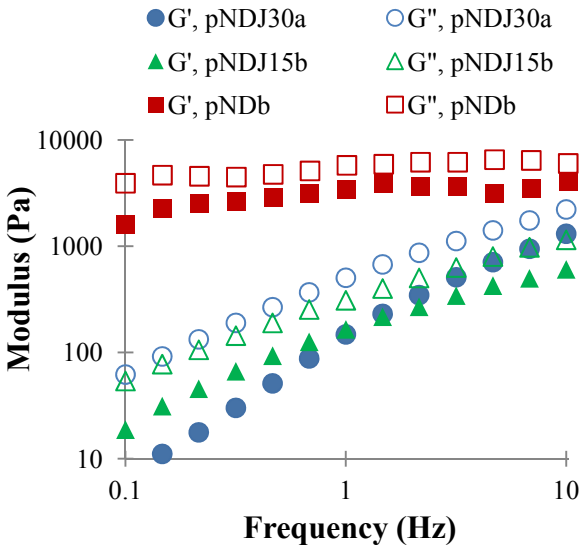

Figure 5.4. Frequency sweep showing the storage (solid icons) and loss (open icons) moduli of 30 wt% gels of pNDJ30a (circles), pNDJ15b (triangles), and pNDb (squares) at 37°C. pNDJ gels are weaker and more sensitive to frequency than pND gels.

Rheological properties of 30 wt% hydrogels at 37°C as a function of temperature are shown in Figure 5.5. All of the gels were viscoelastic and pNDJ

gels showed G" > G' over the range tested. pND in both the sol and gel state had the highest moduli. pNDJ15 and pNDJ30 gels were both considerably weaker in both the sol and gel states, but both showed an approximately 50-fold increase in complex modulus when heated from a sol to a gel. pNDJ15 became stronger over the temperature range 15-21°C, whereas pNDJ became stronger over 20-40°C. The slight decrease in modulus observed at temperatures above 37°C for pNDJ gels may have to do with stronger physical crosslinking at these temperatures leading to shrinking and poor contact with the rheometer resulting in a measurement of lower modulus, a finding consistent with other gels which do not shrink at 37°C but do shrink at higher temperatures.[147]

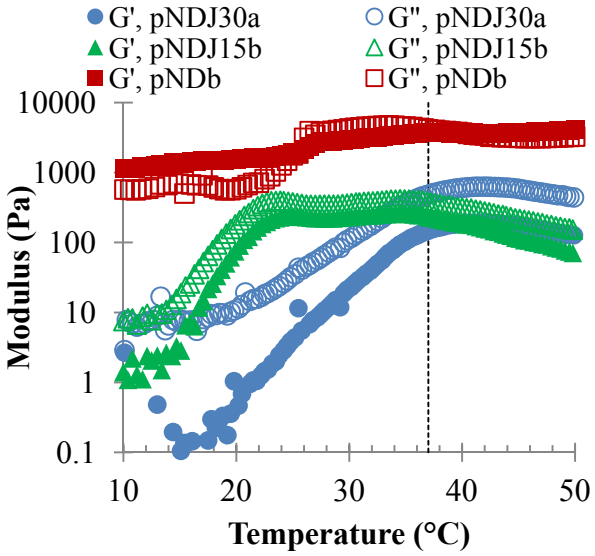

Figure 5.5. Temperature sweep showing the storage (solid icons) and loss (open icons) moduli of 30 wt% gels of pNDJ30a (circles), pNDJ15b (triangles), and pNDb (squares) at 37°C. pNDJ solutions form less viscous solutions below the LCST and less strong gels above the LCST compared to pND. Both pNDJ solutions increase in modulus by about 50-fold through the sol-gel transition.

In most of the samples, the complex modulus was linearly related to the frequency of the applied strain on the material over most of the frequency range tested. Therefore complex viscosity (i.e. complex modulus divided by angular frequency in rad/s) was used a single measure of the gels' strength. Complex viscosity as a function of polymer concentration and drug loading is shown in the top of Figure 5.6 for the polymer solutions at room temperature (21.3°C) and at body temperature (37°C). The gels show increased complex viscosity by 20-50 fold in most cases at body temperature relative to room temperature. At room temperature, the gels show phase angles exceeding 75°, characteristic of a viscous fluid, whereas the polymer solutions above the LCST behave as more viscoelastic fluids with phase angles between 60-75°. Concentration also has a meaningful effect on the rheological properties of the polymer solutions and on their handling. At 40 wt%, the polymer solution is so viscous that drug cannot be mixed into it using a vortex mixer. There was some inconsistency in measuring the complex viscosity of the gels at higher concentrations. For example, the 30 wt% gel has higher complex viscosity than the 35 wt% gel. This is likely due to incomplete contact of the gel with the rotating head of the rheometer, as it is clear that the modulus should increase with concentration, an effect easily observed at room temperature.

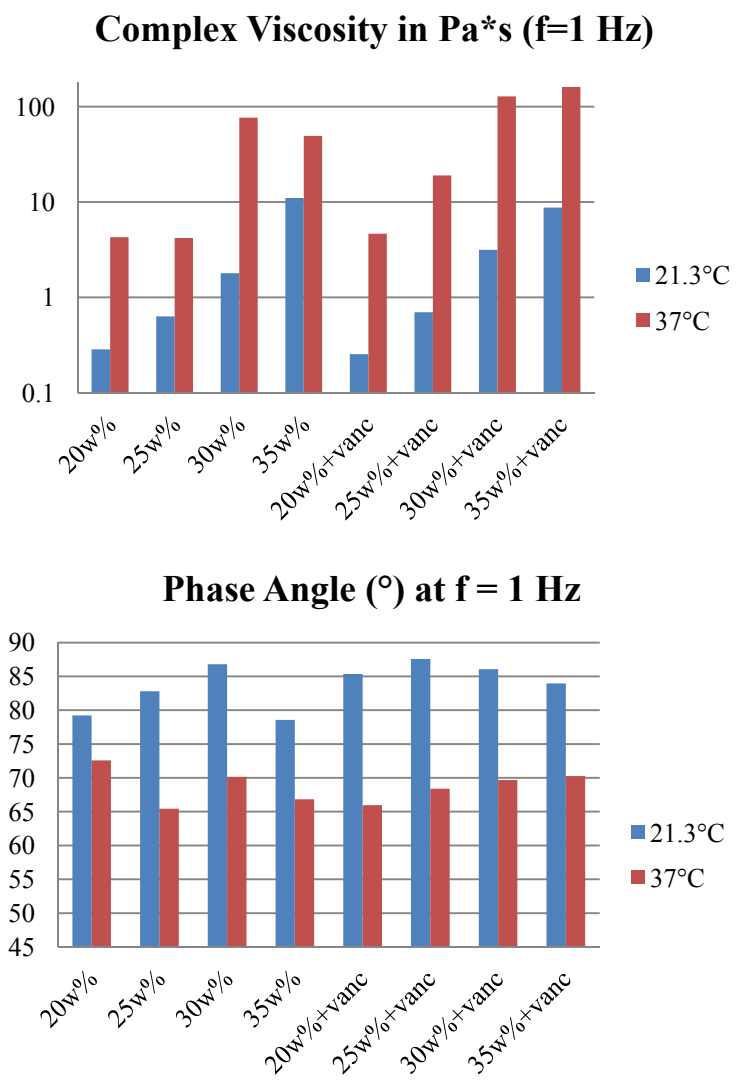

Figure 5.6. Complex viscosity (top) and phase angle (bottom) of pNDJ30b with or without 50 mg/mL vancomycin hydrochloride. Gels show increased viscosity and decreased phase angle when heated from room temperature to body temperature.

5.3.4. Distribution in Cadaveric Human Femur

After reaming but prior to the application of the hydrogel (Figure 5.7A), the jagged surface of the firmly inserted implant is clearly visible on both the lateral (top in the image) and medial (bottom) sides of the implant. After filling with

radio-opaque polymer solution and re-insertion of the implant (Figure 5.7B), none of the surface features along the entire length of the implant were visible. The images also show penetration of the polymer solution into the cancellous bone slightly lateral to the proximal portion of the implant.

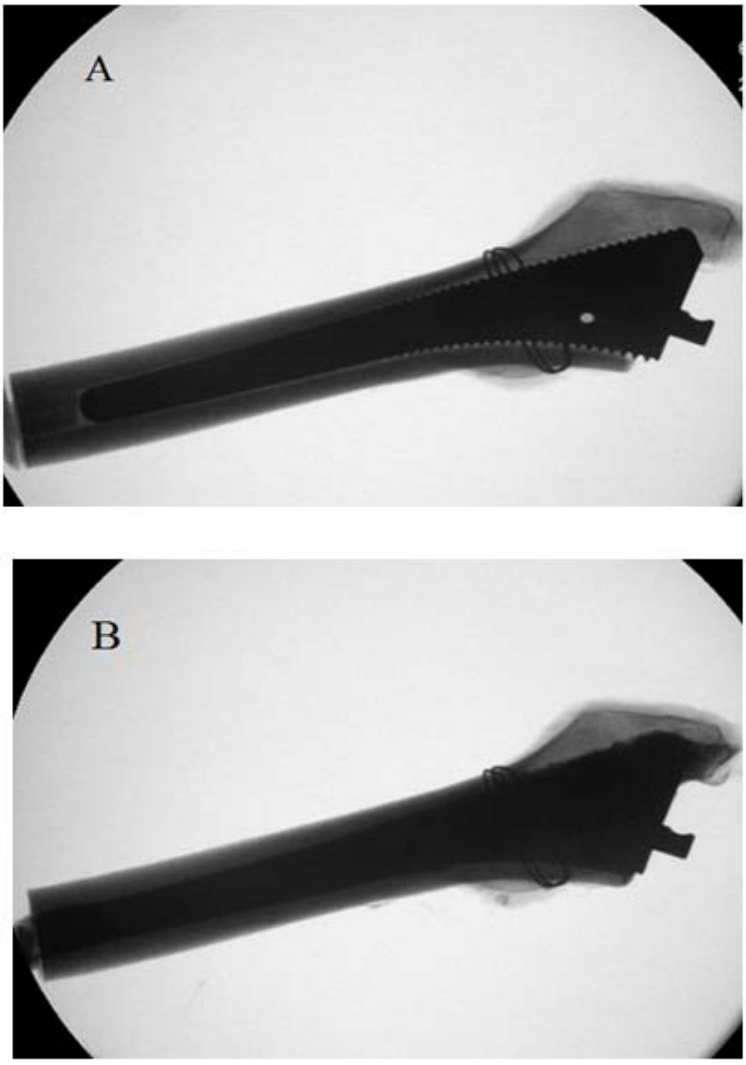

Figure 5.7. Biomet Exact® implant in cadaveric human femur (A) uncoated and (B) coated with mock p(NDJ30) above the LCST. Inserting the implant into viscous hydrogel provides complete coverage of the gel on the implant surface.

5.3.5. *In Vitro* Antimicrobial Release

Drug release profiles from 2 mm-thick discs of pND, pNDJ15, and pNDJ30 hydrogels are shown in Figure 5.8. Data are reported as the cumulative amount of drug released (M_t) normalized to the cumulative amount of drug released after 168 hr ($M_{168\ hr}$), because the release rate by 168 hr was very slow for all hydrogels tested. The percentage of the loaded drug that was released from each material within 168 hr is reported in Table 5.2. For each hydrogel/drug combination, at least 65% of the drug loaded into the gels was released within 168 hr. Cumulative release of cefazolin was over 85% from pNDJ gels, and as low as 65% from pND gels, whereas only 70-85% of vancomycin was measured as having been released from any of the gel formulations. Incomplete release over this timeframe may be due to some combination of drug retention within the gel or degradation of the drugs—vancomycin[309,310] and cefazolin[311,312] both are known to be unstable under conditions similar to those used in these studies. pNDJ30 gels became translucent by 72 hr and were dissolved in the release media by 120 or 168 hr. Both pNDJ15 and pND gels remained intact throughout the studies.

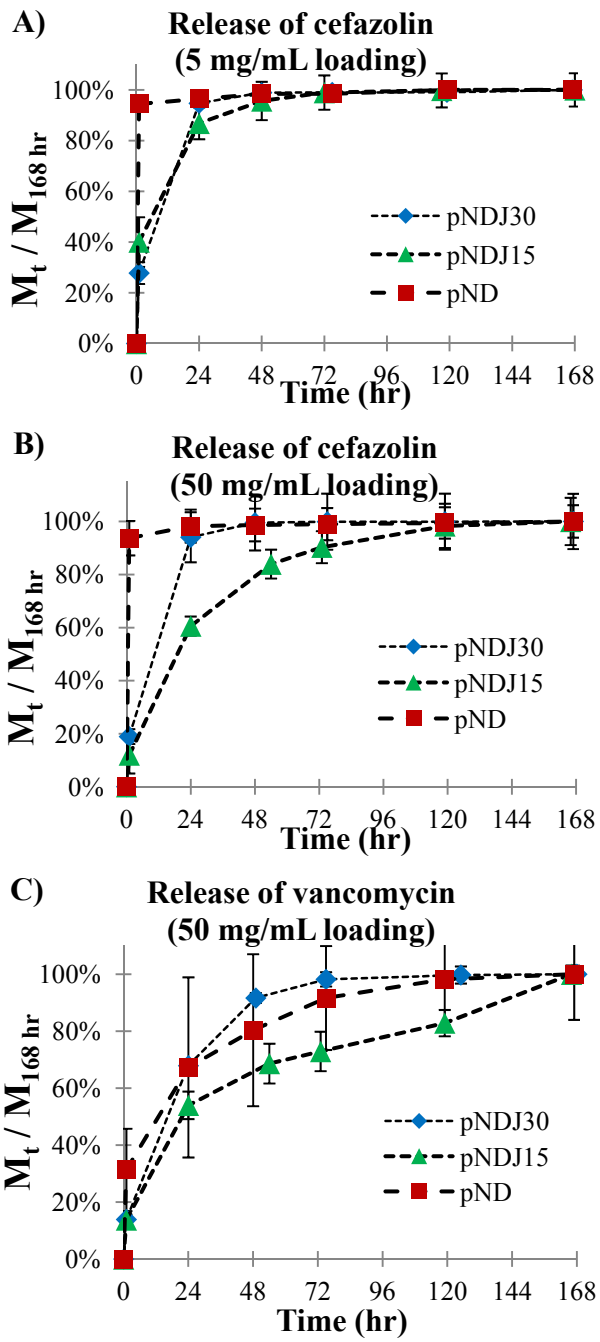

Figure 5.8. Release of model drugs from 2 mm thick discs of resorbable temperature-responsive hydrogels (30 wt%). Release is dependent on JAAm graft content, drug, and drug loading. Data are reported as mean ± s.d. (n = 3).

Table 5.2. Cumulative fraction of entrapped drug ($M_{168\ hr}$/ Loading) released after 168 hr.

	Low Dose* Cefazolin	High Dose* Cefazolin	High Dose* Vancomycin
pND	65.3 ± 1.2	78.1 ± 4.8	72.8 ± 11.7
pNDJ15	86.3 ± 6.6	99.4 ± 8.8	70.5 ± 2.2
pNDJ30	100.0 ± 1.7	92.6 ± 9.7	86.6 ± 2.6
pMMA	16.6 ± 3.4	46.7 ± 6.8	29.8 ± 0.6

**Low dose loading: Hydrogels 5 mg; pMMA 16.4 mg*
*** High dose loading: Hydrogels 50 mg; pMMA 143 mg*

pMMA cement released the lowest fraction of the drug loaded into it in all cases. The fraction of drug released was particularly low (16.6%) when the cement was prepared with the low dose (16.4 mg per g) of cefazolin. Release is known to be relatively fast and incomplete from bone cement, as a fraction of the drug mixed into cement remains trapped.[38,39] Higher doses of drug increase the fraction of drug released because the drugs can act as pore-forming agents which allow access of a greater volume fraction of the cement to the surrounding aqueous medium.[39]

When loaded with 5 mg/mL cefazolin, pND gels provided high burst release, with 94% release observed within 1 hr after gelation. Gels with JAAm showed reduced burst release (under 40% within 1 hr) but over 85% release after 24 hr. When loaded with 50 mg/mL cefazolin, similar release profiles were observed both from pND and pNDJ30, with slower release observed over about 5 days from pNDJ15 gels. pNDJ15 released 12% within 1 hr, 61% within 24 hr, and 90% within 72 hr. Gels loaded with 50 mg/mL vancomycin showed slower release from each hydrogel formulation. pND gels released drug with high

sample-to-sample variability, but on average released 31% within 1 hr, 67% within 24 hr, and 92% in 72 hr. pNDJ30 gels provided low burst release, but release was 98% complete within 72 hr. pNDJ15 gels provided the slowest release of vancomycin, with 54% release within 24 hr and approximately linear release for 6 days thereafter.

Figure 5.9 shows the mass of drug released with time from pNDJ15 hydrogels (the slowest releasing hydrogel formulation) and from pMMA cement. For each set of conditions tested, the mass of drug released was similar between pNDJ15 gels and pMMA cement, despite the loading of the cement samples being approximately 3 times that of the hydrogels.

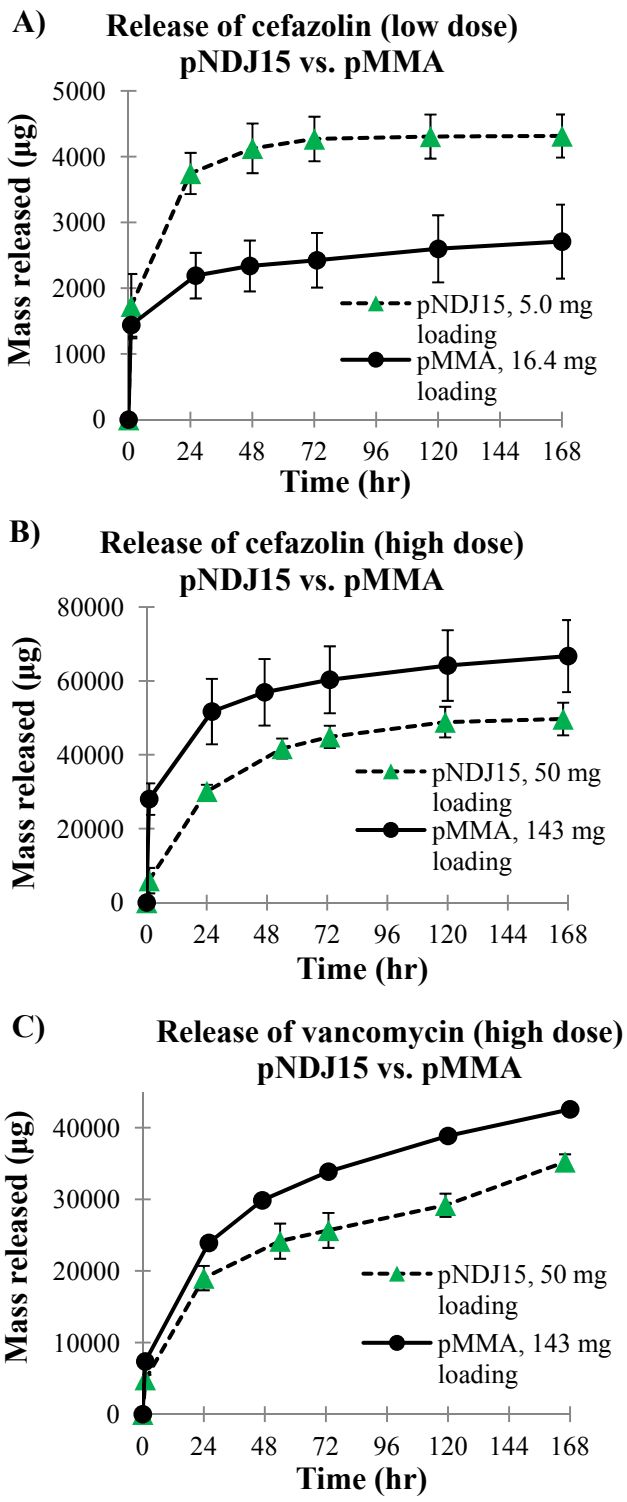

Figure 5.9. Cumulative mass of model antimicrobials released from 2 mm thick discs of pNDJ15 resorbable temperature-responsive hydrogels or pMMA bone

cement. The extent and rate of release from hydrogels is similar to that of cement loaded with approximately 3 times as much drug. Data are reported as mean ± s.d. (n = 3). Some error bars are smaller than the data points.

5.3.6. *In Vitro* Cytocompatibility

Results from *in vitro* cytocompatibility studies on pNDJ30a degradation byproducts are shown in Figure 5.10. The number reported represent the number of live cells present per well of a 24 well plate. The number of living NIH3T3 fibroblasts after 3 days was greatly increased from the initial seeding of 10,000 cells in every concentration of the polymer solution tested, and no significant differences in cell number between negative control media without polymer and any of the individual polymer concentrations were found. The number of living MC3T3 osteoblasts after 6 days in culture was also greatly increased relative to the initial cell seeding density. A significant difference (p = 0.007) in cell number was observed between control and 2.5 wt% degraded pNCJ30a, with 2.5 wt% having a greater number of cells present. This difference may have been caused by greater initial cell seeding density or more uniform initial cell density within the wells, as all of the wells (including controls) were observed to have variable cell density from location to location within a single well. Representative images of high cell density areas in the presence of control media or 2.5 wt% degraded pNDJ30 for both cell types prior to performing the MTS assay are shown in Figure 5.11. Cells cultured in up to 2.5 wt% degraded polymer displayed spread or spindle-like morphology as cells cultured in standard media.

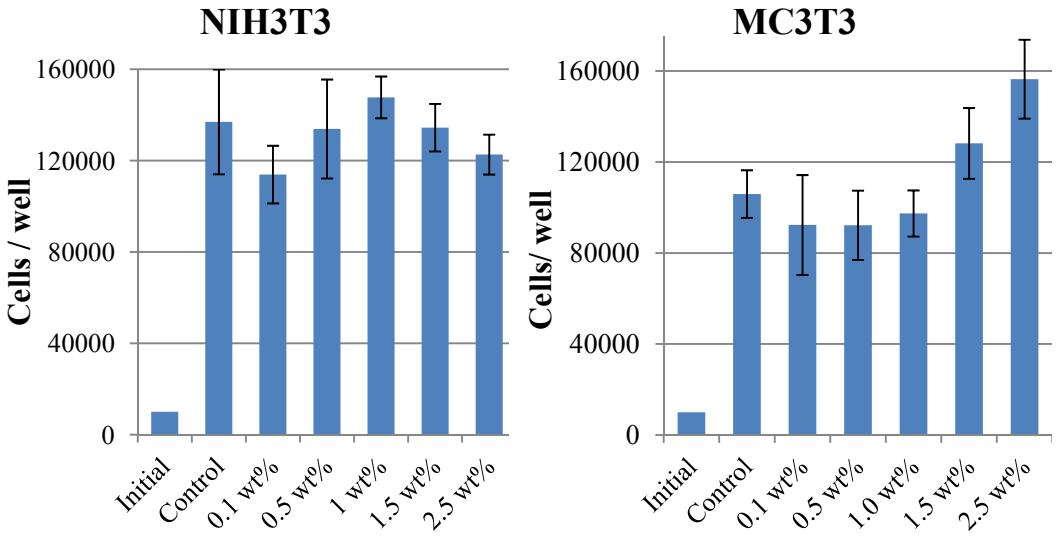

Figure 5.10. Cytocompatibility of pNDJ30a degradation byproducts to NIH3T3 fibroblasts (left) and MC3T3 osteoblasts (right). Both cell types were able to proliferate when cultured in degraded pNDJ30a at concentrations up to 2.5 wt%.

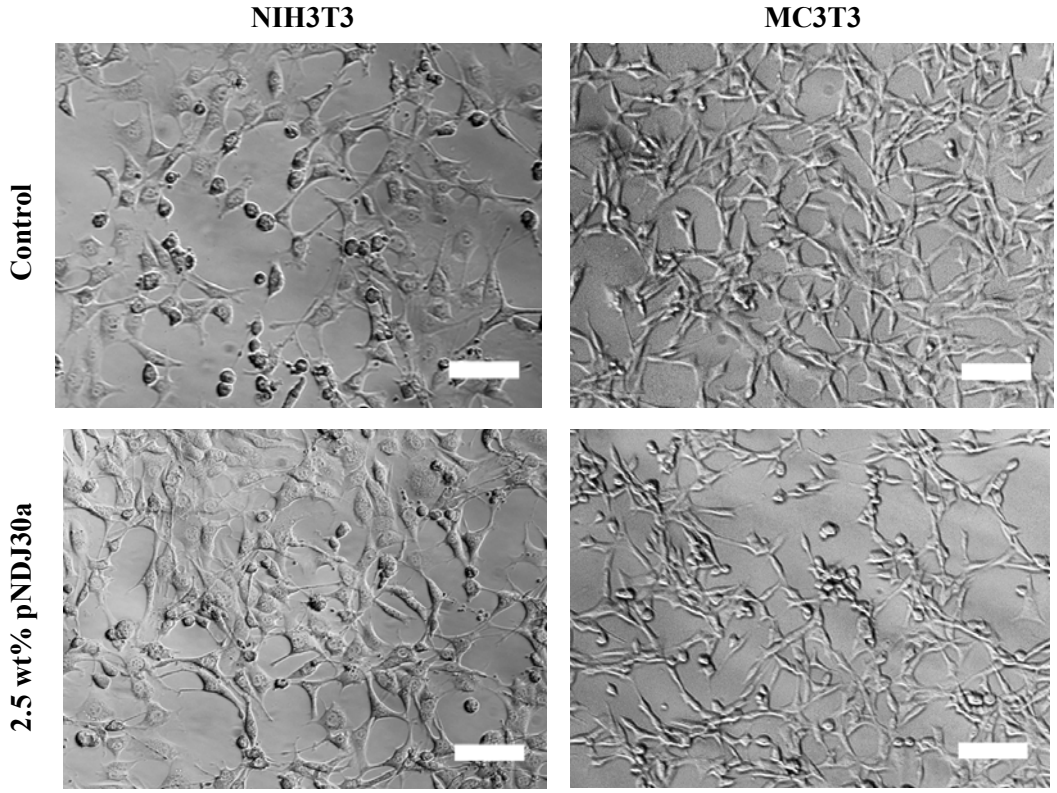

Figure 5.11. Light microscopy photographs of NIH3T3 fibroblasts (left) and MC3T3 mouse osteoblasts (right). Cell density and morphology is similar when cultured in standard media without polymer (top) or 2.5 wt% degraded pNDJ30a (bottom). Scale bars are each 100 μm.

5.4. Discussion

The inclusion of hydrophilic JAAm grafts in temperature-responsive resorbable copolymers results in increased water content in the corresponding hydrogels. JAAm can therefore be used to control gel properties relevant to local drug delivery (degradation kinetics, drug release, and rheological properties). The

pNDJ gels reported in this work display a unique combination of attributes (highly viscous, controlled release, and degradable over 1-8 weeks) for an injectable and degradable drug carrier. While the relatively fast degradation time and viscous nature of the hydrogels limits their feasibility for some applications, it may enable their feasibility in others, particularly in sites with irregular geometries or sites under mechanical load which are unsuitable for pre-formed solid implants or drug-loaded microspheres.

5.4.1. Swelling and Degradation Relationship

The degradation and swelling behavior of pNDJ hydrogels changes greatly due to JAAm. Incorporation of JAAm in the polymer led to reduced shrinking and more uniform degradation throughout the gel. The initially slow change in LCST observed in pNDJ15 gels agrees well with previous published data on pND gels.[122] The acceleration of the LCST increase observed in pNDJ15 is thought to be attributed to the degradable ester groups on the butyrolactone ring being hydrolyzed to pendent hydroxyl and carboxyl groups still bound to the polymer. Along with increasing the LCST, this increases the accessibility of the water to the remaining intact esters of the polymer. In pNDJ30 gels, the polymer is so hydrophilic that the degradation occurs at a faster rate even before hydrolysis. Despite the fact that the degradation time of NIPAAm-based gels can be easily controlled using small molecules like AAc,[123,124,135] the graft copolymer approach used in this work results controls swelling to a greater extent, which is important

for maintaining the interfacial contact between the gel and the implantation site as well as for providing controlled release of low molecular weight drugs.

It is important to note that gelation of these copolymers is concentration-dependent and the polymer molecules within each batch are heterogeneous in both content and molecular weight. Accordingly, the gels are likely to weaken or macroscopically degrade slightly prior to the average LCST increasing to body temperature. *In vitro*, this results in the gel becoming a translucent solution, and eventually a transparent solution. While undisturbed pNDJ30 gels remained somewhat intact at 7 or even 13 days, it was observed that even gentle replacement of release media on pNDJ30 gels in the release studies caused pNDJ30 gels to partially mix with the release medium as early as 5 days post-gelation.

5.4.2. Rheological and Handling Properties

All of the gels tested could be characterized as viscoelastic fluids, with G" > G' above the LCST. All of the polymer solutions were observed to become stronger upon heating above their LCST. pND gels macroscopically behaved as solid materials after shrinking—the gels retained their shape and were not prone to flow. On the other hand, pNDJ15 and pNDJ30 gels had much lower modulus, and were even prone to slow flow over a period of days at 37°C. The gels would not noticeably flow in an inverted vial for 30 seconds, but if left overnight, the gels would flow. These gels therefore would be unsuitable for use in sites where external forces would deform the gel undesirably or cause displacement of the gel

from the site. All of the hydrogels tested would be prone to creep. However, these properties are likely to be acceptable or even advantageous in irregular geometries, in sites where the material would remain in the site due to its viscosity (such as a thin coating on an implant), or in sites where gel cohesion is desired rather than strength. The pNDJ hydrogels reported in this work could provide complete interfacial contact even at temperatures above the LCST, as they behave more like very viscous liquids than elastic gels.

The difference in rheological properties is meaningful for the handling and use of the material. Below the LCST such as at room temperature, pNDJ30 is a liquid with a viscosity similar to warm honey. Above the LCST, the gel/fluid is so thick that it will not flow when inverted for up to minute. In a large container such as a mason jar, the material will begin to flow if inverted for over 30 seconds. Such a material is likely to maintain its location adequately (i.e. not flow) in a closed space, such as around an orthopaedic implant.

5.4.3. *In Vitro* Antimicrobial Release Kinetics

Drug release kinetics from the gels varied depending on the drug choice, drug loading, and polymer JAAm content. Vancomycin release was sustained for a period of 3-7 days from gels based on all three polymers. On account of vancomycin's higher molecular weight and lower solubility at neutral pH, vancomycin release was slower than cefazolin release for all gels tested. While pND gels did show the greatest amount of release over the first hour when gel shrinking occurs, they nevertheless provided sustained release over at least 5-7

days, which is evidence that vancomycin distributes predominantly into the polymer-rich gel phase when the polymer solution is heated above its LCST. The shortest duration of vancomycin release was observed from pNDJ30 gels. These gels became translucent within 72 hr of release and partially mixed with the release media by 120 hr. Therefore, the faster release from pNDJ30 may be caused by partial degradation of the gel, resulting in increased diffusivity of the drug in the gel and faster release.

When heated above the LCST, pND gels released a large fraction of the loaded cefazolin within 15 minutes regardless of drug loading. Because cefazolin is hydrophilic, it is likely to partition predominantly into the solvent phase as the pND phase-separates following gelation. pNDJ30 gels showed slower cefazolin release over 24-48 hr without the large initial burst observed from pND gels. Though the release was still relatively rapid, a majority of the cefazolin was retained in the gels at 1 hr, indicating controlled release. The slowest cefazolin release was observed from pNDJ15 gels, which exhibit intermediate hydrophilicity and reduced phase separation. Even though a small fraction of water separates from pNDJ15 gels, the release data suggests that most of the cefazolin was retained within the gel after the transition. Release then occurs almost entirely by diffusion, as these gels did not degrade much within the first week.

The release rate being the slowest from pNDJ15 gels is evidence that a balance was achieved in these gels between low phase separation (achieved by more JAAm) and slow degradation (achieved by less JAAm). Even with further

optimization, it is anticipated that the release of small hydrophilic drugs such as cefazolin could not be prolonged by much longer than 5-7 days by this system, simply due to the diffusivity of the drug within the polymer gel. This duration of release is shorter than what might be achieved by injectable gels with much longer degradation times containing drug-loaded microspheres.[293] Differences in the final polymer content in the gel (after shrinking) did not seem to strongly affect the diffusivity of the drugs remaining in the gel phase, as the release of vancomycin was similar between pND and pNDJ15 gels. While release could be somewhat controlled by polymer concentration in the gel, the concentration must not exceed about 40 wt% because the polymer solution can become too viscous and eventually the polymer itself would not be soluble. Alternatively, the release of hydrophobic drugs could be prolonged for a much longer time, perhaps up to 20 weeks from pND gels, particularly if the drug were loaded well above its solubility, resulting in partition-controlled release.[212] Sustained release beyond the degradation time of pND would require changes to the polymer composition not explored in this work.

pNDJ15 sustained the release of both drugs for the longest time, providing a similar release profile to pMMA cement over the first 7 days. While the 40 day degradation time of pNDJ15 is very close to the time at which bone healing onto implants can be seen radiographically (6-8 weeks), the amount of JAAm in the polymer could be increased to provide faster gel degradation. Optimization of the hydrogel degradation time may be required to facilitate clearance of the gel

degradation products from a bone-implant interface and allow for implant fixation.

It is important to note that the release kinetics from these gels *in vivo* are expected to depend on the gel shape and the surrounding fluid environment (viscosity, flow, pH). Release was evaluated from discs with 2 mm diameter in infinite sink conditions to reliably compare the materials under conditions prone to fast release. Release would be sustained over a longer time *in vivo* if the gel had a lower surface area-to-volume ratio or if the drug were cleared slowly from the local tissue.

5.4.4. Implications for Prevention of Prosthetic Joint Infection

Release of both antimicrobials was more complete from the pNDJ15 hydrogels than from the cement after 168 hr, but with similar release profiles. Release is known to continue at a very low rate from antimicrobial-loaded bone cement for extended periods of time (months to years).[38,39,313,314] This may provide subtherapeutic local concentrations which allow the emergence of resistant organisms,[315,316] and has led some to advocate against the use of antimicrobial-loaded bone cement for prophylaxis in routine primary arthroplasty.[317] At the lower dose, pNDJ15 hydrogels showed greater mass release than pMMA, whereas at the higher dose, pMMA showed greater mass release. This difference is attributed to the fact that the pMMA becomes more porous with higher drug loading and hence releases a greater fraction of the entrapped drug more quickly. Nevertheless, given that the shape of the high-dose release profiles

are similar between the cement and hydrogel formulations, it seems likely that similar antimicrobial concentrations as those provided high-dose pMMA formulations used for infection management could be provided from the hydrogel delivery vehicle either for infection management or for prophylaxis. By providing increased and sustained delivery relative to ALBC that is safe for fixation, these new hydrogel materials may be able to more effective in preventing infections while being compatible with cementless fixation.

The complete surface coverage shown by the radio-opaque PEG mock is a strong indication that the hydrogel would provide complete surface coverage on a hip implant. Infusion of the hydrogel into interstices in the bone exposed before insertion of an implant is promising because those interstices comprise part of the surface area of the wound created during an arthroplasty. The ability of a polymer with the rheological characteristics of pNDJ30 (and very similar to pNDJ15 as well) to thoroughly cover the surface of the implant as well as to be driven into cavities within the nearby bone is promising for the prevention of infections on or near these implants. Though the anatomical features of the surgical wound are certain to affect the concentration profile in and around the surgical site, direct contact of the delivery vehicle to the desired site is the best way to provide the most drug to vulnerable surfaces.

Additionally, because the polymer solution is capable of flowing, it yields easily when the implant is inserted and so it does not negatively affect the quality of fit between the implant and the bone in the way that a pre-formed solid implant might. Such a fluid-like controlled release vehicle which provides release over a

complete surface is not currently available for any indication and to my knowledge has not been reported elsewhere in the literature.

5.4.5. *In Vitro* Cytocompatibility

While microscopy shows more rounded cells at higher polymer concentrations, the MTS assay data is evidence that the polymer does not slow cell growth and division and is not cytotoxic. At any location not within the hydrogel, it is unlikely that the polymer concentration will exceed the concentrations tested here for multiple days, as the degradation products are expected to diffuse from the delivery site once soluble. While only one degraded polymer, pNDJ30, was tested, it is expected that the other polymers would perform similarly as they are made of the same components, and all are predominantly composed of NIPAAm repeat units. These results also agree well with previous *in vivo* biocompatibility studies on subcutaneous injections of poly(NIPAAm-*co*-DBLA-*co*-AAc) where the injection site was indistinguishable from native tissue after degradation of the gels were complete.[123] Future work will be required to determine what concentrations, if any, affect either the mineralization of osteoblasts or the osseointegration of bone onto an implant surface in the presence of gel, as would be required to safely use the gel on a femoral prosthesis indicated for cementless fixation.

5.5. Conclusions

In situ forming, temperature-responsive, degradable polymers were successfully synthesized and characterized for the controlled release of the model drugs cefazolin and vancomycin. To our knowledge, these are the first purely physical gels based on NIPAAm demonstrated for the sustained release of hydrophilic low molecular weight drugs with minimal burst release. The gels provide controlled release over days without relying on drug-polymer interactions or co-delivered microparticles. Gel degradation and drug release was controlled by varying the amount of hydrophilic JAAm grafts on the polymer backbone. Gels with greater JAAm content shrank less upon heating above their LCST, which resulted in reduced burst release, particularly for cefazolin. Gels with JAAm were viscoelastic and weak with storage and loss moduli in the 100-500 Pa range at 1 Hz. Drug release from pNDJ15 gels was sustained for both drugs tested, and nearly complete elution occurred within 7 days. Hydrogels provided similar elution over 7 days to pMMA cement when loaded with approximately 1/3 as much drug. The degradation byproducts of one hydrogel formulation were shown to be cytocompatible to NIH 3T3 fibroblasts and MC3T3 osteoblasts at concentrations up to 2.5 wt%. Given their unique combination of fluid-like handling properties, controlled release, and rapid degradability, these new hydrogels are promising as sustained release carriers of low molecular weight drugs for applications where administration of multiple doses, percutaneous injection, or delivery to sites with irregular geometries is desired. In particular, these gels have potential for enabling drug delivery in joint spaces, overcoming

the limitations of currently available hard materials (PLGA, cement) and implant surface coatings.

Chapter 6: *IN SITU* CROSSLINKING TEMPERATURE-RESPONSIVE HYDROGELS WITH IMPROVED DELIVERY, SWELLING, AND ELASTICITY FOR ENDOVASCULAR EMBOLIZATION

6.1. Introduction

Hemorrhage results from approximately 30,000 cerebral aneurysms annually in the United States, about half of which are fatal.[54] Endovascular embolization is a common method of pre-emptive cerebral aneurysm treatment owing to its minimal invasiveness and enabled by the development of endovascular coils—flexible platinum coils inserted into the aneurysm. Coils occlude less than half of an aneurysm, relying on clot formation to occlude the remaining volume.[83] Though coils are considered the most effective endovascular approach, they are associated with poor recanalization rates (>25%) in large or wide-neck aneurysms,[59,61,75,318] which is attributed to the low volume fraction that the coils occupy within the aneurysm.[62–64]

In situ forming materials are a promising alternative to endovascular coils because the shape of an *in situ* forming implant is defined by its local environment, allowing complete filling of the aneurysm sac. While one liquid embolic formulation—poly(ethylene-*co*-vinyl alcohol) in dimethyl sulfoxide, marketed under the name Onyx® (Covidien, Mansfield, MA, USA)—which forms by solvent exchange precipitation has been FDA approved for use, there are concerns over solvent toxicity including vessel necrosis and vasospasm.[89,92,319] Another unavoidable limitation of the solvent exchange approach is that the

delivery procedure is complicated and time intensive, requiring repeated steps allowing for the DMSO to gradually leave the aneurysm site and be replaced by water, precipitating the polymer *in situ* often over the course of an hour or more—even up to 6 hr in some cases.[81] Water-borne gelling systems based on poly(NIPAAm),[85] alginate,[86] chitosan,[320] and acrylated oligomeric precursors[84,321] have been more recently investigated, though none are yet approved.

Temperature-responsive polymers based on *N*-isopropylacrylamide (NIPAAm) provide a potentially useful platform for embolization because they quickly precipitate from aqueous solution when heated to body temperature and can be modified easily through copolymerization with other monomers. Despite these advantages, NIPAAm-based systems also have major limitations to practical use as liquid embolics. As the polymer solution in the catheter is warmed to body temperature, the polymer is liable to gel inside the catheter, preventing its delivery, yet the hydrogel must also be sufficiently strong and highly elastic after delivery. Though chemical crosslinking (most commonly done via Michael addition between thiols and acrylates) can result in a stronger and elastic gel forming *in situ*,[142,275,277,278] this reaction takes place much more quickly below the polymer's LCST, presumably due to the hydrophobicity of the polymer.[274] Embolization also requires that the material maintain its volume after delivery, whereas poly(NIPAAm) typically undergoes shrinking within hours after gelation.[144,235,274]

This Chapter reports on the development of a polymer system that would be initially flowable at body temperature, chemically crosslink *in situ* within a

reasonable time, and adequately maintain its shape and volume. The material is based on a copolymer consisting of repeat units of NIPAAm, repeat units with pendent thiol groups for chemical crosslinking, and Jeffamine® M-1000 acrylamide (JAAm) to increase the hydrophilicity of the copolymer. Upon mixing with an alkaline solution of poly(ethylene glycol diacrylate) (PEGDA), the polymer begins to chemically crosslink by Michael addition. Previously, it has been demonstrated that JAAm grafts on NIPAAm-based polymers cause weakened physical crosslinking and controlled gel swelling.[322] The hypothesis for this work was that combining the NIPAAm-JAAm graft copolymer design with physiologically compatible *in situ* crosslinking would provide a viable candidate material for endovascular embolization of cerebral aneurysms.

6.2. Materials and Methods

6.2.1. Materials

All materials were reagent grade and obtained from Aldrich unless otherwise noted. The polymerization solvent was HPLC grade Tetrahydrofuran (THF). Dichloromethane (DCM) was distilled and stored under nitrogen. Jeffamine® M-1000 was donated by Huntsman Corporation (The Woodlands, TX, USA).

6.2.2. Synthesis

Jeffamine® M-1000 acrylamide (JAAm) was synthesized from Jeffamine® M-1000 by acryloylation with acryloyl chloride as reported in Chapter 5. Poly(NIPAAm-*co*-*N*-acryloxysuccinimide-*co*-JAAm) copolymers (pNNJ), with 5 mol % *N*-acryloxysuccinimide (NASI) and varying feed ratios of JAAm (0, 10, and 20 wt% relative to the amount of NIPAAm monomer) were synthesized by radical polymerization in THF (10 wt%) as depicted in Figure 6.1. The monomer solution was bubbled with nitrogen for 20 minutes before the addition of the initiator to reduce dissolved oxygen. The reaction was initiated with AIBN (0.007 mol AIBN per mol monomer), and conducted at 65°C for 24 hr under slightly positive nitrogen pressure. pNNJ copolymers were obtained by precipitation in 10-fold (0 JAAm) or 15-fold (10%, 20% JAAm) excess of diethyl ether at 0°C, and then filtered and vacuum-dried overnight.

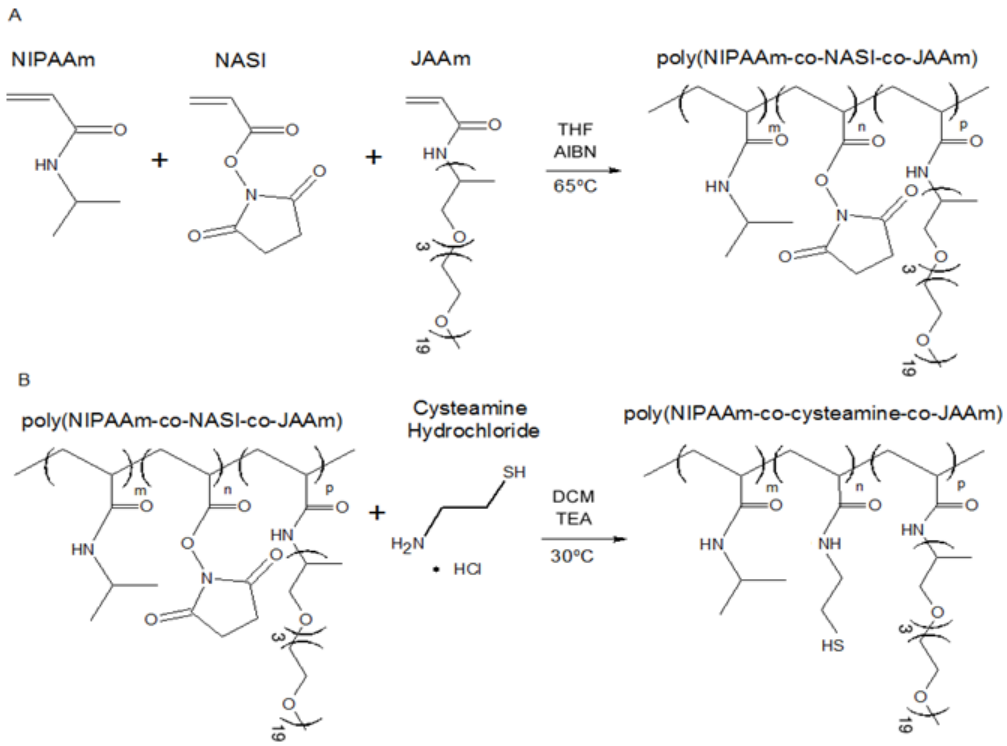

Figure 6.1. (A) Synthesis of poly(NIPAAm-*co*-NASI-*co*-JAAm) intermediate (B) Substitution of cysteamine to form poly(NIPAAm-*co*-cysteamine-*co*-JAAm).

NASI side groups were converted to pendent thiols by nucleophilic substitution with cysteamine.[275] Cysteamine hydrochloride was measured in a two-fold excess over the NASI and dried under vacuum at 60°C for 24 hours to reduce moisture. DCM was added to the cysteamine hydrochloride and a 1.5x excess of triethylamine was added to deprotect hydrochloride. The solution was allowed to dissolve under stirring for 30 minutes; if cysteamine hydrochloride remained partially undissolved, the solution was vacuum filtered to remove excess cysteamine. pNNJ was then added to this solution and allowed to dissolve, resulting in a final pNNJ concentration of 10 wt%. This reaction was allowed to

proceed under nitrogen at 30°C for 72 hr. The resulting polymers, poly(NIPAAm-*co*-cysteamine-*co*-JAAm) (abbreviated pNC, pNCJ10, and pNCJ20), were precipitated in diethyl ether, filtered and vacuum-dried overnight. Polymers were then dissolved in 5 mM HCl with a stoichoimetric amount of dithiothreitol (DTT) to reduce disulfide linkages and dialyzed (3500 MWCO) against 5 mM HCl for 7 days with frequent exchange of the dialysis solution to remove the DTT. The pNCJ solution was then lyophilized and stored at -20°C under nitrogen until use.

6.2.3. Hydrogel Preparation

Unless otherwise noted, hydrogels were prepared as shown in Figure 6.2. Each pNCJ copolymer was dissolved in 5 mM HCl at 33 wt% and stored at 4°C for less than 48 hrs prior to use. To induce chemical crosslinking, the polymer solution was mixed with a solution of PEGDA (MW 700) (acrylates equimolar to thiols on pNCJ) in 750 mM phosphate buffered saline (PBS) titrated to pH 10 with 1 M NaOH. PEGDA solution was prepared immediately before mixing of the two precursor solutions. Syringes (1 mL) were loaded with the precursor solutions and connected by a syringe coupler. The solutions were mixed for 15 seconds and used immediately. The pNCJ concentration in the gels after mixing was 30 wt%.

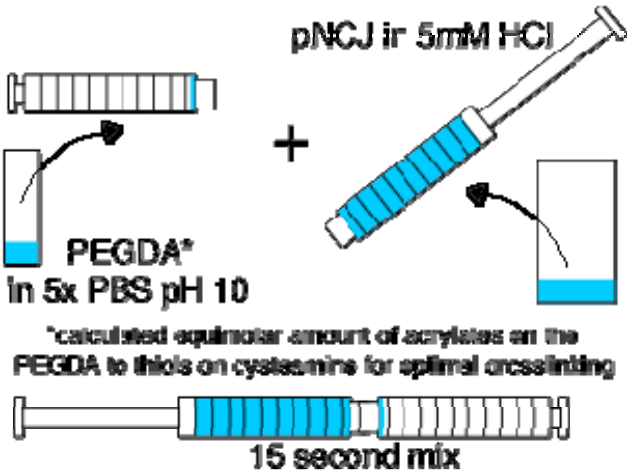

Figure 6.2. Method used for preparing *in situ* crosslinking hydrogels by mixing aqueous solutions of temperature-responsive polymers with poly(ethylene glycol) diacrylate (PEGDA).

6.2.4. Composition and LCST Transition

Polymer composition and molecular weight were determined by ^{1}H NMR and GPC as reported in Section 5.2.3. To determine the LCST of the synthesized copolymers, solutions were prepared at 0.25 wt% in 150 mM PBS titrated to pH 5 using 1 N HCl to reduce disulfide bonding. Cuvettes containing polymer solution were allowed to equilibrate for 90 seconds before each absorbance measurement. Absorbance (λ = 450 nm) was measured using a UV/Vis spectrometer (Fluostar Omega, BMG Labtech) every 1°C from 25-45°C with buffer alone as a reference. For samples which precipitated and formed aggregates at higher temperatures, the highest absorbance value before this aggregation was recorded as the maximum value. All absorbance values measured were normalized to the maximum value

measured for that sample. If the polymer did not aggregate, values were normalized to the absorbance at 55°C.

6.2.5. Equilibrium Swelling

Polymer solutions were mixed as described above to obtain final polymer concentrations of 5, 10, 20, and 30 wt%. Immediately after mixing, the solutions were pushed to one syringe and submerged in a water bath at 37°C for 2 minutes. The gels were then incubated for an additional 24 hours at 37°C to allow the gels to crosslink. After 24 hr, the syringe was cut and the gel inside was removed and sliced into 3 approximately equal pieces. Each gel piece was placed into a vial filled with pre-warmed 37°C PBS (pH 7.4) to allow the gel to swell or shrink to equilibrium. After 5 days, the gel sections were removed from the vials, excess water was removed, and the gel pieces were weighed to determine the wet mass (W). Each piece was then lyophilized and again weighed to obtain the measured dry mass (D_m). The dry mass was calculated as:

$$D = D_m - 0.017W$$

to correct for the salt content (1.7 wt%) of the PBS in the polymer. The swelling ratio (S) for each piece of gel was calculated as

$$S = \frac{1.017W - D}{D - 0.017W}$$

The initial swelling ratio S_0 was calculated based on the initial gel concentration (i.e. for a 20 wt% gel, $S_0 = 4$). The relative change in gel volume after 5 days (V/V_0) was then calculated as

$$\frac{V}{V_0} = \frac{S+1}{S_0+1}$$

and reported. Significant differences in relative volume ratio (V/V_0) between gels prepared at the same polymer concentration were determined by Student's *t*-test ($\alpha = 0.05$).

6.2.6. Gelation Kinetics and Rheometry

Hydrogel samples were prepared as described above. The gelation kinetics were measured for the first 30 minutes after mixing. For each sample, 400 mL of prepared polymer solution was placed between the flat 25 mm plates of the rheometer (Anton Paar MCR-101) at a gap height of approximately 0.5 mm. The stage was maintained at 37°C. The experiment was started approximately 60 seconds after the polymer solutions were syringe mixed to allow the gelling solution to reach temperature. The storage and loss moduli were measured under oscillation (0.5% strain, f = 1Hz) for 30 minutes (time sweep) with a humidity chamber placed over the sample to limit evaporation. Normal force control was not used because the gels were initially very weak. Immediately after 30 minutes had elapsed, a frequency sweep was conducted from 0.1-10 Hz (0.5% strain) with the normal force maintained at 100 ± 50 mN.

Hydrogels were evaluated separately to assess their susceptibility to creep after crosslinking. For this test, the hydrogel was allowed to cure for 30 minutes at 37°C under oscillation (0.5% strain, f = 1Hz) under a humidity chamber to limit

evaporation. Immediately after the 30 minute curing period, the strain of each gel was measured under a constant shear stress (5 Pa) for 90 minutes.

6.2.7. Delivery Window Characterization

The delivery window of each polymer system was tested using a 3.0 French polyethylene microcatheter with an inner diameter of 0.018 in (0.46 mm) and length of 55 cm (DHN1, Cook Medical, Bloomington, IN). The microcatheter was primed using normal saline and the length of the catheter, except for about 5 cm at either end, was submerged in a recirculating water bath maintained at 37°C. The saline solution was allowed to equilibrate before the study started. Each polymer solution (30 wt%, 1.1 mL) was prepared by syringe mixing using the method described above. After mixing, the syringe was quickly attached to the microcatheter and 0.4 mL of polymer solution was injected into the catheter 10 seconds after mixing, filling the catheter with polymer solution. At 30 second intervals after the initial injection, 100 μL of polymer solution was injected into the catheter. To test the control of the delivery, the polymer was injected through the catheter using only the thumb, with the syringe held by the first two fingers of the same hand. The end of the delivery window was determined to be when injection of 100 μL of the gelling solution could not be performed or controlled using only the thumb.

6.2.8. *In Vitro* Embolization Model

A stability test for gels based on pNC and pNCJ20 was performed in glass aneurysm models under flow in the parent vessel. The hydrogels were injected into the models at room temperature to assess the stability in the model aneurysm independently of the deliverability of the gels. Glass aneurysm models were obtained from a custom glassblowing shop and consisted of a hollow glass parent vessel of approximately 7 mm inner diameter with an attached spherical side-wall aneurysm with a dome-to-neck ratio of 1.5 and dome width of approximately 10 mm. Such a large neck aneurysm model was intended to present a challenge to this material,[323,324] as temperature-responsive hydrogels previously used in these geometries are associated with a risk of recanalization unless co-delivered with protection devices such as coils or stents.[85]

Precursor solutions were mixed for 15 sec and then immediately injected at room temperature through a cut-off microcatheter into the side-wall aneurysm of the glass model until filling was complete. The models were oriented to allow the polymer solution to settle into the aneurysm and the model was submerged in a 37°C water bath for 10 min to allow for chemical crosslinking to proceed *in situ*. After 10 min, the glass models were placed in series with the recirculating line of a recirculating water bath filled with PBS (pH 7.4) and maintained at 37°C with a flow rate of 40 mL/sec. This flow rate was chosen because it imparts similar shear stress on the gel as that which might be experienced in the carotid artery, where liquid embolic agents have previously been evaluated in pre-clinical experiments.[82,85] Photographs were taken after 7 days to show gel morphology.

6.2.9. *In Vitro* Cytocompatibility

To evaluate cytocompatibility of the hydrogels, an indirect contact methodology was used. Precursor solutions were filter sterilized and gels were left inside one of the coupled syringes overnight at 37°C. Under sterile conditions, the end of the syringe containing the crosslinked gels was cut and the gels were ejected and placed in 10 mL of sterile media pre-warmed to 37°C. The gels were incubated for 1 week with the media changed twice. This step was done to allow the alkaline buffer to exchange out of the gel so that the toxicity of the polymer rather than its pH could be evaluated.

NIH3T3 cells, clone A31, from the American Tissue Culture Collection (ATCC) were seeded in a 24 well plate (10,000 cells/well) and allowed to adhere for 24 hrs (37°C, 5% CO_2) in 550 μL control media (DMEM supplemented with 1% glutamine, 1% pen-strep, and 10% bovine calf serum) per well. Then the gels (which floated in the media) were added to the wells (n = 4). Four wells were also left without gels as a control. Cells were incubated for an additional 72 hr, washed with PBS, and then evaluated for cell number using the CellTiter 96® AQueous Cell Proliferation Assay (Promega, Inc.) according to the manufacturer's instructions. Significant differences in cell number between cells in media without polymer and cells in each concentration of polymer were determined using Student's t-test ($\alpha = 0.05$).

6.3. Results

6.3.1. Composition and Molecular Weight

Poly(NIPAAm-*co*-cysteamine-*co*-JAAm) was successfully synthesized using three feed ratios of JAAm, 0, 10, and 20 wt% as a fraction of all monomers (abbreviated pNC, pNCJ10, and pNCJ20, respectively). A representative ^{1}H NMR spectrum for the pNCJ polymers is shown in Figure 6.3. The molar ratio of cysteamine to NIPAAm and JAAm in each polymer was calculated by comparing the area under the curve (AUC) of the peaks attributed to cysteamine (2H) at 3.4 ppm to the AUC of the peak attributed to the isopropyl proton of NIPAAm (1H) at 4.1 ppm and the peak attributed to the protons of the ethylene oxide repeat units of JAAm (76H) at 3.7 ppm. The results are shown in Table 6.1.

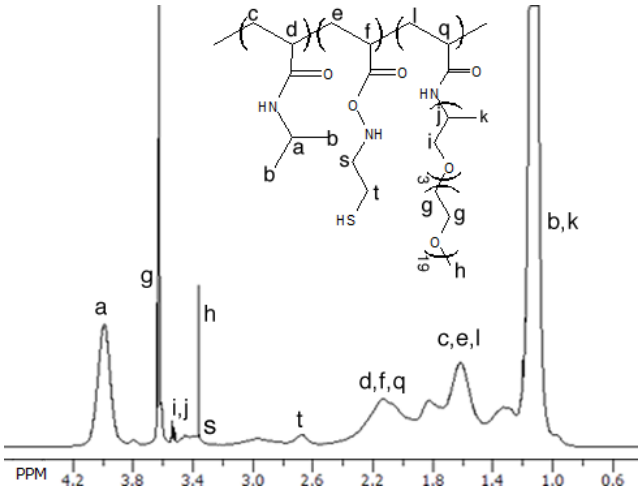

Figure 6.3. ^{1}H NMR spectrum for poly(NIPAAm-*co*-cysteamine-*co*-JAAm).

Table 6.1. Selected properties of *in situ* crosslinking temperature-responsive copolymers

Polymer	Content in Feed Ratio (mol%)			Content by ^{1}H NMR (mol %)			M_n (Da)	P_d	LCST (°C)
	NIPAAm	Cyst	JAAm	NIPAAm	Cyst	JAAm			
pNC	95.0	5.0	0.0	94.7	5.3	0.0	6247	2.13	27
pNCJ10	93.8	4.9	1.3	95.6	3.4	1.0	9584	3.37	29
pNCJ20	92.3	4.9	2.8	93.5	4.4	2.1	15990	4.54	33

Average molecular weight and polydispersity of the synthesized copolymers both increase with increasing JAAm content. This may be attributed to light crosslinking of pendent thiol groups with greater amounts of JAAm during dialysis or storage. Similar polymerizations with THF as the solvent yield number-average molecular weights near 10 kDa.[137]

6.3.2. LCST Transition

The polymer LCST in PBS (pH 5) was between 27-33°C for all polymers tested, as seen in Figure 6.4. The LCST = was evaluated at pH 5 to avoid self-crosslinking. Because the pKa of the thiol of pNC is above 9, the fraction of thiols that are deprotonated will be near zero both at pH 5 and at physiological pH.[325] JAAm increases the LCST slightly for these polymers; however, the LCST is still low enough that the majority of the polymer is physically crosslinked at 37°C. Physical crosslinking is important because it prevents the polymer from diluting in the surrounding aqueous medium prior to chemical crosslinking.

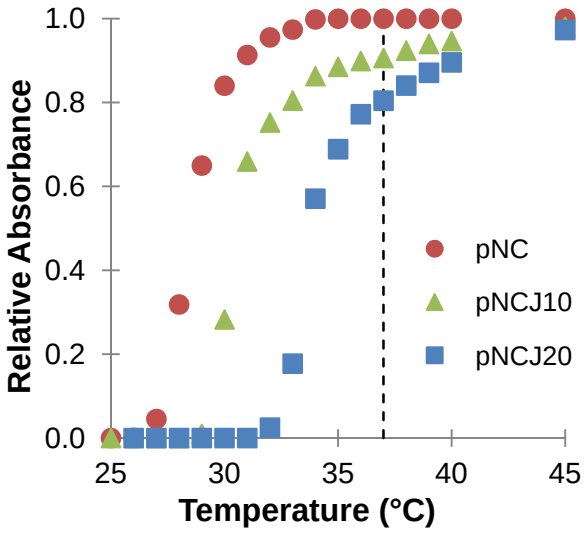

Figure 6.4. Relative absorbance at 450 nm for each of the temperature-responsive polymers pNC (circles), pNCJ10 (triangles), and pNCJ20 (squares) at 0.25 wt% (150 mM PBS, pH 5). LCST increased with JAAm content in the copolymers.

6.3.3. Swelling

Gel swelling was dependent on polymer concentration and JAAm content as shown in Figure 6.5. Retention of volume is reported rather than swelling ratio because was deemed more relevant to assessing potential for effective aneurysm embolization and also because the swelling ratio (defined as the ratio of wet weight to dry weight) of these gels varies with concentration. Both copolymer gels containing JAAm showed significantly increased relative volume ratio ($p < 0.05$) relative to pNC gels at every concentration tested. pNC gels shrank from their initial volume in all cases. At 5 wt%, both gels with JAAm shrank, with pNCJ20 gels being slightly more swollen than pNCJ10 gels. At 10 and 20 wt% polymer concentration, the equilibrium volume of pNCJ10 and pNCJ20 gels

remained within 20% of their initial volume. This demonstrates the gels having some shape memory because they were crosslinked inside a closed container (in this case, a syringe). At 30 wt% polymer concentration, both gels containing JAAm swelled beyond their initial volume, with pNCJ20 gels increasing in volume by about 75%.

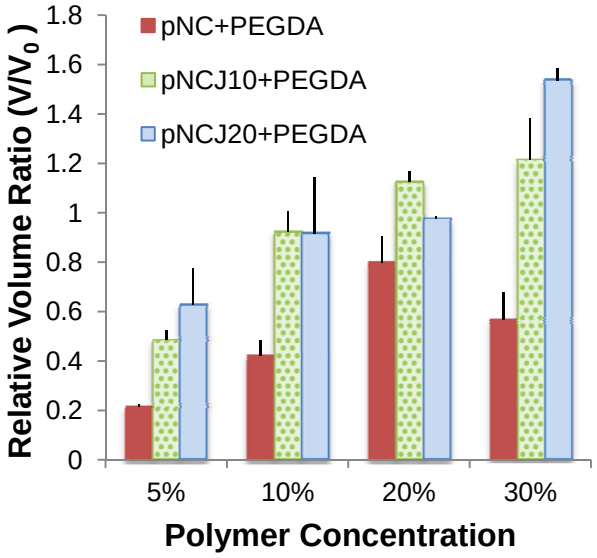

Figure 6.5. Equilibrium gel volume to original gel volume ratio for each polymer system at various hydrogel concentrations. JAAm had a positive effect on hydrogel swelling. Data are reported as mean +/- s.d (n = 3).

6.3.4. Gelation Kinetics and Rheometry

The rheological properties of each gelling system during the first 30 minutes at 37°C are shown in Figure 6.6, with the frequency response of each system after 30 minutes shown in Figure 6.7. Immediately upon heating, the pNC+PEGDA gelling system becomes a viscoelastic gel with storage and loss moduli both above 1000 Pa. Over the following 30 minutes, the storage modulus

of the pNC system increases the least. After 30 minutes, the rheological properties of the pNC gelling system are frequency dependent, characteristic of a viscoelastic material.[144,246,250] The initial strength of the pNC gel is derived from physical crosslinking between pNC chains, while the small increase in storage modulus indicates that chemical crosslinking between pNC and PEGDA is slow and incomplete.

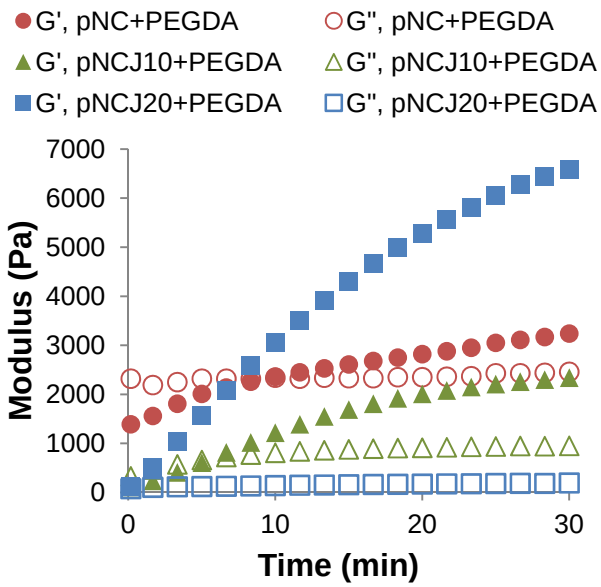

Figure 6.6. Time sweeps showing the storage (solid icons) and loss (open icons) moduli of pNC+PEGDA (circles), pNCJ10+PEGDA (triangles), and pNCJ20+PEGDA (squares) hydrogels at 30 wt%. Hydrogels with greater JAAm content have lower loss modulus and become elastic more quickly.

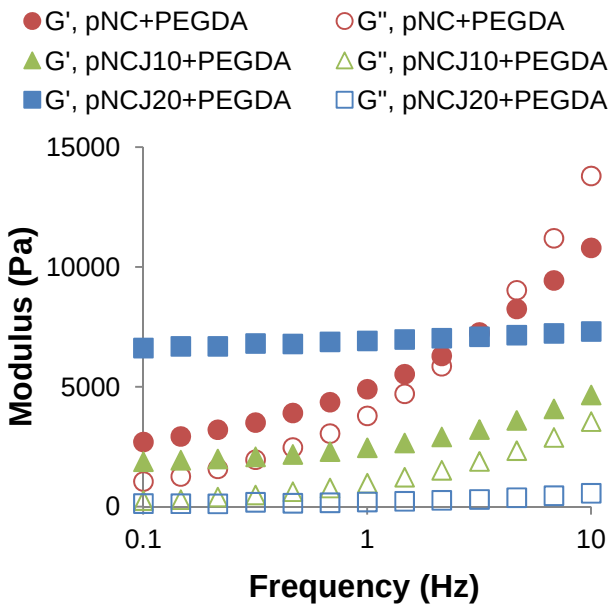

Figure 6.7. Frequency sweeps showing the storage (solid icons) and loss (open icons) moduli of pNC+PEGDA (circles), pNCJ10+PEGDA (triangles), and pNCJ20+PEGDA (squares) hydrogels at 30 wt %. Frequency dependence decreases and elasticity increases with increasing JAAm content.

The pNCJ20+PEGDA gelling system is initially weak, with storage and loss moduli below 200 Pa. While the loss modulus remains nearly constant throughout gelation, the storage modulus increases to over 6000 Pa after 30 minutes, the highest of all formulations tested The moduli of the crosslinked pNCJ20+PEGDA gel are relatively independent of frequency, characteristic of an elastic gel.[275,278] The pNCJ10+PEGDA gel has intermediate properties in terms of its increase in storage modulus, initial strength, and frequency response after 30 minutes. pNCJ10 gels have the lowest storage modulus after 30 minutes and an intermediate ratio of G' to G", indicating that the increase in chemical

crosslinking relative to pNC is not enough to overcome the hindered physical crosslinking caused by JAAm.

Creep characterization for pNC and pNCJ20 gelling systems after 30 minutes at 37°C is shown in Figure 6.8. pNC gels show significant creep under a low constant shear stress, deforming by up to 40% within 1 hr. pNCJ20 gels show very little creep and only about 0.05% strain over 1 hour, evidence of purely elastic behavior.

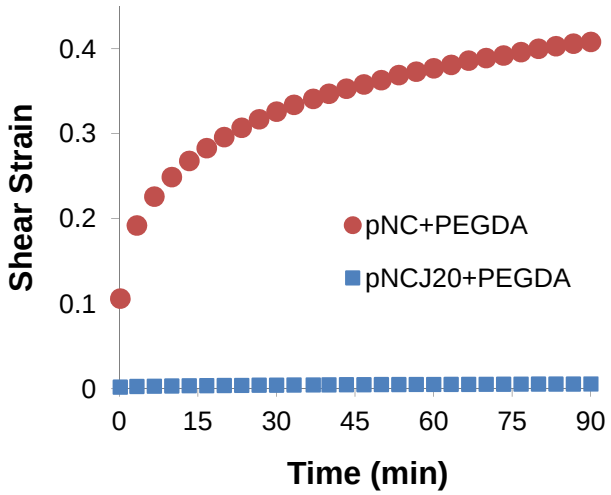

Figure 6.8. Creep test showing the shear strain of the hydrogels, pNC+PEGDA (circles) and pNCJ20+PEGDA (squares). The pNC+PEGDA hydrogel is prone to creep under a constant shear stress whereas the pNCJ20+PEGDA hydrogel is not.

6.3.5. Delivery Window

The delivery window for each hydrogel is shown in Table 6.2. While the pNC system can be quickly injected into a microcatheter filled with warm saline, it gels inside the catheter within 30 seconds. Polymers with greater JAAm content

was deliverable for a longer time, and the pNCJ20 system was injectable for all time points (up to 220 sec) tested. However, increased pressure was required to deliver the pNCJ20 system 220 sec after mixing.

Table 6.2. Delivery window of physical-chemical gelling polymer systems at 37°C

Polymer System	End of Delivery Window (post-mixing)
pNC+PEGDA	Less than 40 sec
pNCJ10+PEGDA	160 sec
pNCJ20+PEGDA	Over 220 sec

6.3.6. *In Vitro* Embolization Model

Photographs of physical-chemical gels inside glass model aneurysms after 1 week at 37°C are shown in Figure 6.9. Both hydrogels remained in the model aneurysms throughout the experiment and did not visibly deform or show recanalization of the aneurysm. Because the gels were delivered at room temperature, this test was not affected by the poor deliverability of the pNC gelling system.

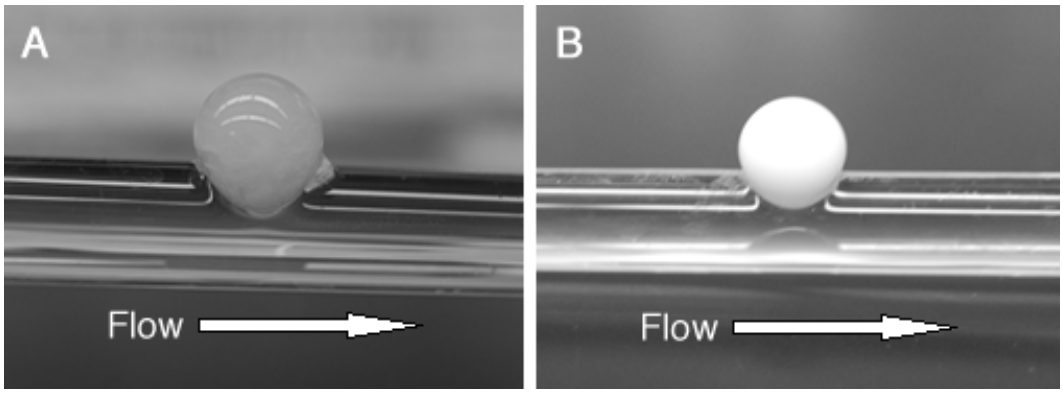

Figure 6.9. Pictures of glass model aneurysms with (A) pNC+PEGDA and (B) pNCJ20+PEGDA hydrogels after 7 days at 37°C. Flow in the parent vessel (d = 0.7 cm) was maintained at 40 mL/sec.

6.3.7. *In Vitro* Cytocompatibility

In vitro cytocompatibility results are shown in Figure 6.10. Hydrogels were allowed to crosslink for 24 hr and then soak in media for 1 week prior to the study to allow the initiating solution to rinse out of the gel. Fibroblasts were able to proliferate in the presence of each hydrogel. The number of cells after 72 hr was lower in both cases when cultured in the presence of hydrogel compared to control. pNC+PEGDA gels showed significantly lower cell number than control ($p < 0.001$), while the difference between pNCJ20+PEGDA and control was not significant ($p = 0.15$).

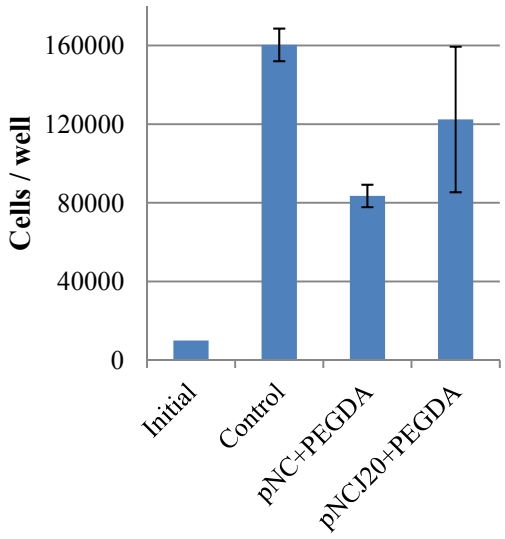

Figure 6.10. NIH3T3 fibroblasts present per well after 72 hrs in culture with or without hydrogels in each well. Data are reported as mean +/- s.d. (n=3).

6.4. Discussion

6.4.1. Swelling

Equilibrium swelling greater than the initial volume, as exhibited by pNCJ20+PEGDA, is likely to be tolerable or perhaps advantageous for a liquid embolic agent. These gels may not be so strong as to cause the aneurysm sac to distend, and instead the gel may permanently remain at a volume below that dictated by its equilibrium swelling. Accordingly, the tendency of the gels to expand inside the aneurysm could provide some interfacial pressure between the gel and aneurysm wall, reducing recanalization.

6.4.2. Gelation Kinetics and Delivery

Unlike pNC, the pNCJ20 gelling system's high increase in rheological properties is strong evidence that chemical crosslinking between pNCJ20 and PEGDA is faster and more complete within a timeframe relevant for endovascular embolization (i.e. 10-30 minutes). The gel's modulus after 30 minutes is approximately an order of magnitude greater than previously reported lightly crosslinked NIPAAm-based hydrogels used for embolization.[85,119] The difference in creep despite these materials having similar complex moduli demonstrates the importance of elasticity derived from chemical crosslinking on the stability of these hydrogels for embolization, which requires the gel to retain its shape after many repeated stresses.

Physical temperature-induced crosslinking observed in the pNC system cannot be slowed adequately in this system without a cooling jacket, as the temperature surrounding the microcatheter in an endovascular procedure is always physiological. The delivery window for the polymer systems containing JAAm grafts could potentially be controlled by changing the pH of the PEGDA precursor solution (controlling the rate of chemical crosslink formation), with higher pH leading to faster gelation and a shorter required delivery time.

6.4.3. *In Vitro* Embolization Model and Cytocompatibility

The lack of shrinking observed in the pNC gel (Figure 6.9A) suggests that the gel may have adhered to the glass, resulting in either no recanalization or gel collapse and recanalization only in the center of the aneurysm where it could not

be seen. Another important limitation of this study was the use of constant rather than pulsatile flow. By approximating the shear stress to which the gel would be exposed *in vivo*, the glass model experiment demonstrates that the pNCJ20+PEGDA gel (Figure 6.9B) is strong enough to withstand a shear stress of similar magnitude to physiological after 10 minutes of crosslinking. As gels with about 0.1 times the shear modulus of the gels reported in this work have been retained inside model aneurysms in swine,[85] it is reasonable to expect that these materials would perform at least as well *in vivo*.

A noticeable difference between the gels in glass models was that the pNCJ20 gels appeared bright white while the pNC gels were off-white and slightly less opaque. A small portion of the pNC+PEGDA gelling solution was carried away from the aneurysm in the parent vessel over the first 15 minutes of flow, and the recirculating fluid in the parent vessel for the pNC study was slightly turbid after the study. It is possible that the pNC gels had a broader LCST transition after crosslinking due to incomplete crosslinking with PEGDA. If a fraction of the PEGDA was bound on one end and free on the other, the thiol-bearing repeat units becoming more hydrophilic would lead to an increase in LCST. On the other hand, the pNCJ20 gels became more opaque than when initially heated to 37°C due to the high extent of crosslinking causing an effective increase in polymer molecular weight, which is known to decrease the LCST.[100,285]

The significantly lower cytocompatibility of the pNC+PEGDA gelling system may also be attributed to poor crosslinking and leaching of soluble

PEGDA from the pNC physically crosslinked network into the culture media. Acrylate species on otherwise cytocompatible polymers including PEG are known to be cytotoxic.[326,327] Without additional data, it is not possible to determine whether PEGDA or some other leachable was responsible for the lower cell numbers observed in cultures with polymer gels. *In vivo* studies would be required to assess the local biocompatibility of the device because the present study did not evaluate cell attachment on the hydrogel and thus the potential to allow a neointimal layer to form over the gel is unknown and the short-term toxicity due to the high pH of the gel was not explored. An *in vitro* cytotoxicity test which adequately predicts this system's *in vivo* toxicity is difficult at best because the spatially variable exchange of alkaline buffer out of the gel *in vivo* is difficult to reproduce.

6.4.4. Comparison of pNCJ20 and pNC Gelling Systems for Embolization

There are three major flaws of the pNC physical-chemical gelling system, namely: 1) it shrinks rapidly after gelation; 2) it is too strong to be injectable at body temperature; and 3) it is liable to creep because of poor crosslinking at temperatures above the LCST.

First, JAAm grafts improve gel swelling due to their hydrophilicity. Second, JAAm grafts weaken the physical interaction between polymer chains above the LCST, resulting in lower initial gel strength when physically crosslinked. Thus the requirement of a cooling catheter for endovascular delivery can be avoided, and the gelling solution can be delivered for up to 4 minutes after

mixing. Third, JAAm grafts increase the rate of chemical reaction on the polymer when heated above its LCST. While similar polymer systems without hydrophilic grafts are able to crosslink below the LCST[275] or to a lesser extent when the mixing time at room temperature is long,[274] the pNCJ20+PEGDA material reported in this work is the first based on NIPAAm in which chemical crosslinking above the LCST results in a purely elastic gel. It is by coincidence that adding JAAm to the polymer causes changes in three properties (swelling, delivery time, and final strength) which all improve the ability of the polymer system to serve as a liquid embolic.

6.5. Conclusions

Hydrogels capable of simultaneous physical and chemical crosslinking were successfully prepared by mixing aqueous precursor solutions of poly(NIPAAm-*co*-cysteamine-*co*-JAAm) and poly(ethylene glycol) diacrylate. Fast physical crosslinking is intended to prevent dilution of the polymer upon delivery into an aneurysm while subsequent chemical crosslinking increases the strength and elasticity of the gel. Polymers with JAAm grafts are deliverable through a microcatheter and undergo more rapid and complete crosslinking, yielding an elastic gel with an elastic shear modulus over 6000 Pa within 30 minutes at 37°C. Gel swelling was also determined to be dependent on JAAm content. Further testing *in vivo* will be required to assess whether this swelling behavior is acceptable or if it may require a modification to the delivery procedure such as sub-complete aneurysm filling.[84] The pNCJ20+PEGDA system

reported in this work combines the capability to completely fill an aneurysm while enabling a faster and simpler delivery procedure than solvent-exchange precipitating materials allow. Taken together, the data on the pNCJ20+PEGDA system reported in this work supports the further investigation and development of these hydrogels for endovascular embolization of cerebral aneurysms.

Chapter 7: CONCLUSIONS AND FUTURE WORK

This dissertation reports on the development of temperature-responsive polymers based on *N*-isopropylacrylamide (NIPAAm) with hydrophilic side-chain grafts of Jeffamine® M-1000 acrylamide (JAAm). Because of the graft copolymer architecture, the water content within the gels at body temperature can be controlled over a wide range without undesirably altering the LCST. Other approaches such as copolymerization with low molecular weight monomers, introduction of crosslinkers, and mixing with hydrophilic chain molecules produce hydrogels which have inherent limitations for most applications (including burst release, LCST above body temperature, poor delivery characteristics).

The experimental approach to this work was to first synthesize and characterize these copolymers in terms of their capability for gelation, swelling, and drug release, with the hypothesis that controlled gel swelling would affect release rates from the hydrogels. Following this initial phase of investigation, the utility of this graft copolymer design was explored by developing resorbable hydrogels for drug delivery and *in situ* crosslinkable hydrogels for endovascular embolization. In all of the gels, JAAm incorporation allowed for controlled water content without unacceptable effects on LCST or delivery properties. JAAm grafts led to other (often unanticipated) changes in gel properties which in almost every respect bode well for the further development of these gels toward clinical applications in embolization and especially drug delivery.

7.1. Temperature-Responsive Graft Copolymer Design

Temperature-responsive graft copolymers of NIPAAm and JAAm were made in an attempt to combine the desirable LCST property of poly(NIPAAm) with the hydrophilicity imparted by JAAm, a PEG-based macromer. The objective of this work was to demonstrate proof-of-principle for controlling gel swelling nearly independently of LCST, and to characterize important differences in other properties relevant to potential applications as materials in medicine.

This work demonstrated that JAAm provides excellent control over swelling with a low impact on LCST, eliminating the design tradeoffs inherent with using acrylic acid or PEGDA to control swelling. The gels were very soft, behaving as viscoelastic fluids above the LCST. Copolymers also required higher concentrations to form gels. Finally, copolymer gels significantly slowed the release of ovalbumin whereas homopolymer gels released nearly 100% within minutes.

The weak physical crosslinking and controlled release properties observed in this material provided valuable proof-of-concept to justify the subsequent work. The poly(NIPAAm-*co*-JAAm), while not necessarily useful on its own, demonstrated for the first time controlled swelling above the LCST without confounding effects on LCST, degradation, or delivery properties. The principle of using polymer architecture is not completely new, but further research in biomaterials and other areas are likely to find more materials problems that graft copolymers will address in an improved way.

7.2. Resorbable Temperature-Responsive Graft Copolymer Hydrogels for Drug Delivery

The graft copolymers of NIPAAm and JAAm were made resorbable by copolymerization with DBLA, a comonomer which causes an increase in LCST upon degradation. JAAm led to controlled gel swelling, slower drug release (particularly for cefazolin, a hydrophilic antimicrobial), weaker gelation, and faster degradation. An interesting and new property of these materials is that they are both water-insoluble and liquid-like above the LCST, allowing for the gel to deform yet remain cohesive *in situ*.

In terms of their appropriateness for preventing prosthetic joint infection, the poly(NIPAAm-*co*-DBLA-*co*-JAAm) hydrogels reported in this work have properties which may enable local delivery to joint replacement sites. While local delivery is likely to be required for effective antimicrobial prophylaxis in joints, it remains impossible using materials currently in FDA-approved products. Because the pNDJ gels are viscoelastic fluids, they can completely coat a joint prosthesis without generating wear debris like a hard material such as PLGA or bone cement. The hydrogels can be loaded with much higher amounts of drugs than bone cement, and provide complete release within about one week, providing a similar release profile to surgeon-mixed bone cements used clinically for infection management. Finally, the rapid degradation of the gels may enable their use in sites through which healing takes place within weeks, whereas harder materials already in FDA-approved products are degradable only over months or more. The

gels may also be suitable for a variety of other applications, including in fractures or to protect other device surfaces against infection.

Future work on antimicrobial-loaded hydrogels for prevention of prosthetic joint infection should consist of *in vivo* evaluation of biocompatibility, demonstration of bone healing through an implant-bone interface with gel present simulating, and anti-infection effectiveness on an implanted material. Because the hydrogel on its own has no therapeutic effect, a final product to be considered for regulatory approval would consist of the gelling solution and one or more active ingredients. Because it is likely most cost-effective to use a single antimicrobial, the antimicrobial should be chosen such that it is effective against a broad spectrum of organisms which are responsible for prosthetic joint infection. If these early *in vivo* experiments are successful, then the pursuit of approval as a new drug product is warranted. While developing new drugs is both time and resource intensive, the reasonable cost of the polymer, clinical need, and market size all help to justify the high cost and risk associated with commercializing this polymer.

7.3. *In Situ* Crosslinking Temperature-Responsive Graft Copolymer Hydrogels for Embolization

Simultaneously physical-chemical gelling hydrogels were made by mixing aqueous solutions of PEGDA and poly(NIPAAm-*co*-JAAm-*co*-cysteamine), a thiol-modified polymer. This design was pursued as PEGDA is soluble and mobile in water, allowing it to more completely crosslink the polymer network.

The molecular weight of the temperature-responsive polymer (pNCJ) was intended to be low (around 10 kDa) to allow the gelling solution to be delivered through a microcatheter under physiological conditions. JAAm affected the swelling of the networks, led to a longer delivery window, and higher final strength.

The biocompatibility and ability of the hydrogels to embolize cerebral aneurysms will require *in vivo* validation. Such a material would likely have to address large or giant aneurysms where coils tend to fail, because coils are popular and easy to use in most cases. This system represents a clear improvement in terms of procedure cost, delivery properties, and final properties relative to previously reported NIPAAm-based embolic agents in the literature. However, it remains unclear which, if any, *in situ* forming liquid embolic hydrogels are most effective in the indications which are poorly treated by available materials and therefore represent the best opportunity both for a viable path to market and improved patient care.

REFERENCES

1. Van Vlierberghe, S., Dubruel, P. & Schacht, E. Biopolymer-based hydrogels as scaffolds for tissue engineering applications: a review. *Biomacromolecules* **12**, 1387–1408 (2011).

2. Hou, Q., De Bank, P. A. & Shakesheff, K. M. Injectable scaffolds for tissue regeneration. *J Mater Chem* **14**, 1915–1923 (2004).

3. Nelson, D. M., Ma, Z., Fujimoto, K. L., Hashizume, R. & Wagner, W. R. Intra-myocardial biomaterial injection therapy in the treatment of heart failure: Materials, outcomes and challenges. *Acta Biomaterialia* **7**, 1–15 (2011).

4. Sawhney, A. S., Pathak, C. P., van Rensburg, J. J., Dunn, R. C. & Hubbell, J. A. Optimization of photopolymerized bioerodible hydrogel properties for adhesion prevention. *J Biomed Mater Res* **28**, 831–838 (1994).

5. Hill-West, J. L., Chowdhury, S. M., Slepian, M. J. & Hubbell, J. A. Inhibition of thrombosis and intimal thickening by *in situ* photopolymerization of thin hydrogel barriers. *Proc. Natl. Acad. Sci. USA* **91**, 5967–5971 (1994).

6. Jeong, B., Choi, Y. K., Bae, Y. H., Zentner, G. M. & Kim, S. W. New biodegradable polymers for injectable drug delivery systems. *J. Control. Rel.* **62**, 109–114 (1999).

7. Hatefi, A. & Amsden, B. Biodegradable injectable in situ forming drug delivery systems. *J Control Rel* **80**, 9–28 (2002).

8. Garrett, W. E. American Board of Orthopaedic Surgery Practice of the Orthopaedic Surgeon: Part-II, Certification Examination Case Mix. *J. Bone Joint Surg Am* **88**, 660–667 (2006).

9. Kurtz, S., Ong, K., Lau, E., Mowat, F. & Halpern, M. Projections of Primary and Revision Hip and Knee Arthroplasty in the United States from 2005 to 2030. *J. Bone Joint Surg Am* **89**, 780–785 (2007).

10. Khanuja, H. S., Vakil, J. J., Goddard, M. S. & Mont, M. A. Cementless femoral fixation in total hip arthroplasty. *J Bone Joint Surg Am* **93**, 500–509 (2011).

11. Dunbar, M. J. Cemented femoral fixation: the North Atlantic divide. *Orthopedics* **32**, (2009).

12. Insall, J. N., Binazzi, R., Soudry, M. & Mestriner, L. A. Total knee arthroplasty. *Clin. Orthop. Relat. Res.* 13–22 (1985).

13. Font-Rodriguez, D. E., Scuderi, G. R. & Insall, J. N. Survivorship of cemented total knee arthroplasty. *Clin. Orthop. Relat. Res.* 79–86 (1997).

14. Hirakawa, K., Bauer, T. W., Stulberg, B. N. & Wilde, A. H. Comparison and quantitation of wear debris of failed total hip and total knee arthroplasty. *J Biomed Mater Res* **31**, 257–263 (1996).

15. Shanbhag, A. S. *et al.* Quantitative analysis of ultrahigh molecular weight polyethylene (UHMWPE) wear debris associated with total knee replacements. *J. Biomed. Mater. Res.* **53**, 100–110 (2000).

16. Sharkey, P. F., Hozack, W. J., Rothman, R. H., Shastri, S. & Jacoby, S. M. Insall Award paper. Why are total knee arthroplasties failing today? *Clin. Orthop. Relat. Res.* 7–13 (2002).

17. Wasielewski, R. C., Galante, J. O., Leighty, R. M., Natarajan, R. N. & Rosenberg, A. G. Wear patterns on retrieved polyethylene tibial inserts and their relationship to technical considerations during total knee arthroplasty. *Clin. Orthop. Relat. Res.* 31–43 (1994).

18. Darwiche, H., Barsoum, W. K., Klika, A., Krebs, V. E. & Molloy, R. Retrospective Analysis of Infection Rate After Early Reoperation in Total Hip Arthroplasty. *Clin. Orthop. Relat. Res.* **468**, 2392–2396 (2010).

19. Lentino, J. R. Prosthetic joint infections: bane of orthopedists, challenge for infectious disease specialists. *Clin Infect Dis* **36**, 1157 (2003).

20. Senthi, S., Munro, J. T. & Pitto, R. P. Infection in total hip replacement: meta-analysis. *Int Orthop* **35**, 253–260 (2010).

21. Haddad, F. S., Muirhead-Allwood, S. K., Manktelow, A. R. J. & Bacarese-Hamilton, I. Two-stage uncemented revision hip arthroplasty for infection. *J Bone Joint Surg Br* **82**, 689–694 (2000).

22. Kraay, M. J., Goldberg, V. M., Fitzgerald, S. J. & Salata, M. J. Cementless Two-staged Total Hip Arthroplasty for Deep Periprosthetic Infection. *Clin Orthop Relat Res* **441**, 243–249 (2005).

23. Berbari, E. F. *et al.* Risk factors for prosthetic joint infection: case-control study. *Clin Infect Dis* **27**, 1247–1254 (1998).

24. Bernthal, N. M. *et al.* A Mouse Model of Post-Arthroplasty Staphylococcus aureus Joint Infection to Evaluate In Vivo the Efficacy of Antimicrobial Implant Coatings. *PLoS ONE* **5**, e12580 (2010).

25. Bozic, K. J. & Ries, M. D. The impact of infection after total hip arthroplasty on hospital and surgeon resource utilization. *J. Bone Joint Surg Am* **87**, 1746–1751 (2005).

26. Gristina, A. Biomaterial-centered infection: microbial adhesion versus tissue integration. *Science* **237**, 1588–1595 (1987).

27. Costerton, J. W., Stewart, P. S. & Greenberg, E. P. Bacterial Biofilms: A Common Cause of Persistent Infections. *Science* **284**, 1318–1322 (1999).

28. Ceri, H. *et al.* The Calgary Biofilm Device: new technology for rapid determination of antibiotic susceptibilities of bacterial biofilms. *J Clin Microbiol* **37**, 1771–1776 (1999).

29. Cerca, N. *et al.* Comparative assessment of antibiotic susceptibility of coagulase-negative staphylococci in biofilm versus planktonic culture as assessed by bacterial enumeration or rapid XTT colorimetry. *J Antimicrob Microbiol* **56**, 331–336 (2005).

30. Ashby, M. J., Neale, J. E., Knott, S. J. & Critchley, I. A. Effect of antibiotics on non-growing planktonic cells and biofilms of Escherichia coli. *J Antimicrob Chemother* **33**, 443–452 (1994).

31. Hanssen, A. D. & Rand, J. A. Instructional Course Lectures, The American Academy of Orthopaedic Surgeons-Evaluation and Treatment of Infection at the Site of a Total Hip or Knee Arthroplasty. *J Bone Joint Surg Am* **80**, 910–922 (1998).

32. Ong, K. L. *et al.* Prosthetic joint infection risk after total hip arthroplasty in the Medicare population. *J. Arthroplasty* **24**, 105–109 (2009).

33. Kurtz, S. M. *et al.* Prosthetic Joint Infection Risk after TKA in the Medicare Population. *Clin. Orthop. Relat. Res.* **468**, 52–56 (2009).

34. Bourne, R. B. Prophylactic use of antibiotic bone cement:: an emerging standard–in the affirmative. *J Arthroplasty* **19**, 69–72 (2004).

35. Hanssen, A. D. & Spangehl, M. J. Practical Applications of Antibiotic-Loaded Bone Cement for Treatment of Infected Joint Replacements. *Clin. Orthop. Relat. Res.* **427**, 79–85 (2004).

36. Moran, J. M., Greenwald, A. S. & Matejczyk, M.-B. Effect of Gentamicin on Shear and Interface Strengths of Bone Cement. *Clin Orthop Relat Res* **141**, 96–101 (1979).

37. Davies, J. P., O'Connor, D. O., Burke, D. W. & Harris, W. H. Influence of antibiotic impregnation on the fatigue life of simplex P and palacos R acrylic

bone cements, with and without centrifugation. *J Biomed Mater Res* **23**, 379–397 (1989).

38. Penner, M. J., Duncan, C. P. & Masri, B. A. The in vitro elution characteristics of antibiotic-loaded CMW and Palacos-R bone cements. *J Arthroplasty* **14**, 209–214 (1999).

39. Miller, R. B., McLaren, A. C., Leon, C. M., Vernon, B. L. & McLemore, R. Surfactant-stabilized Emulsion Increases Gentamicin Elution From Bone Cement. *Clin Orthop Relat Res* **469**, 2995–3001 (2011).

40. Hope, P., Kristinsson, K., Norman, P. & Elson, R. Deep infection of cemented total hip arthroplasties caused by coagulase-negative staphylococci. *J. Bone Joint Surg Br* **71**, 851–855 (1989).

41. Bohner, M. *et al.* Gentamicin-loaded hydraulic calcium phosphate bone cement as antibiotic delivery system. *J. Pharm. Sci.* **86**, 565–572 (1997).

42. Barralet, J., Gaunt, T., Wright, A., Gibson, I. & Knowles, J. Effect of porosity reduction by compaction on compressive strength and microstructure of calcium phosphate cement. *J. Biomed. Mater. Res. (Appl. Biomater.)* **63**, 1–9 (2002).

43. Hak, D. J. The use of osteoconductive bone graft substitutes in orthopaedic trauma. *J Am Acad Orthop Surg* **15**, 525–536 (2007).

44. Alt, V. *et al.* Effects of gentamicin and gentamicin–RGD coatings on bone ingrowth and biocompatibility of cementless joint prostheses: An experimental study in rabbits. *Acta Biomaterialia* **7**, 1274–1280 (2011).

45. Parvizi, J. *et al.* Titanium Surface with Biologic Activity against Infection. *Clin. Orthop. Relat. Res.* **429**, 33–38 (2004).

46. Antoci Jr, V. *et al.* The inhibition of Staphylococcus epidermidis biofilm formation by vancomycin-modified titanium alloy and implications for the treatment of periprosthetic infection. *Biomaterials* **29**, 4684–4690 (2008).

47. Lucke, M. *et al.* Gentamicin coating of metallic implants reduces implant-related osteomyelitis in rats. *Bone* **32**, 521–531 (2003).

48. Price, J. S., Tencer, A. F., Arm, D. M. & Bohach, G. A. Controlled release of antibiotics from coated orthopedic implants. *J. Biomed. Mater. Res.* **30**, 281–286 (1996).

49. Gollwitzer, H. Antibacterial poly(D,L-lactic acid) coating of medical implants using a biodegradable drug delivery technology. *J. Antimicrob. Chemother.* **51**, 585–591 (2003).

50. De Giglio, E. *et al.* Ciprofloxacin-modified electrosynthesised hydrogel coatings to prevent titanium implant-associated infections. *Acta Biomaterialia* (2010).

51. Changez, M., Koul, V. & Dinda, A. K. Efficacy of antibiotics-loaded interpenetrating network (IPNs) hydrogel based on poly(acrylic acid) and gelatin for treatment of experimental osteomyelitis: in vivo study. *Biomaterials* **26**, 2095–2104 (2005).

52. Inagawa, T. & Hirano, A. Autopsy study of unruptured incidental intracranial aneurysms. *Surg Neurol* **34**, 361–365 (1990).

53. Juvela, S., Porras, M. & Heiskanen, O. Natural history of unruptured intracranial aneurysms: a long-term follow-up study. *J. Neurosurg.* **79**, 174–182 (1993).

54. Schievink, W. I. Intracranial aneurysms. *N Engl J Med* **336**, 28–40 (1997).

55. Molyneux, A. International Subarachnoid Aneurysm Trial (ISAT) of neurosurgical clipping versus endovascular coiling in 2143 patients with ruptured intracranial aneurysms: a randomised trial. *The Lancet* **360**, 1267–1274 (2002).

56. McKissock, W., Richardson, A. & Walsh, L. Anterior Communicating Aneurysms: A Trial of Conservative and Surgical Treatment. *Lancet* **1**, 874–876 (1965).

57. Kanaan, Y., Kaneshiro, D., Fraser, K., Wang, D. & Lanzino, G. Evolution of endovascular therapy for aneurysm treatment. Historical overview. *Neurosurg Focus* **18**, E2 (2005).

58. Linfante, I. & Wakhloo, A. K. Brain aneurysms and arteriovenous malformations: advancements and emerging treatments in endovascular embolization. *Stroke* **38**, 1411–1417 (2007).

59. Hayakawa, M. *et al.* Natural history of the neck remnant of a cerebral aneurysm treated with the Guglielmi detachable coil system. *J. Neurosurg.* **93**, 561–568 (2000).

60. Murayama, Y. *et al.* Guglielmi detachable coil embolization of cerebral aneurysms: 11 years' experience. *J. Neurosurg.* **98**, 959–966 (2003).

61. Sluzewski, M., Menovsky, T., van Rooij, W. J. & Wijnalda, D. Coiling of very large or giant cerebral aneurysms: long-term clinical and serial angiographic results. *Am J Neuroradiol* **24**, 257–262 (2003).

62. Kawanabe, Y., Sadato, A., Taki, W. & Hashimoto, N. Endovascular occlusion of intracranial aneurysms with Guglielmi detachable coils: correlation between coil packing density and coil compaction. *Acta Neurochir (Wien)* **143**, 451–455 (2001).

63. Piotin, M. *et al.* Dense packing of cerebral aneurysms: an in vitro study with detachable platinum coils. *AJNR Am J Neuroradiol* **21**, 757–760 (2000).

64. Slob, M. J., Sluzewski, M. & van Rooij, W. J. The relation between packing and reopening in coiled intracranial aneurysms: a prospective study. *Neuroradiology* **47**, 942–945 (2005).

65. Tamatani, S. *et al.* Evaluation of the stability of aneurysms after embolization using detachable coils: correlation between stability of aneurysms and embolized volume of aneurysms. *AJNR Am J Neuroradiol* **23**, 762–767 (2002).

66. Cloft, H. J. & Kallmes, D. F. Aneurysm packing with HydroCoil Embolic System versus platinum coils: initial clinical experience. *AJNR Am J Neuroradiol* **25**, 60–62 (2004).

67. Fiorella, D., Albuquerque, F. C., Woo, H. H., McDougall, C. G. & Rasmussen, P. A. The role of neuroendovascular therapy for the treatment of brain arteriovenous malformations. *Neurosurgery* **59**, S163–177; discussion S3–13 (2006).

68. Slob, M. J., van Rooij, W. J. & Sluzewski, M. Coil thickness and packing of cerebral aneurysms: a comparative study of two types of coils. *AJNR Am J Neuroradiol* **26**, 901–903 (2005).

69. Taha, M. M. *et al.* Endovascular embolization vs surgical clipping in treatment of cerebral aneurysms: morbidity and mortality with short-term outcome. *Surg Neurol* **66**, 277–284; discussion 284 (2006).

70. Lanzino, G., Kanaan, Y., Perrini, P., Dayoub, H. & Fraser, K. Emerging concepts in the treatment of intracranial aneurysms: stents, coated coils, and liquid embolic agents. *Neurosurgery* **57**, 449–459; discussion 449–459 (2005).

71. Arthur, A. S., Wilson, S. A., Dixit, S. & Barr, J. D. Hydrogel-coated coils for the treatment of cerebral aneurysms: preliminary results. *Neurosurg Focus* **18**, E1 (2005).

72. Fanning, N. F., Berentei, Z., Brennan, P. R. & Thornton, J. HydroCoil as an adjuvant to bare platinum coil treatment of 100 cerebral aneurysms. *Neuroradiology* **49**, 139–148 (2007).

73. Kang, H.-S. *et al.* Embolization of intracranial aneurysms with hydrogel-coated coils: result of a Korean multicenter trial. *Neurosurgery* **61**, 51–58; discussion 58–59 (2007).

74. Fiorella, D., Albuquerque, F. C. & McDougall, C. G. Durability of aneurysm embolization with matrix detachable coils. *Neurosurgery* **58**, 51–59; discussion 51–59 (2006).

75. Murayama, Y., Tateshima, S., Gonzalez, N. R. & Vinuela, F. Matrix and bioabsorbable polymeric coils accelerate healing of intracranial aneurysms: long-term experimental study. *Stroke* **34**, 2031–2037 (2003).

76. Taschner, C. A., Leclerc, X., Rachdi, H., Barros, A. M. & Pruvo, J.-P. Matrix detachable coils for the endovascular treatment of intracranial aneurysms: analysis of early angiographic and clinical outcomes. *Stroke* **36**, 2176–2180 (2005).

77. Bendszus, M., Bartsch, A. J. & Solymosi, L. Endovascular occlusion of aneurysms using a new bioactive coil: a matched pair analysis with bare platinum coils. *Stroke* **38**, 2855–2857 (2007).

78. Bendszus, M. & Solymosi, L. Cerecyte coils in the treatment of intracranial aneurysms: a preliminary clinical study. *AJNR Am J Neuroradiol* **27**, 2053–2057 (2006).

79. White, P. M. & Raymond, J. Endovascular Coiling of Cerebral Aneurysms Using 'Bioactive' or Coated-Coil Technologies: A Systematic Review of the Literature. *Am J Neuroradiol* **30**, 219–226 (2008).

80. Mawad, M. E., Cekirge, S., Ciceri, E. & Saatci, I. Endovascular treatment of giant and large intracranial aneurysms by using a combination of stent placement and liquid polymer injection. *J. Neurosurg.* **96**, 474–482 (2002).

81. Molyneux, A. J., Cekirge, S., Saatci, I. & Gál, G. Cerebral Aneurysm Multicenter European Onyx (CAMEO) trial: results of a prospective observational study in 20 European centers. *Am. J. Neuroradiol.* **25**, 39–51 (2004).

82. Murayama, Y., Viñuela, F., Tateshima, S., Viñuela, F., Jr & Akiba, Y. Endovascular treatment of experimental aneurysms by use of a combination of liquid embolic agents and protective devices. *AJNR Am J Neuroradiol* **21**, 1726–1735 (2000).

83. Riley, C. M., McLemore, R., Preul, M. C. & Vernon, B. L. Gelling process differences in reverse emulsion, in situ gelling polymeric materials for intracranial aneurysm embolization, formulated with injectable contrast agents. *J. Biomed. Mater. Res. B* **96B**, 47–56 (2011).

84. Brennecka, C. R., Preul, M. C., Bichard, W. D. & Vernon, B. L. In Vivo Experimental Aneurysm Embolization in a Swine Model with a Liquid-to-Solid Gelling Polymer System: Initial Biocompatibility and Delivery Strategy Analysis. *World Neurosurg.* (2011).

85. Takao, H. *et al.* Endovascular treatment of experimental aneurysms using a combination of thermoreversible gelation polymer and protection devices: feasibility study. *Neurosurgery* **65**, 601 (2009).

86. Becker, T. A., Kipke, D. R. & Brandon, T. Calcium alginate gel: a biocompatible and mechanically stable polymer for endovascular embolization. *J. Biomed. Mater. Res.* **54**, 76–86 (2001).

87. He, H. *et al.* Endovascular treatment of cerebral arteriovenous malformations with Onyx embolization. *Chin. Med. J.* **118**, 2041–2045 (2005).

88. Lauriola, W. *et al.* Treatment of Large and Giant Intracranial Aneurysms with Onyx. Preliminary Findings. *Riv Neuroradiol* **18**, 101–112 (2005).

89. Murayama, Y. *et al.* Nonadhesive liquid embolic agent for cerebral arteriovenous malformations: preliminary histopathological studies in swine rete mirabile. *Neurosurgery* **43**, 1164–1175 (1998).

90. Song, D., Leng, B., Zhou, L., Gu, Y. & Chen, X. Onyx in treatment of large and giant cerebral aneurysms and arteriovenous malformations. *Chin. Med. J.* **117**, 1869–1872 (2004).

91. Weber, W., Siekmann, R., Kis, B. & Kuehne, D. Treatment and follow-up of 22 unruptured wide-necked intracranial aneurysms of the internal carotid artery with Onyx HD 500. *AJNR Am J Neuroradiol* **26**, 1909–1915 (2005).

92. Pamuk, A. G., Saatci, I., Cekirge, H. S. & Aypar, U. A contribution to the controversy over dimethyl sulfoxide toxicity: anesthesia monitoring results in patients treated with Onyx embolization for intracranial aneurysms. *Neuroradiology* **47**, 380–386 (2005).

93. Raftopoulos, C. *et al.* Prospective analysis of aneurysm treatment in a series of 103 consecutive patients when endovascular embolization is considered the first option. *J. Neurosurg.* **93**, 175–182 (2000).

94. Becker, T. A., Preul, M. C., Bichard, W. D., Kipke, D. R. & McDougall, C. G. Calcium alginate gel as a biocompatible material for endovascular arteriovenous malformation embolization: six-month results in an animal model. *Neurosurgery* **56**, 793–801; discussion 793–801 (2005).

95. Becker, T. A., Preul, M. C., Bichard, W. D., Kipke, D. R. & McDougall, C. G. PRELIMINARY INVESTIGATION OF CALCIUM ALGINATE GEL AS A BIOCOMPATIBLE MATERIAL FOR ENDOVASCULAR ANEURYSM EMBOLIZATION IN VIVO. *Neurosurgery* **60**, 1119???1128 (2007).

96. Liu, H. & Zhu, X. Lower critical solution temperatures of N-substituted acrylamide copolymers in aqueous solutions. *Polymer* **40**, 6985–6990 (1999).

97. Schild, H. G. Poly(*N*-isopropylacrylamide): Experiment, Theory and Application. *Prog Polym Sci* **17**, 163–249 (1992).

98. Feil, H., Bae, Y. H., Feijen, J. & Kim, S. W. Effect of comonomer hydrophilicity and ionization on the lower critical solution temperature of *N*-isopropylacrylamide copolymers. *Macromolecules* **26**, 2496–2500 (1993).

99. He, C., Kim, S. W. & Lee, D. S. In situ gelling stimuli-sensitive block copolymer hydrogels for drug delivery. *J. Control. Rel.* **127**, 189–207 (2008).

100. Xia, Y., Yin, X., Burke, N. A. D. & Stöver, H. D. H. Thermal response of narrow-disperse poly(*N*-isopropylacrylamide) prepared by atom transfer radical polymerization. *Macromolecules* **38**, 5937–5943 (2005).

101. Fujishige, S., Kubota, K. & Ando, I. Phase transition of aqueous solutions of poly(*N*-isopropylacrylamide) and poly (*N*-isopropylmethacrylamide). *J. Phys. Chem.* **93**, 3311–3313 (1989).

102. Comolli, N., Neuhuber, B., Fischer, I. & Lowman, A. In vitro analysis of PNIPAAm-PEG, a novel, injectable scaffold for spinal cord repair. *Acta Biomaterialia* **5**, 1046–1055 (2009).

103. Yin, X., Hoffman, A. S. & Stayton, P. S. Poly(*N*-isopropylacrylamide-*co*-propylacrylic acid) copolymers that respond sharply to temperature and pH. *Biomacromolecules* **7**, 1381–1385 (2006).

104. Park, T. G. & Hoffman, A. S. Sodium chloride-induced phase transition in nonionic poly(*N*-isopropylacrylamide gel. *Macromolecules* **26**, 5045–5048 (1993).

105. Vernon, B. L., Kim, S. W. & Bae, Y. H. Thermoreversible copolymer gels for extracellular matrix. *J Biomed Mater Res A* **51**, 69–79 (2000).

106. Qiu, L. Y. & Bae, Y. H. Polymer Architecture and Drug Delivery. *Pharm Res* **23**, 1–30 (2006).

107. Yoshida, R. *et al.* Comb-type grafted hydrogels with rapid deswelling response to temperature changes. *Nature* **374**, 240–242 (1995).

108. Reed, A. M. & Gilding, D. K. Biodegradable polymers for use in surgery--poly(glycolic)/poly(lactic acid) homo and copolymers: 2. In vitro degradation. *Polymer* **22**, 494–498 (1981).

109. Chen, G. & Hoffman, A. S. Temperature-induced phase transition behaviors of random vs. graft copolymers of *N*-isopropylacrylamide and acrylic acid. *Macromol. Rapid Commun.* **16**, 175–182 (1995).

110. Weiss-Malik, R. A., Solis, F. J. & Vernon, B. L. Independent control of lower critical solution temperature and swelling behavior with pH for poly(*N*-isopropylacrylamide-*co*-maleic acid). *J. Appl. Polym. Sci.* **94**, 2110–2116 (2004).

111. Chen, G. & Hoffman, A. S. Graft copolymers that exhibit temperature-induced phase transitions over a wide range of pH. *Nature* **373**, 49–52 (1995).

112. Chiang, W.-H., Hsu, Y.-H., Chen, Y.-W., Chern, C.-S. & Chiu, H.-C. Thermoresponsive Interpolymeric Complex Assemblies from Co-association of Linear PAAc Homopolymers with PNIPAAm Segments Containing PAAc-Based Graft Copolymer. *Macromolecular Chemistry and Physics* n/a–n/a (2011).doi:10.1002/macp.201100124

113. Oh, Y. J., In, I. & Park, S. Y. Temperature-sensitive hydrogel prepared by graft polymerization of N-isopropylacrylamide onto macroradical Pluronic. *J Indust Eng Chem* **18**, 321–324 (2012).

114. Suzuki, A., Yoshikawa, S. & Bai, G. Shrinking pattern and phase transition velocity of poly(*N*-isopropylacrylamide gel). *J. Chem. Phys.* **111**, 360–367 (1999).

115. Kaneko, Y. *et al.* Rapid deswelling response of poly (*N*-isopropylacrylamide) hydrogels by the formation of water release channels using poly(ethylene oxide) graft chains. *Macromolecules* **31**, 6099–6105 (1998).

116. Gutowska, A. *et al.* Squeezing hydrogels for controlled oral drug delivery. *J Control Rel* **48**, 141–148 (1997).

117. Okano, T., Bae, Y. H., Jacobs, H. & Kim, S. W. Thermally on-off switching polymers for drug permeation and release. *J Control Rel* **11**, 255–265 (1990).

118. Stile, R. A., Burghardt, W. R. & Healy, K. E. Synthesis and characterization of injectable poly(*N*-isopropylacrylamide)-based hydrogels that support tissue formation in vitro. *Macromolecules* **32**, 7370–7379 (1999).

119. Yoshioka, H., Mikami, M. & Mori, Y. A synthetic hydrogel with thermoreversible gelation. I. Preparation and Rheological Properties. *J. Macromol. Sci. Pure Appl. Chem.* **A31**, 113–120 (1994).

120. Brazel, C. S. & Peppas, N. A. Pulsatile local delivery of thrombolytic and antithrombotic agents using poly (N-isopropylacrylamide-co-methacrylic acid) hydrogels. *Journal of controlled release* **39**, 57–64 (1996).

121. Kim, S. & Healy, K. E. Synthesis and Characterization of Injectable Poly(*N*-isopropylacrylamide-*co*-acrylic acid) Hydrogels with Proteolytically Degradable Cross-Links. *Biomacromolecules* **4**, 1214–1223 (2003).

122. Cui, Z., Lee, B. H. & Vernon, B. L. New hydrolysis-dependent thermosensitive polymer for an injectable degradable system. *Biomacromolecules* **8**, 1280–1286 (2007).

123. Henderson, E. *et al. In vivo* evaluation of injectable thermosensitive polymer with time-dependent LCST. *J Biomed Mater Res A* **90A**, 1186–1197 (2009).

124. Li, Z., Wang, F., Roy, S., Sen, C. K. & Guan, J. Injectable, highly flexible, and thermosensitive hydrogels capable of delivering superoxide dismutase. *Biomacromolecules* **10**, 3306–3316 (2009).

125. Hoare, T. R. & Kohane, D. S. Hydrogels in drug delivery: Progress and challenges. *Polymer* **49**, 1993–2007 (2008).

126. Overstreet, D. J., Vernon, B. L. & von Recum, H. A. Drug delivery applications of injectable biomaterials. *Injectable Biomaterials: Science and Applications* (2011).

127. Van Tomme, S. R., Storm, G. & Hennink, W. E. In situ gelling hydrogels for pharmaceutical and biomedical applications. *Int. J. Pharm.* **355**, 1–18 (2008).

128. Kretlow, J. D., Klouda, L. & Mikos, A. G. Injectable matrices and scaffolds for drug delivery in tissue engineering. *Adv. Drug Deliv. Rev.* **59**, 263–273 (2007).

129. McLemore, R., Preul, M. C. & Vernon, B. L. Controlling delivery properties of a waterborne, *in-situ*-forming biomaterial. *J Biomed Mater Res B* **79B**, 398–410 (2006).

130. Pollock, J. F. & Healy, K. E. Mechanical and swelling characterization of poly(*N*-isopropyl acrylamide -co- methoxy poly(ethylene glycol) methacrylate) sol–gels. *Acta Biomaterialia* **6**, 1307–1318 (2010).

131. Huynh, C. T., Nguyen, M. K. & Lee, D. S. Injectable Block Copolymer Hydrogels: Achievements and Future Challenges for Biomedical Applications. *Macromolecules* **44**, 6629–6636 (2011).

132. Talukdar, M. M., Vinckier, I., Moldenaers, P. & Kinget, R. Rheological characterization of xanthan gum and hydroxypropylmethyl cellulose with respect to controlled-release drug delivery. *J. Pharm. Sci.* **85**, 537–540 (1996).

133. Neradovic, D., Hinrichs, W. L. J., Kettenes-van dan Bosch, J. J. & Hennink, W. E. Poly(*N*-isopropylacrylamide) with hydrolyzable lactid acid ester side groups: a new type of thermosensitive polymer. *Macromol. Rapid Commun.* **20**, 577–581 (1999).

134. Guan, J., Hong, Y., Ma, Z. & Wagner, W. R. Protein-Reactive, Thermoresponsive Copolymers with High Flexibility and Biodegradability. *Biomacromolecules* **9**, 1283–1292 (2008).

135. Ma, Z., Nelson, D. M., Hong, Y. & Wagner, W. R. Thermally Responsive Injectable Hydrogel Incorporating Methacrylate-Polylactide for Hydrolytic Lability. *Biomacromolecules* **11**, 1873–1881 (2010).

136. Lee, B. H. & Vernon, B. Copolymers of *N*-isopropylacrylamide, HEMA-lactate and acrylic acid with time-dependent lower critical solution temperature as a bioresorbable carrier. *Polym Int* **54**, 418–422 (2005).

137. Overstreet, D. J., Dhruv, H. D. & Vernon, B. L. Bioresponsive copolymers of poly (*N*-isopropylacrylamide) with enzyme-dependent lower critical solution temperatures. *Biomacromolecules* **11**, 1154–1159 (2010).

138. Huang, X., Nayak, B. R. & Lowe, T. L. Synthesis and characterization of novel thermoresponsive-*co*-biodegradable hydrogels composed of *N*-isopropylacrylamide, poly(L-lactic acid), and dextran. *J. Polym. Sci. A Polym. Chem.* **42**, 5054–5066 (2004).

139. Huang, X. & Lowe, T. L. Biodegradable Thermoresponsive Hydrogels for Aqueous Encapsulation and Controlled Release of Hydrophilic Model Drugs. *Biomacromolecules* **6**, 2131–2139 (2005).

140. Yoshida, T., Aoyagi, T., Kokufuta, E. & Okano, T. Newly Designed Hydrogel with Both Sensitive Thermoresponse and Biodegradability. *J. Polym. Sci. A Polym. Chem.* **41**, 779–787 (2003).

141. Leon, C., Solis, F. J. & Vernon, B. Phase behavior and shrinking kinetics of thermo-reversible poly(*N*-isopropylacrylamide-2-hydroxyethyl methacrylate). *Mater Res Soc Symp Proc* **1190**, (2009).

142. Lee, B. H., West, B., McLemore, R., Pauken, C. & Vernon, B. L. In-situ injectable physically and chemically gelling NIPAAm-based copolymer system for embolization. *Biomacromolecules* **7**, 2059–2064 (2006).

143. Gutowska, A., Bae, Y. H., Feijen, J. & Kim, S. W. Heparin release from thermosensitive hydrogels. *J Control Rel* **22**, 95–104 (1992).

144. Overstreet, D. J., McLemore, R. Y., Doan, B. D., Farag, A. & Vernon, B. L. Temperature-responsive graft copolymer hydrogels for controlled swelling and drug delivery. *Soft Materials - in press* (2012).

145. Shah, S. S., Wertheim, J., Wang, C. T. & Pitt, C. G. Polymer-drug conjugates: manipulating drug delivery kinetics using model LCST systems. *J. Control. Rel.* **45**, 95–101 (1997).

146. Nagase, K. *et al.* Preparation of Thermoresponsive Cationic Copolymer Brush Surfaces and Application of the Surface to Separation of Biomolecules. *Biomacromolecules* **9**, 1340–1347 (2008).

147. Garbern, J. C., Hoffman, A. S. & Stayton, P. S. Injectable pH- and temperature-responsive poly(*N*-isopropylacrylamide-*co*-propylacrylic acid) copolymers for delivery of angiogenic growth factors. *Biomacromolecules* **11**, 5891–5905 (2010).

148. Loh, X. J., Goh, S. H. & Li, J. New Biodegradable Thermogelling Copolymers Having Very Low Gelation Concentrations. *Biomacromolecules* **8**, 585–593 (2007).

149. Attwood, D., Collett, J. H. & Tait, C. J. The micellar properties of the poly(oxyethylene)-poly(oxypropylene) copolymer Pluronic F127 in water and electrolyte solution. *Int. J. Pharm.* **26**, 25–33 (1985).

150. Vadnere, M., Amidon, G., Lindenbaum, S. & Haslam, J. L. Thermodynamic studies on the sol-gel transition of some pluronic polyols. *Int. J. Pharm.* **22**, 207–218 (1984).

151. Alexandridis, P. & Hatton, T. A. Poly(ethylene oxide)-poly(propylene oxide)-poly (ethylene oxide) block copolymer surfactants in aqueous solutions and at interfaces: thermodynamics, structure, dynamics, and modeling. *Colloids Surf. A* **96**, 1–46 (1994).

152. Brown, W., Schillen, K. & Almgren, M. Micelle and Gel Formation in a Poly(ethylene oxide)/Poly(propylene oxide)/ Poly(ethylene oxide) Triblock

Copolymer in Water Solution. Dynamic and Static Light Scattering and Oscillatory Shear Measurements. *J. Phys. Chem.* **95**, 1850–1858 (1991).

153. Glatter, O. & Scherf, G. Characterization of a poly(ethylene oxide)-poly(propylene oxide) triblock copolymer (EO_{27}-PO_{39}-EO_{27}) in Aqueous Solution. *Macromolecules* **27**, 6046–6054 (1994).

154. Jorgensen, E. B., Hvidt, S., Brown, W. & Schillen, K. Effects of salts on the micellization and gelation of a triblock copolymer studied by rheology and light scattering. *Macromolecules* **30**, 2355–2364 (1997).

155. Jeong, B., Bae, Y. H., Lee, D. S. & Kim, S. W. Biodegradable block copolymers as injectable drug-delivery systems. *Nature* **388**, 860–862 (1997).

156. Jeong, B., Bae, Y. H. & Kim, S. W. Drug release from biodegradable injectable thermosensitive hydrogel of PEG–PLGA–PEG triblock copolymers. *J Control Rel* **63**, 155–163 (2000).

157. Kim, S. Y. *et al.* Reverse Thermal Gelling PEG−PTMC Diblock Copolymer Aqueous Solution. *Macromolecules* **40**, 5519–5525 (2007).

158. Bae, S. J. *et al.* Gelation Behavior of Poly(ethylene glycol) and Polycaprolactone Triblock and Multiblock Copolymer Aqueous Solutions. *Macromolecules* **39**, 4873–4879 (2006).

159. Bae, S. J. *et al.* Thermogelling Poly(caprolactone-*b*-ethylene glycol-*b*-caprolactone) Aqueous Solutions. *Macromolecules* **38**, 5260–5265 (2005).

160. Xiong, X. Y., Tam, K. C. & Gan, L. H. Synthesis and thermal responsive properties of P(LA-*b*-EO-*b*-PO-*b*-EO-*b*-LA) block copolymers with short hydrophobic poly(lactic acid) (PLA) segments. *Polymer* **46**, 1841–1850 (2005).

161. Xiong, X. Y., Tam, K. C. & Gan, L. H. Synthesis and thermally responsive properties of novel Pluronic F87/polycaprolactone (PCL) block copolymers with short PCL blocks. *J. Appl. Polym. Sci.* **100**, 4163–4172 (2006).

162. Ahn, J. S., Suh, J. M., Lee, M. & Jeong, B. Slow eroding biodegradable multiblock poloxamer copolymers. *Polym. Int.* **54**, 842–847 (2005).

163. Jeong, Y. *et al.* Enzymatically degradable temperature-sensitive polypeptide as a new in-situ gelling biomaterial. *J. Control. Rel.* **137**, 25–30 (2009).

164. Li, C. *et al.* Synthesis and Characterization of Biocompatible, Thermoresponsive ABC and ABA Triblock Copolymer Gelators. *Langmuir* **21**, 11026–11033 (2005).

165. Li, C. *et al.* Synthesis and Characterization of Biocompatible Thermo-Responsive Gelators Based on ABA Triblock Copolymers. *Biomacromolecules* **6**, 994–999 (2005).

166. Zentner, G. M. *et al.* Biodegradable block copolymers for delivery of proteins and water-insoluble drugs. *J. Control. Rel.* **72**, 203–215 (2001).

167. Choi, S., Baudys, M. & Kim, S. W. Control of Blood Glucose by Novel GLP-1 Delivery Using Biodegradable Triblock Copolymer of PLGA-PEG-PLGA in Type 2 Diabetic Rats. *Pharm. Res.* **21**, 827–831 (2004).

168. Huynh, D. P. *et al.* Functionalized injectable hydrogels for controlled insulin delivery. *Biomaterials* **29**, 2527–2534 (2008).

169. Gong, C. Y. *et al.* Synthesis and characterization of PEG-PCL-PEG thermosensitive hydrogel. *Int. J. Pharm.* **365**, 89–99 (2009).

170. Tang, Y. & Singh, J. Biodegradable and biocompatible thermosensitive polymer based injectable implant for controlled release of protein. *Int. J. Pharm.* **365**, 34–43 (2009).

171. Determan, M. D., Cox, J. P. & Mallapragada, S. K. Drug release from pH-responsive thermogelling pentablock copolymers. *J. Biomed. Mater. Res.* **81A**, 326–333 (2007).

172. Garripelli, V. K. *et al.* A novel thermosensitive polymer with pH-dependent degradation for drug delivery. *Acta Biomaterialia* **6**, 477–485 (2010).

173. Chenite, A. *et al.* Novel injectable neutral solutions of chitosan form biodegradable gels in situ. *Biomaterials* **21**, 2155–2161 (2000).

174. Ganji, F., Abdekhodaie, M. J. & Ramazani S.A., A. Gelation time and degradation rate of chitosan-based injectable hydrogel. *J. Sol-Gel Sci. Techn.* **42**, 47–53 (2007).

175. Ruel-Gariepy, E. *et al.* A thermosensitive chitosan-based hydrogel for the local delivery of paclitaxel. *Eur J Pharm Biopharm* **57**, 53–63 (2004).

176. Zan, J., Chen, H., Jiang, G., Lin, Y. & Ding, F. Preparation and properties of crosslinked chitosan thermosensitive hydrogel for injectable drug delivery systems. *J. Appl. Polym. Sci.* **101**, 1892–1898 (2006).

177. Ha, D. I. *et al.* Preparation of thermo-responsive and injectable hydrogels based on hyaluronic acid and poly(*N*-isopropylacrylamide) and their drug release behaviors. *Macromol. Res.* **14**, 87 (2006).

178. Lee, W.-F. & Lee, S.-C. Effect of gelatin on the drug release behaviors for the organic hybrid gels based on N-isopropylacrylamide and gelatin. *J. Mater. Sci.-Mater M.* **18**, 1089–1096 (2007).

179. Fang, J. Y., Chen, J. P., Leu, Y. L. & Hu, J. W. Temperature-sensitive hydrogels composed of chitosan and hyaluronic acid as injectable carriers for drug delivery. *Eur. J. Pharm. Biopharm.* **68**, 626–636 (2008).

180. Cao, Y. *et al.* Poly(*N*-isopropylacrylamide)-chitosan as thermosensitive in situ gel-forming system for ocular drug delivery. *J. Control. Rel.* **120**, 186–194 (2007).

181. Bae, J. W., Go, D. H., Park, K. D. & Lee, S. J. Thermosensitive chitosan as an injectable carrier for local drug delivery. *Macromol. Res.* **14**, 461 (2006).

182. Allcock, H. R., Austin, P. E. & Neenan, T. X. Phosphazene high polymers with bioactive substituent groups: prospective anesthetic aminophosphazenes. *Macromolecules* **15**, 689–693 (1982).

183. Grolleman, C., De Visser, A., Wolke, J., Van der Goot, H. & Timmerman, H. Studies on a bioerodible drug carrier system based on polyphosphazene Part I. Synthesis. *J. Control. Rel.* **3**, 143–154 (1986).

184. Lakshmi, S., Katti, D. & Laurencin, C. Biodegradable polyphosphazenes for drug delivery applications. *Adv. Drug Deliv. Rev.* **55**, 467–482 (2003).

185. Kang, G. D., Cheon, S. H., Khang, G. & Song, S. C. Thermosensitive poly (organophosphazene) hydrogels for a controlled drug delivery. *Eur. J. Pharm. Biopharm.* **63**, 340–346 (2006).

186. Kang, G. D., Cheon, S. H. & Song, S. C. Controlled release of doxorubicin from thermosensitive poly (organophosphazene) hydrogels. *Int. J. Pharm.* **319**, 29–36 (2006).

187. Urry, D. W. Free-energy transduction in polypeptides and proteins based on inverse temperature transitions. *Prog. Biophys. Molec. Biol.* **57**, 23–57 (1992).

188. Bidwell III, G. L., Fokt, I., Priebe, W. & Raucher, D. Development of elastin-like polypeptide for thermally targeted delivery of doxorubicin. *Biochem. Pharmacol.* **73**, 620–631 (2007).

189. Liu, W. *et al.* Tumor accumulation, degradation and pharmacokinetics of elastin-like polypeptides in nude mice. *J. Control. Rel.* **116**, 170–178 (2006).

190. Massodi, I., Bidwell III, G. L. & Raucher, D. Evaluation of cell penetrating peptides fused to elastin-like polypeptide for drug delivery. *J. Control. Rel.* **108**, 396–408 (2005).

191. Shamji, M. F. *et al.* An injectable and in situ-gelling biopolymer for sustained drug release following perineural administration. *Spine* **33**, 748 (2008).

192. Simnick, A. J., Lim, D. W., Chow, D. & Chilkoti, A. Biomedical and Biotechnological Applications of Elastin-Like Polypeptides. *Polym. Rev.* **47**, 121–154 (2007).

193. Dinerman, A. A., Cappello, J., Ghandehari, H. & Hoag, S. W. Solute diffusion in genetically engineered silk-elastinlike protein polymer hydrogels. *J. Control. Rel.* **82**, 277–287 (2002).

194. Balakrishnan, B. & Jayakrishnan, A. Self-cross-linking biopolymers as injectable in situ forming biodegradable scaffolds. *Biomaterials* **26**, 3941–3951 (2005).

195. Lee, K. Y., Alsberg, E. & Mooney, D. J. Degradable and injectable poly (aldehyde guluronate) hydrogels for bone tissue engineering. *J. Biomed. Mater. Res.* **56**, 228–233 (2001).

196. Salem, A. K. *et al.* Porous polymer and cell composites that self-assemble in situ. *Adv. Mater.* **15**, 210–213 (2003).

197. Cai, S., Liu, Y., Zheng Shu, X. & Prestwich, G. D. Injectable glycosaminoglycan hydrogels for controlled release of human basic fibroblast growth factor. *Biomaterials* **26**, 6054–6067 (2005).

198. Hiemstra, C., van der Aa, L. J., Zhong, Z., Dijkstra, P. J. & Feijen, J. Rapidly in Situ-Forming Degradable Hydrogels from Dextran Thiols through Michael Addition. *Biomacromolecules* **8**, 1548–1556 (2007).

199. Jin, R., Hiemstra, C., Zhong, Z. & Feijen, J. Enzyme-mediated fast in situ formation of hydrogels from dextran-tyramine conjugates. *Biomaterials* **28**, 2791–2800 (2007).

200. Lee, F., Chung, J. E. & Kurisawa, M. An injectable hyaluronic acid-tyramine hydrogel system for protein delivery. *J. Control. Rel.* **134**, 186–193 (2009).

201. Ishihara, M. *et al.* Chitosan hydrogel as a drug delivery carrier to control angiogenesis. *J. Artif. Organs* **9**, 8–16 (2006).

202. Ishihara, M. *et al.* Controlled release of fibroblast growth factors and heparin from photocrosslinked chitosan hydrogels and subsequent effect on in vivo vascularization. *J. Biomed. Mater. Res. A* **64**, 551–559 (2003).

203. Obara, K. *et al.* Photocrosslinkable chitosan hydrogel containing fibroblast growth factor-2 stimulates wound healing in healing-impaired< i> db/db</i> mice. *Biomaterials* **24**, 3437–3444 (2003).

204. West, J. L. & Hubbell, J. A. Photopolymerized hydrogel materials for drug delivery applications. *React. Polym.* **25**, 139–147 (1995).

205. West, J. L. & Hubbell, J. A. Polymeric Biomaterials with Degradation Sites for Proteases Involved in Cell Migration. *Macromolecules* **32**, 241–244 (1999).

206. Sharifi, S. *et al.* Injectable in situ forming drug delivery system based on poly ([epsilon]-caprolactone fumarate) for tamoxifen citrate delivery: Gelation characteristics, in vitro drug release and anti-cancer evaluation. *Acta Biomaterialia* **5**, 1966–1978 (2009).

207. Shin, H., Temenoff, J. S. & Mikos, A. G. In Vitro Cytotoxicity of Unsaturated Oligo[poly(ethylene glycol) fumarate] Macromers and Their Cross-Linked Hydrogels. *Biomacromolecules* **4**, 552–560 (2003).

208. Temenoff, J. S., Shin, H., Conway, D. E., Engel, P. S. & Mikos, A. G. In Vitro Cytotoxicity of Redox Radical Initiators for Cross-Linking of Oligo(poly(ethylene glycol) fumarate) Macromers. *Biomacromolecules* **4**, 1605–1613 (2003).

209. Flory, P. J. *Principles of polymer chemistry*. (Cornell University Press: Ithaca, NY, 1953).

210. Metters, A. T. & Hubbell, J. A. Network formation and degradation behavior of hydrogels formed by Michael-type addition reactions. *Biomacromolecules* **6**, 290–301 (2005).

211. Elbert, D. L., Pratt, A. B., Lutolf, M. P., Halstenberg, S. & Hubbell, J. A. Protein delivery from materials formed by self-selective conjugate addition reactions. *J. Control. Rel.* **76**, 11–25 (2001).

212. Vernon, B. L., Fusaro, F., Borden, B. & Roy, K. H. Partition-controlled progesterone release from waterborne, in situ-gelling materials. *Int J Pharm* **274**, 191–200 (2004).

213. Rupenthal, I. D., Alany, R. G. & Green, C. R. Ion-Activated In Situ Gelling Systems for Antisense Oligodeoxynucleotide Delivery to the Ocular Surface. *Mol. Pharmaceutics* **8**, 2282–2290 (2011).

214. Hao, X. *et al.* Angiogenic effects of sequential release of VEGF-A165 and PDGF-BB with alginate hydrogels after myocardial infarction. *Cardiovasc. Res.* **75**, 178 (2007).

215. Silva, E. & Mooney, D. Spatiotemporal control of vascular endothelial growth factor delivery from injectable hydrogels enhances angiogenesis. *J. Thromb. Haemost.* **5**, 590–598 (2007).

216. Emerich, D. F., Mooney, D. J., Storrie, H., Babu, R. S. & Kordower, J. H. Injectable Hydrogels Providing Sustained Delivery of Vascular Endothelial Growth Factor are Neuroprotective in a Rat Model of Huntington's Disease. *Neurotox. Res.* **17**, 66–74 (2009).

217. Lansdown, A. B. & Payne, M. J. An evaluation of the local reaction and biodegradation of calcium sodium alginate (Kaltostat) following subcutaneous implantation in the rat. *J R Coll Surg Edinb* **39**, 284–288 (1994).

218. Cohen, S., Lobel, E., Trevgoda, A. & Peled, Y. A novel in situ-forming ophthalmic drug delivery system from alginates undergoing gelation in the eye. *J. Control. Rel.* **44**, 201–208 (1997).

219. Liu, Z. *et al.* Study of an alginate/HPMC-based in situ gelling ophthalmic delivery system for gatifloxacin. *Int. J. Pharm.* **315**, 12–17 (2006).

220. Van Tomme, S. R., van Steenbergen, M. J., De Smedt, S. C., van Nostrum, C. F. & Hennink, W. E. Self-gelling hydrogels based on oppositely charged dextran microspheres. *Biomaterials* **26**, 2129–2135 (2005).

221. Van Tomme, S. R., Van Nostrum, C. F., De Smedt, S. C. & Hennink, W. E. Degradation behavior of dextran hydrogels composed of positively and negatively charged microspheres. *Biomaterials* **27**, 4141–4148 (2006).

222. Jin, K. M. & Kim, Y. H. Injectable, thermo-reversible and complex coacervate combination gels for protein drug delivery. *J. Control. Rel.* **127**, 249–256 (2008).

223. Hsieh, P. C. H., Davis, M. E., Gannon, J., MacGillivray, C. & Lee, R. T. Controlled delivery of PDGF-BB for myocardial protection using injectable self-assembling peptide nanofibers. *J. Clin. Invest.* **116**, 237 (2006).

224. Chiu, Y. L. *et al.* pH-triggered injectable hydrogels prepared from aqueous N-palmitoyl chitosan: In vitro characteristics and in vivo biocompatibility. *Biomaterials* **30**, 4877–4888 (2009).

225. Vemula, P. K., Cruikshank, G. A., Karp, J. M. & John, G. Self-assembled prodrugs: An enzymatically triggered drug-delivery platform. *Biomaterials* **30**, 383–393 (2009).

226. Vemula, P. K. *et al.* On-demand drug delivery from self-assembled nanofibrous gels: A new approach for treatment of proteolytic disease. *J Biomed Mater Res A* **97A**, 103–110 (2011).

227. Yu, L., Zhang, Z., Zhang, H. & Ding, J. Mixing a Sol and a Precipitate of Block Copolymers with Different Block Ratios Leads to an Injectable Hydrogel. *Biomacromolecules* **10**, 1547–1553 (2009).

228. Tsuji, H. Poly(lactide) Stereocomplexes: Formation, Structure, Properties, Degradation, and Applications. *Macromol. Biosci.* **5**, 569–597 (2005).

229. Zhang, S. Fabrication of novel biomaterials through molecular self-assembly. *Nat. Biotechnol.* **21**, 1171–1178 (2003).

230. Li, J., Ni, X. & Leong, K. W. Injectable drug-delivery systems based on supramolecular hydrogels formed by poly (ethylene oxide) s and α-cyclodextrin. *J. Biomed. Mater. Res. A* **65**, 196–202 (2003).

231. Li, J. *et al.* Self-assembled supramolecular hydrogels formed by biodegradable PEO-PHB-PEO triblock copolymers and [alpha]-cyclodextrin for controlled drug delivery. *Biomaterials* **27**, 4132–4140 (2006).

232. Harada, A., Li, J. & Kamachi, M. The molecular necklace: a rotaxane containing many threaded α-cyclodextrins. *Nature* **356**, 325–327 (1992).

233. Wenz, G. & Keller, B. Threading cyclodextrin rings on polymer chains. *Angew. Chem. Int. Edit.* **31**, 197–199 (1992).

234. Cloyd, J. M. *et al.* Material properties in unconfined compression of human nucleus pulposus, injectable hyaluronic acid-based hydrogels and tissue engineering scaffolds. *Eur. Spine J.* **16**, 1892–1898 (2007).

235. Vernengo, J., Fussell, G. W., Smith, N. G. & Lowman, A. M. Evaluation of novel injectable hydrogels for nucleus pulposus replacement. *J Biomed Mater Res B* **84B**, 64–69 (2008).

236. Gloria, A., Borzacchiello, A., Causa, F. & Ambrosio, L. Rheological Characterization of Hyaluronic Acid Derivatives as Injectable Materials Toward Nucleus Pulposus Regeneration. *Journal of Biomaterials Applications* (2010).doi:10.1177/0885328210387174

237. McLemore, R. *et al.* Tubal sterilization with a waterborne polyethylene glycol in situ cross-linking material: a minimally invasive approach. *Fertil. Steril.* **83**, 1284–1292 (2005).

238. Wei, C. Z. *et al.* A thermosensitive chitosan-based hydrogel barrier for post-operative adhesions' prevention. *Biomaterials* **30**, 5534–5540 (2009).

239. Amin, S. P., Marmur, E. S. & Goldberg, D. J. Complications from injectable polyacrylamide gel, a new nonbiodegradable soft tissue filler. *Dermatol. Surg.* **30**, 1507–1509 (2004).

240. Bergeret-Galley, C., Latouche, X. & Illouz, Y.-G. The Value of a New Filler Material in Corrective and Cosmetic Surgery: DermaLive and DermaDeep. *Aesthet. Plast. Surg.* **25**, 249–255 (2001).

241. Christensen, L., Breiting, V., Janssen, M., Vuust, J. & Hogdall, E. Adverse Reactions to Injectable Soft Tissue Permanent Fillers. *Aesthet. Plast. Surg.* **29**, 34–48 (2005).

242. Narins, R. S. & Beer, K. Liquid Injectable Silicone: A Review of Its History, Immunology, Technical Considerations, Complications, and Potential. *Plast. Reconstr. Surg.* **118**, 77S–84S (2006).

243. Thornton, A. J., Alsberg, E., Hill, E. E. & Mooney, D. J. Shape retaining injectable hydrogels for minimally invasive bulking. *J. Urology* **172**, 763–768 (2004).

244. Vaizey, C. J. & Kamm, M. A. Injectable bulking agents for treating faecal incontinence. *Brit. J. Surg.* **92**, 521–527 (2005).

245. Yu, R. N. Treatment of Vesicoureteral Reflux Using Endoscopic Injection of Nonanimal Stabilized Hyaluronic Acid/Dextranomer Gel: Initial Experience in Pediatric Patients by a Single Surgeon. *Pediatrics* **118**, 698–703 (2006).

246. Bossard, F., Sfika, V. & Tsitsilianis, C. Rheological Properties of Physical Gel Formed by Triblock Polyampholyte in Salt-Free Aqueous Solutions. *Macromolecules* **37**, 3899–3904 (2004).

247. Solis, F. J., Weiss-Malik, R. & Vernon, B. Local Monomer Activation Model for Phase Behavior and Calorimetric Properties of LCST Gel-Forming Polymers. *Macromolecules* **38**, 4456–4464 (2005).

248. Rzaev, Z. M. O., Dincer, S. & Piskin, E. Functional copolymers of *N*-isopropylacrylamide for bioengineering applications. *Prog. Polym. Sci.* **32**, 534–595 (2007).

249. Tian, J., Seery, T. A. P. & Weiss, R. A. Physically Cross-Linked Alkylacrylamide Hydrogels: Phase Behavior and Microstructure. *Macromolecules* **37**, 9994–10000 (2004).

250. Lin, H. H. & Cheng, Y. L. In-Situ Thermoreversible Gelation of Block and Star Copolymers of Poly(ethylene glycol) and Poly(*N*-isopropylacrylamide) of Varying Architectures. *Macromolecules* **34**, 3710–3715 (2001).

251. Potta, T., Chun, C. J. & Song, S. C. Design of Polyphosphazene Hydrogels with Improved Structural Properties by Use of Star-Shaped Multithiol Crosslinkers. *Macromol Biosci* **11**, 689–699 (2011).

252. Wall, S. T., Walker, J. C., Healy, K. E., Ratcliffe, M. B. & Guccione, J. M. Theoretical Impact of the Injection of Material Into the Myocardium: A Finite Element Model Simulation. *Circulation* **114**, 2627–2635 (2006).

253. Fujimoto, K. L. *et al.* Synthesis, characterization and therapeutic efficacy of a biodegradable, thermoresponsive hydrogel designed for application in chronic infarcted myocardium. *Biomaterials* **30**, 4357–4368 (2009).

254. Hsieh, P. C. H. Local Controlled Intramyocardial Delivery of Platelet-Derived Growth Factor Improves Postinfarction Ventricular Function Without Pulmonary Toxicity. *Circulation* **114**, 637–644 (2006).

255. Segers, V. F. M. *et al.* Local Delivery of Protease-Resistant Stromal Cell Derived Factor-1 for Stem Cell Recruitment After Myocardial Infarction. *Circulation* **116**, 1683–1692 (2007).

256. Hiemstra, C., Zhang, Z., Dijkstra, P. J. & Feijen, J. Stereocomplex mediated gelation of PEG-$(PLA)_2$ and PEG-$(PLA)_8$ block copolymers. *Macromol. Symp.* **224**, 119–131 (2005).

257. Yoshioka, H., Mikami, M., Mori, Y. & Tsuchida, E. Preparation of poly(*N*-isopropylacrylamide)-*b*-poly(ethylene glycol) and calorimetric analysis of its aqueous solution. *J. Macromol. Sci. Part A Pure Appl. Chem.* **31**, 109–112 (1994).

258. Wu, D.-Q. *et al.* Toward the Development of Partially Biodegradable and Injectable Thermoresponsive Hydrogels for Potential Biomedical Applications. *ACS Appl Mater Interfaces* **1**, 319–327 (2009).

259. Wang, T. *et al.* Novel thermosensitive hydrogel injection inhibits post-infarct ventricle remodelling. *Eur. J. Heart Fail.* **11**, 14–19 (2009).

260. Landa, N. *et al.* Effect of Injectable Alginate Implant on Cardiac Remodeling and Function After Recent and Old Infarcts in Rat. *Circulation* **117**, 1388–1396 (2008).

261. Rane, A. A. *et al.* Increased Infarct Wall Thickness by a Bio-Inert Material Is Insufficient to Prevent Negative Left Ventricular Remodeling after Myocardial Infarction. *PLoS ONE* **6**, e21571 (2011).

262. Garbern, J. C., Minami, E., Stayton, P. S. & Murry, C. E. Delivery of basic fibroblast growth factor with a pH-responsive, injectable hydrogel to improve angiogenesis in infarcted myocardium. *Biomaterials* **32**, 2407–2416 (2011).

263. Dobner, S., Bezuidenhout, D., Govender, P., Zilla, P. & Davies, N. A Synthetic Non-degradable Polyethylene Glycol Hydrogel Retards Adverse Post-infarct Left Ventricular Remodeling. *Journal of Cardiac Failure* **15**, 629–636 (2009).

264. Vernon, B. L., Tirelli, N., Bachi, T., Haldimann, D. & Hubbell, J. A. Water-borne, in situ crosslinked biomaterials from phase-segregated precursors. *J. Biomed. Mater. Res. A* **64A**, 447–456 (2003).

265. Piske, R. L. *et al.* Evaluation of Onyx HD-500 Embolic System in the Treatment of 84 Wide-Neck Intracranial Aneurysms. *Neurosurgery* **64**, E865–E875 (2009).

266. Ito, T. *et al.* The prevention of peritoneal adhesions by in situ cross-linking hydrogels of hyaluronic acid and cellulose derivatives. *Biomaterials* **28**, 975–983 (2007).

267. Gibble, J. & Ness, P. Fibrin glue: the perfect operative sealant? *Transfusion* **30**, 741–747 (1990).

268. McCarthy, P. M. *et al.* The Effectiveness of Fibrin Glue Sealant for Reducing Experimental Pulmonary Air Leak. *Ann. Thorac. Surg.* **45**, 203–205 (1988).

269. Venkatesh, K. S. & Ramanujam, P. Fibrin glue application in the treatment of recurrent anorectal fistulas. *Dis. Colon Rectum* **42**, 1136–1139 (1999).

270. Mukherjee, R. *et al.* Targeted Myocardial Microinjections of a Biocomposite Material Reduces Infarct Expansion in Pigs. *Ann. Thorac. Surg.* **86**, 1268–1276 (2008).

271. Christman, K. L., Fok, H. H., Sievers, R. E., Fang, Q. & Lee, R. J. Fibrin glue alone and skeletal myoblasts in a fibrin scaffold preserve cardiac function after myocardial infarction. *Tissue Eng.* **10**, 403–409 (2004).

272. Christman, K. L. *et al.* Injectable Fibrin Scaffold Improves Cell Transplant Survival, Reduces Infarct Expansion, and Induces Neovasculature Formation in Ischemic Myocardium. *J. Am. Coll. Cardiol.* **44**, 654–660 (2004).

273. Wang, Z. C. *et al.* In Situ Formation of Thermosensitive PNIPAAm-Based Hydrogels by Michael-Type Addition Reaction. *ACS Applied Materials & Interfaces* **2**, 1009–1018 (2010).

274. Bearat, H. H., Lee, B. H., Valdez, J. & Vernon, B. L. Synthesis, Characterization and Properties of a Physically and Chemically Gelling Polymer System Using Poly(NIPAAm-co-HEMA-acrylate) and Poly(NIPAAm-co-cysteamine). *J Biomater Sci Polym Ed* **22**, 1299–1318 (2011).

275. Robb, S. A., Lee, B. H., McLemore, R. & Vernon, B. L. Simultaneously physically and chemically gelling polymer system utilizing a poly(NIPAAm-*co*-cysteamine)-based copolymer. *Biomacromolecules* **8**, 2294–2300 (2007).

276. Hacker, M. C., Klouda, L., Ma, B. B., Kretlow, J. D. & Mikos, A. G. Synthesis and Characterization of Injectable, Thermally and Chemically Gelable, Amphiphilic Poly(*N*-isopropylacrylamide)-Based Macromers. *Biomacromolecules* **9**, 1558–1570 (2008).

277. Potta, T., Chun, C. & Song, S.-C. Injectable, dual cross-linkable polyphosphazene blend hydrogels. *Biomaterials* **31**, 8107–8120 (2010).

278. Potta, T., Chun, C. & Song, S.-C. Chemically crosslinkable thermosensitive polyphosphazene gels as injectable materials for biomedical applications. *Biomaterials* **30**, 6178–6192 (2009).

279. Bae, Y. H., Okano, T. & Kim, S. W. 'On–Off' thermocontrol of solute transport. I. Temperature dependence of swelling of *N*-isopropylacrylamide networks modified with hydrophobic components in water. *Pharm. Res.* **8**, 531–537 (1991).

280. Beltran, S., Baker, J. P., Hooper, H. H., Blanch, H. W. & Prausnitz, J. M. Swelling equilibria for weakly ionizable, temperature-sensitive hydrogels. *Macromolecules* **24**, 549–551 (1991).

281. Martens, P. J., Bryant, S. J. & Anseth, K. S. Tailoring the degradation of hydrogels formed from multivinyl poly(ethylene glycol) and poly(vinyl alcohol) macromers for cartilage tissue engineering. *Biomacromolecules* **4**, 283–292 (2003).

282. Huntsman Corporation Technical Bulletin for Jeffamine® M-1000 Polyetheramine (XTJ-506). (2006).at <http://products.brenntagspecialties.com/huntsman/JEFFAMINE_M-1000.pdf>

283. Berlinova, I. V., Dimitrov, I. V., Vladimirov, N. G., Samichkov, V. & Ivanov, Y. Associative graft copolymers comprising a poly (*N*-

isopropylacrylamide) backbone and end-functionalized polyoxyethylene side chains. Synthesis and aqueous solution properties. *Polymer* **42**, 5963–5971 (2001).

284. Han, C. K. & Bae, Y. H. Inverse thermally-reversible gelation of aqueous N-isopropylacrylamide copolymer solutions. *Polymer* **39**, 2809–2814 (1998).

285. Schild, H. G. & Tirrell, D. A. Microcalorimetric detection of lower critical solution temperatures in aqueous polymer solutions. *J Phys Chem* **94**, 4352–4356 (1990).

286. Tasdelen, B., Kayaman-Apohan, N., Guven, O. & Baysal, B. M. Preparation of poly(*N*-isopropylacrylamide/itaconic acid) copolymeric hydrogels and their drug release behavior. *Int. J. Pharm.* **278**, 343–351 (2004).

287. Erbil, C., Aras, S. & Uyanik, N. Investigation of the effect of type and concentration of ionizable comonomer on the collapse behavior of *N*-isopropylacrylamide copolymer gels in water. *J. Polym. Sci. A Polym. Chem.* **37**, 1847–1855 (1999).

288. Yaszemski, M. J., Payne, R. G., Hayes, W. C., Langer, R. & Mikos, A. G. Evolution of bone transplantation: molecular, cellular and tissue strategies to engineer human bone. *Biomaterials* **17**, 175–185 (1996).

289. Saha, K. *et al.* Substrate modulus directs neural stem cell behavior. *Biophys J* **95**, 4426–4438 (2008).

290. Roy, S., Ghosh, D. & Guha, S. K. Polyelectrolyte polymer properties in relation to male contraceptive RISUG® action. *Colloid Surface B* **69**, 77–84 (2009).

291. Van Dyke, T. E., Offenbacher, S., Braswell, L. & Lessem, J. Enhancing the value of scaling and root-planing: Arestin clinical trial results. *J Int Acad Periodontol* **4**, 72–76 (2002).

292. Peeling, W. B. Phase III studies to compare goserelin (Zoladex) with orchiectomy and with diethylstilbestrol in treatment of prostatic carcinoma. *Urology* **33**, 45–52 (1989).

293. Nelson, D. M., Ma, Z., Leeson, C. E. & Wagner, W. R. Extended and sequential delivery of protein from injectable thermoresponsive hydrogels. *J Biomed Mater Res A* **100A**, 776–785 (2012).

294. Morscher, E. W., Hefti, A. & Aebi, U. Severe osteolysis after third-body wear due to hydroxyapatite particles from acetabular cup coating. *J Bone Joint Surg Br* **80**, 267–272 (1998).

295. Trumpy, I. G. & Lyberg, T. In vivo deterioration of proplast-teflon temporomandibular joint interpositional implants: a scanning electron microscopic and energy-dispersive X-ray analysis. *J Oral Maxillofac Surg* **51**, 624–629 (1993).

296. Landes, C. A., Ballon, A. & Roth, C. In-patient versusin vitro degradation of P(L/DL)LA and PLGA. *J Biomed Mater Res B* **76B**, 403–411 (2006).

297. Heskins, M. & Guillet, J. E. Solution Properties of Poly(*N*-isopropylacrylamide). *J Macromol Sci Chem* **2**, 1441–1455 (1968).

298. Milasinovic, N., Kalagasidis Krusic, M., Knezevic-Jugovic, Z. & Filipovic, J. Hydrogels of *N*-isopropylacrylamide copolymers with controlled release of a model protein. *Int J Pharm* **383**, 53–61 (2010).

299. Bae, Y. H., Okano, T. & Kim, S. W. 'On-Off' Thermocontrol of Solute Transport. II. Solute Release from Thermosensitive Hydrogels. *Pharm Res* **8**, 624–628 (1991).

300. Kim, S. Y. & Lee, S. C. Thermo-responsive injectable hydrogel system based on poly(*N*-isopropylacrylamide-*co*-vinylphosphonic acid). I. Biomineralization and protein delivery. *J Appl Polym Sci* **113**, 3460–3469 (2009).

301. Kucers, A., Crowe, S. M., Grayson, M. L. & Hoy, J. F. *The use of antibiotics: a clinical review of antibacterial, antifungal, and antiviral drugs*. (Butterworth Heinemann: Oxford, 1997).

302. Levine, D. P. Vancomycin: A History. *Clin Infect Dis* **42**, S5–S12 (2006).

303. Walsh, C. Deconstructing Vancomycin. *Science* **284**, 442–443 (1999).

304. McLaren, A. C. *et al.* Hand-mixed and Premixed Antibiotic-loaded Bone Cement Have Similar Homogeneity. *Clin Orthop Relat Res* **467**, 1693–1698 (2009).

305. Jiranek, W. A., Hanssen, A. D. & Greenwald, A. S. Antibiotic-loaded bone cement in aseptic total joint replacement: whys, wherefores and caveats. *American Academy of Orthopaedic Surgeons, Committee on Infections* (2005).

306. Galperin, A., Long, T. J. & Ratner, B. D. Degradable, Thermo-Sensitive Poly(*N*-isopropylacrylamide)-Based Scaffolds with Controlled Porosity for Tissue Engineering Applications. *Biomacromolecules* **11**, 2583–2592 (2010).

307. DeNardo, S. J. *et al.* Effect of Molecular Size of Pegylated Peptide on the Pharmacokinetics and Tumor Targeting in Lymphoma-Bearing Mice. *Clin Cancer Res* **9**, 3854S–3864S (2003).

308. Peppas, N. A. & Khare, A. R. Preparation, structure and diffusional behavior of hydrogels in controlled release. *Adv Drug Deliv Rev* **11**, 1–35 (1993).

309. Mathew, M. & Das Gupta, V. Stability of Vancomycin Hydrochloride Solutions at Various pH Values as Determined by High-Performance Liquid Chromatography. *Drug Dev Ind Pharm* **21**, 257–264 (1995).

310. Antipas, A. S., Velde, D. V. & Stella, V. J. Factors affecting the deamidation of vancomycin in aqueous solutions. *Int J Pharm* **109**, 261–269 (1994).

311. Ahmed, I. & Day, P. Stability of cefazolin sodium in various artificial tear solutions and aqueous vehicles. *Am J Hosp Pharm* **44**, 2287–2290 (1987).

312. Galanti, L. M., Hecq, J. D., Vanbeckbergen, D. & Jamart, J. Long-term stability of cefuroxime and cefazolin sodium in intravenous infusions. *J Clin Pharm Ther* **21**, 185–189 (1996).

313. van de Belt, H. *et al.* Gentamicin release from polymethylmethacrylate bone cements and Staphylococcus aureus biofilm formation. *Acta Orthop Scand* **71**, 625–629 (2000).

314. van de Belt, H. *et al.* Staphylococcus aureus biofilm formation on different gentamicin-loaded polymethylmethacrylate bone cements. *Biomaterials* **22**, 1607–1611 (2001).

315. Kendall, R. W., Duncan, C. P. & Beauchamp, C. P. Bacterial growth on antibiotic-loaded acrylic cement: A prospective in vivo retrieval study. *J Arthroplasty* **10**, 817–822 (1995).

316. Neut, D. *et al.* Biomaterial-associated infection of gentamicin-loaded PMMA beads in orthopaedic revision surgery. *J Antimicrob Chemother* **47**, 885–891 (2001).

317. Hanssen, A. D. Prophylactic use of antibiotic bone cement: an emerging standard–in opposition. *J Arthroplasty* **19**, 73–77 (2004).

318. Viñuela, F., Duckwiler, G. & Mawad, M. Guglielmi detachable coil embolization of acute intracranial aneurysm: perioperative anatomical and clinical outcome in 403 patients. *J. Neurosurg.* **86**, 475–482 (1997).

319. Chaloupka, J. C. *et al.* A reexamination of the angiotoxicity of superselective injection of DMSO in the swine rete embolization model. *AJNR Am J Neuroradiol* **20**, 401–410 (1999).

320. Wang, Y. *et al.* In vivo assessment of chitosan/β-glycerophosphate as a new liquid embolic agent. *Interv Neuroradiol* **17**, 87–92 (2011).

321. Barnett, B. P., Hughes, A. H., Lin, S., Arepally, A. & Gailloud, P. H. In vitro assessment of EmboGel and UltraGel radiopaque hydrogels for the endovascular treatment of aneurysms. *J Vasc Interv Radiol* **20**, 507–512 (2009).

322. Overstreet, D. J., McLemore, R., Doan, B. D., Farag, A. & Vernon, B. L. Temperature-responsive graft copolymer hydrogels for controlled swelling and drug delivery. *Soft Materials - in press* (2012).

323. Seshadri, S., Janiga, G., Beuing, O., Skalej, M. & Thevenin, D. Impact of Stents and Flow Diverters on Hemodynamics in Idealized Aneurysm Models. *J Biomech Eng-T ASME* **133**, 071005 (2011).

324. Hassan, T., Ahmed, Y. M. & Hassan, A. A. The adverse effects of flow-diverter stent-like devices on the flow pattern of saccular intracranial aneurysm models: computational fluid dynamics study. *Acta Neurochirurgica* **153**, 1633–1640 (2011).

325. McLemore, R., Robb, S. A., Lee, B. H., Caplan, M. R. & Vernon, B. L. Michael-Type Addition Reactions in NIPAAm-Cysteamine Copolymers Follow Second Order Rate Laws with Steric Hindrance. *Annals of Biomedical Engineering* **37**, 2416–2425 (2009).

326. Timmer, M. D., Shin, H., Horch, R. A., Ambrose, C. G. & Mikos, A. G. In Vitro Cytotoxicity of Injectable and Biodegradable Poly(propylene fumarate)-Based Networks: Unreacted Macromers, Cross-Linked Networks, and Degradation Products. *Biomacromolecules* **4**, 1026–1033 (2003).

327. Desai, E. S., Tang, M. Y., Ross, A. E. & Gemeinhart, R. A. Critical factors affecting cell encapsulation in superporous hydrogels. *Biomed Mater* **7**, (2012).

APPENDIX A

STATEMENT OF PERMISSION FROM CO-AUTHORS

Co-authors on the previously published or submitted articles “Injectable Hydrogels”, “Temperature-responsive graft copolymer hydrogels for controlled swelling and drug delivery”, “Temperature-responsive resorbable hydrogels providing controlled release of low molecular weight drugs”, and “*In situ* Crosslinking Temperature-Responsive Hydrogels with Improved Delivery, Swelling, and Elasticity for Endovascular Embolization” have granted their permission for use of the articles in this dissertation.